

**T.C.  
DOKUZ EYLÜL UNIVERSITY  
IZMIR INTERNATIONAL  
BIOMEDICINE AND  
GENOME INSTITUTE**

**DEVELOPMENT AND PHENOTYPE OF  
NKT<sub>FH</sub> CELLS AND THEIR RELATION TO  
NKT10 CELLS**

**BAŐAK GÜNDÜZ**

**MOLECULAR BIOLOGY AND GENETICS**

**MASTER'S THESIS**

**IZMIR-2020**

**THESIS ID: DEU.IBG.MSc/2017850029**

**T.C.  
DOKUZ EYLÜL UNIVERSITY  
IZMIR INTERNATIONAL  
BIOMEDICINE AND GENOME  
INSTITUTE**

**DEVELOPMENT AND PHENOTYPE OF  
NKT<sub>FH</sub> CELLS AND THEIR RELATION TO  
NKT10 CELLS**

**MOLECULAR BIOLOGY AND GENETICS**

**MASTER'S THESIS**

**BAŞAK GÜNDÜZ**

Supervisor: Dr. GERHARD WINGENDER

This research is supported by TUBITAK 1001-117Z216

**THESIS ID: DEU.IBG.MSc/2017850029**



T.C.  
DOKUZ EYLÜL ÜNİVERSİTESİ



İZMİR ULUSLARARASI BİYOTIP VE GENOM ENSTİTÜSÜ

### YÜKSEK LİSANS TEZ SAVUNMA TUTANAĞI

Dokuz Eylül Üniversitesi İzmir Uluslararası Biotıp ve Genom Enstitüsü Genom Bilimleri ve Moleküler Biyoteknoloji Anabilim Dalı, İngilizce Moleküler Biyoloji ve Genetik Yüksek Lisans program, 2017850029 öğrenci numaralı, Başak Gündüz'ün '**NKT<sub>EM</sub> HÜCRELERİNİN GELİŞİMİ, FENOTİPİ VE NKT10 HÜCRELERİ İLE İLİŞKİSİ**' konulu Yüksek Lisans tezini 10.04.2020 tarihinde başarılı olarak tamamlamıştır.

**BAŞKAN**

**Dr. Öğr. Üyesi Gerhard Wingender**

İzmir Uluslararası Biotıp ve Genom Enstitüsü

Biyotıp ve Sağlık Teknolojileri A.D.

**ÜYE**

**Dr. Öğr. Üyesi Zeynep Ahsen Kocer**

İzmir Uluslararası Biotıp ve Genom  
Enstitüsü

**ÜYE**

**Dr. Öğr. Üyesi Çiğdem Tosun**

İzmir Yüksek Teknoloji Enstitüsü

**YEDEK ÜYE**

**Prof. Dr. Yavuz Oktay**

İzmir Uluslararası Biotıp ve Genom  
Enstitüsü

**YEDEK ÜYE**

**Dr. Öğr. Üyesi Gülistan Meşe Özçivici**

İzmir Yüksek Teknoloji Enstitüsü

## INDEXES

Indexes.....	iv
Table index.....	vii
Figure index.....	viii
Abbreviations.....	ix
Summary (English).....	1
Summary (Turkish).....	2
<b>1. INTRODUCTION AND OBJECTIVES.....</b>	<b>3</b>
<b>2. LITERATURE SUMMARY.....</b>	<b>4</b>
2.1. The Immune System.....	4
2.2. The Innate Immune System.....	4
2.3. The Adaptive Immune System.....	5
2.3.1. B Cells.....	7
2.3.2. T Cells.....	7
2.4. Antigen Presenting Cells as The Link Between the Innate Immune System and The Adaptive Immune System.....	9
2.5. Innate-Like T Cells.....	10
2.6. Invariant Natural Killer T Cells.....	10
2.6.1. The Expression of a Semi-Invariant TCR.....	11
2.6.2. The Recognition of CD1d Molecules.....	11
2.6.3. The Antigens of <i>i</i> NKT Cells.....	12
2.6.4. The Effector Functions of <i>i</i> NKT Cells.....	13
2.6.5. The Basic Role of <i>i</i> NKT Cell in Different Diseases.....	13
2.6.6. The Subsets of <i>i</i> NKT Cells.....	14
2.6.7. NKT <sub>FH</sub> Cells.....	15
<b>3. MATERIALS AND METHODS.....</b>	<b>17</b>
3.1. Type of Research.....	17
3.2. The Location and Date of the Research.....	17
3.3. Research Population, Sampling and Experimental Groups.....	17
3.4. Research Materials.....	17
3.5. Research Variables.....	17
3.6. Data Collection Tools.....	18
3.6.1. Laboratory Materials.....	18
3.6.1.1. General Laboratory Equipment.....	18
3.6.1.2. Vivarium Laboratory Equipment.....	19
3.6.1.3. Consumables.....	20

3.6.1.4. Chemicals, Reagents, and Commercial Kits.....	21
3.6.1.5. Antibodies for Flow Cytometry.....	23
3.6.1.6. Other Reagents for Staining.....	27
3.6.1.7. Other Fluorescent Reagents for Flow Cytometry.....	27
3.6.2. Methods.....	28
3.6.2.1. Animal Handling and Experimentation.....	28
3.6.2.1.1. Mouse Handling.....	28
3.6.2.1.2. Mouse Anaesthesia.....	28
3.6.2.1.3. Mouse Injection Methods.....	29
3.6.2.1.4. Mouse Euthanasia by Cervical Dislocation.....	31
3.6.2.1.5. Recovery of Mouse Organs.....	32
3.6.2.2. Cell Isolation.....	36
3.6.2.2.1. Single Cell Suspensions from the Bone Marrow.....	36
3.6.2.2.2. Density Gradient Separation with Lymphoprep.....	37
3.6.2.2.3. Density Gradient Separation with Percoll.....	38
3.6.2.3. <i>In Vitro</i> Stimulation of Single Cell Suspensions.....	40
3.6.2.4. Cell Staining for Flow Cytometry.....	40
3.6.2.4.1. Cell Surface Staining for Flow Cytometry.....	40
3.6.2.4.2. Intracellular Staining for Flow Cytometry.....	41
3.7. Research Plan.....	44
3.8. Evaluation of the Data.....	45
3.9. Limitation of the Research.....	45
4. RESULTS.....	46
4.1. Optimizing the Bcl6 Staining for The Detection of NKT <sub>FH</sub> Cells.....	46
4.1.1. The gating strategy for the identification of <i>n</i> NKT cells.....	46
4.1.2. Germinal center B cells are used as positive control for the Bcl6-expression.....	48
4.1.3. NKT <sub>FH</sub> cells are detectable in C57BL/6 mice six days after injection of $\alpha$ GalCer.....	50
4.1.4. A pre-fix step using Cytofix/Cytoperm at 37°C improves the Bcl6 staining.....	52
4.1.5. The working concentration of $\alpha$ Bcl6-Ab [7D1] was established.....	54
4.1.6. Differences in The Bcl6 Detection Between the $\alpha$ Bcl6-Ab Clones <i>K112-91</i> and Clone <i>7D1</i> .....	55
4.2. The Frequency and Phenotype of Splenic NKT <sub>FH</sub> Cells.....	56
4.3. The Tissue Distribution of NKT <sub>FH</sub> Cells.....	62
4.4. The Cytokine Production of NKT <sub>FH</sub> Cells.....	65
4.5. The Relationship of NKT <sub>FH</sub> And NKT10 Cells.....	67
4.5.1. The frequency of NKT <sub>FH</sub> and NKT10 cells changes over time following antigenic stimulation.....	67

<b>4.5.2. The Importance of NKT<sub>FH</sub> Cells for The Development of NKT10 Cells.....</b>	<b>70</b>
<b>5. DISCUSSION.....</b>	<b>71</b>
<b>6. CONCLUSION.....</b>	<b>74</b>
<b>7. REFERENCES.....</b>	<b>75</b>
<b>8. ADDENDA.....</b>	<b>82</b>
<b>8.1. Research Ethics Committee Approval.....</b>	<b>82</b>
<b>8.2. Curriculum Vitae.....</b>	<b>84</b>



## TABLE INDEX

	Page number
<b>Table 1.</b> The comparison of <i>NKT</i> cell subsets.....	15
<b>Table 2.</b> Antibodies used in the study.....	22
<b>Table 3.</b> Other reagents for staining.....	27
<b>Table 4.</b> Other fluorescent reagents for flow cytometry.....	27



## FIGURE INDEX

	<b>Page number</b>
<b>Figure 1.</b> Following immune activation, the expression of Bcl6 in naïve T cells results in the differentiation of T <sub>FH</sub> cells.....	9
<b>Figure 2.</b> The chemical structure of αGalCer.....	12
<b>Figure 3.</b> NKT <sub>FH</sub> cells arise <i>in vivo</i> following the injection of αGalCer.....	16
<b>Figure 4.</b> The location for the i.p. injections.....	30
<b>Figure 5.</b> A schematic illustration of the mouse liver perfusion.....	35
<b>Figure 6.</b> Schematic illustration of the separation of liver leukocytes by Percoll density gradient.....	39
<b>Figure 7.</b> The gating strategy used to identify <i>IN</i> KT cells.....	47
<b>Figure 8.</b> The gating strategy used to detect GC B cells.....	49
<b>Figure 9.</b> The frequency of NKT <sub>FH</sub> cells and GC B cells is higher following αGalCer injection.....	51
<b>Figure 10.</b> The different pre-fix protocols tested for the optimization of the Bcl6 staining in GC B cells.....	53
<b>Figure 11.</b> The titration of the αBcl6 antibody using GC B cells.....	54
<b>Figure 12.</b> Two different Bcl6 antibody clones were tested to detect Bcl6 <sup>+</sup> cells in splenic <i>IN</i> KT cells.....	55
<b>Figure 13.</b> The frequency of splenic <i>IN</i> KT and NKT <sub>FH</sub> cells following i.v. or i.p. injection of αGalCer.....	56
<b>Figure 14.</b> The phenotype of splenic <i>IN</i> KT and NKT <sub>FH</sub> cells following i.v. or i.p. injection of αGalCer.....	58
<b>Figure 15.</b> The phenotype of splenic <i>IN</i> KT and NKT <sub>FH</sub> cells following i.p. injection of αGalCer.....	59
<b>Figure 16.</b> The expression of PLZF in splenic <i>IN</i> KT and NKT <sub>FH</sub> cells following i.v. or i.p. injection of αGalCer.....	60
<b>Figure 17.</b> The <i>in vivo</i> expansion of NKT <sub>FH</sub> cells in C57BL/6 and BALB/c wild-type mice.....	61
<b>Figure 18.</b> <i>In vivo</i> distribution of <i>IN</i> KT and NKT <sub>FH</sub> cells following i.v. or i.p. injection of αGalCer.....	63
<b>Figure 19.</b> Phenotype differences of <i>IN</i> KT and NKT <sub>FH</sub> cells in various organs following i.v. or i.p. injection of αGalCer.....	64
<b>Figure 20.</b> The expression of CD185 and Bcl6 in NKT <sub>FH</sub> cells following <i>in vitro</i> stimulation with PMA/ionomycin.....	66
<b>Figure 21.</b> The gating strategy of NKT10 cells in C57BL/6 and BALB/c mice.....	68
<b>Figure 22.</b> Time course of the expression of Bcl6 and IL-10 in <i>IN</i> KT cells following αGalCer injection.....	69
<b>Figure 23.</b> NKT10 cell expansion after αGalCer does not depend on Bcl6.....	70



## **ABBREVIATIONS**

$\alpha$ :	anti-
aa:	Amino Acid
$\alpha$ GalCer:	Alpha-galactosylceramide
AF488:	Alexa Flour 488
AF647:	Alexa Flour 647
AF700:	Alexa Flour 700
APCs:	Antigen-presenting cells
APC:	Allophycocyanin
APC-Cy7:	Allophycocyanin-cyanine7
APC-eF780:	Allophycocyanin – eFlour 780
BSA:	Bovine serum albumin
Bcl6:	B cell lymphoma 6
BCR:	B cell receptor
BUV395:	Brilliant Ultraviolet 395
BV421:	Brilliant Violet 421
BV510:	Brilliant Violet 510
BV570:	Brilliant Violet 570
BV605:	Brilliant Violet 605
BV650:	Brilliant Violet 650
BV711:	Brilliant Violet 711
BV785:	Brilliant Violet 785
BV786:	Brilliant Violet 786
C:	Celsius
CD:	Cluster of differentiation
cm:	Centimeter
CTL:	Cytotoxic T cell
cRPMI:	Completed RPMI
CXCL13:	Chemokine (C-X-C Motif) ligand 13
DMSO:	Dimethylsulfoxide
DNA:	Desoxyribonucleic acid
DNase:	Deoxyribonuclease
DCs:	Dendritic cells
EDTA:	Ethylendiamintetraacetat
eF660:	eFlour 660
eFluor 450:	eFlour 450
EtOH:	Ethanol
Fc:	Fragment crystallizable
FACS:	Fluorescent activated cell sorting
FCS:	Foetal calf serum
FITC:	Fluorescein isothiocyanate
FBS:	Fetal Bovin serum
FITC:	Fluorescein isothiocyanate

FoxP3:	Forkhead box P3
FR4:	Folate receptor 4
g:	gram; acceleration of gravity (9.81 m/s <sup>2</sup> )
GC:	Germinal centers (GCs)
h:	hour
IFN:	Interferon
Ig:	Immunoglobulin
IL:	Interleukin
INKT:	Invariant Natural Killer T
IL-10:	Interleukin 10
IL-12:	Interleukin 12
IL-13:	Interleukin 13
IL-17A:	Interleukin 17A
IL-21:	Interleukin 2
IL-4:	Interleukin 4
ILCs:	Innate lymphoid cells
Kb:	Kilobase
kD:	Kilodalton
L:	Liter
μ:	Micro- (10 <sup>-6</sup> )
m:	Meter; milli- (10 <sup>-3</sup> )
M:	Molar
MACS:	Magnetically activated cell sorting
MHC:	Major histocompatibility complex
Min:	Minute
mRNA:	messenger RNA
MW:	Molecular weight
n:	nano- (10 <sup>-9</sup> )
NKT <sub>FH</sub> :	Follicular helper NKT
NaN <sub>3</sub> :	Sodium azide
NK1.1:	Natural Killer 1.1
OD:	Optical density
PBS:	Phosphate buffered saline
PE:	Phycoerythrin
PMA:	Phorbol 12-myristat 13-acetat
PB:	Pacific blue
PE-Cy5:	Phycoerythrin cyanine5
PE-Cy7:	Phycoerythrin cyanine 7
PE-Dazzle 594:	Phycoerythrin Dazzle 594

PE-eFluor610:	Phycoerythrin eFluor610
PerCP-Cy5.5:	Peridinin chlorophyll protein cyanine 5.5
PerCP-eF710:	Peridinin chlorophyll protein – eFluor 710
PLZF:	Promyelocytic leukemia zinc finger
RNA:	Ribonucleic acid
rpm:	Rotations per minute
RT:	Room temperature
RORyt:	RAR-related orphan receptor gamma T
s:	Second
SDS:	Sodium dodecyl sulfate
scWAT:	Subcutaneous white adipose tissue
Slamf6:	Signaling lymphocyte activation molecule 6
SSC-A:	Side scatter area
SSC-W:	Side scatter width
TCR:	T cell receptor
T <sub>FH</sub> :	T follicular helper
Th:	T helper
TNF:	Tumor necrosis factor
Tris:	Tris- (hydroxymethyl) -aminomethan
Tbet:	T-box transcription factor
TRAIL:	Tumor necrosis factor-related apoptosis-inducing ligand
U:	Unit
UV:	Ultraviolet light
v/v:	Volume per volume
Vol:	Volume
W:	Weight
w/v:	Weight per volume

## **ACKNOWLEDGEMENT**

First and foremost, I would like to thank my supervisor, Gerhard Wingender. I can't be grateful enough for constant support and guidance he provided during my MSc studies and his patience with keep handling my mistakes. Whenever I had a question or an urgent problem about ongoing experiment, the door of his office was always opened! Or if, just say, we just needed a chocolate! For countless times I had troubles with experiments and for each of them he had a motivational speech. I could not imagine better opportunity for my first academic step, than be in his lab. Once again, thank you, Gerhard.

A special thanks to coworker of our lab Duygu Sag for showing us how to be a happy scientist. Thanks to my colleagues: Fatma Hapil, who spend so much time giving me practical advise, Resul Ozbilgic, who dedicated his time for my experiments and motivated me whenever I needed, Zeynep Ayyıldız, she always ready to troubleshoot any issues. Big thanks to Muge Ozkan, who taught me handling technical problems and more importantly showed me how to design my experiments. I would like to thank Cem Eskiocak to be there all the time spending his days for my experiments and our nice chats on the ways home. Lastly, I would like to thank to all other members of the Wingender Lab: Zeynep Gulce, Yonca Erdal, Sezgin Bal and Sag Lab for being nice and friendly.

Additionally, I would like to thank my best friends, Ezgi Ozkurt, who always disagrees with me about my perspectives and pushes my limits further, Gizem Tugce Ulu, Ezgi Taş, Irem Tuysuz and Gulsun Bagcı who can bring me into peace with just one smile. Furthermore, I would like to thank my family, my heroes, Melek and Nufel Gunduz and my aunt, Nesli Ayiz for support. They taught me not to give up on my dreams and be a better person. Also, my cousin Cansu, who is brave enough to stand up against my wrong decisions and denote my mistakes. Thank you Cansu for making me a better person! I promise I will share my diploma with you! Lastly, my boyfriend, my best friend, Evgeny Antonyuk, who supports me with endless love. He is always there to make my life easier and better even with all the distance. Thank you for giving me a life which I could not even imagine, my love!

*'Yaşamak şakaya gelmez,  
büyük bir ciddiyetle yaşayacaksın  
bir sincap gibi mesela,  
yani, yaşamının dışında ve ötesinde hiçbir şey beklemeden,  
yani bütün işin gücün yaşamak olacak.  
Yaşamayı ciddiye alacaksın,  
yani o derecede, öylesine ki,  
mesela, kolların bağlı arkadan, sırtın duvarda,  
yahut kocaman gözlüklerin,  
beyaz gömleğinle bir laboratuvar  
insanlar için ölebileceksin,  
hem de yüzünü bile görmediğin insanlar için,  
hem de hiç kimse seni buna zorlamamışken,  
hem de en güzel en gerçek şeyin  
yaşamak olduğunu bildiğin halde.  
Yani, öylesine ciddiye alacaksın ki yaşamayı,  
yetmişinde bile, mesela, zeytin dikeceksin,  
hem de öyle çocuklara falan kalır diye değil,  
ölmekten korktuğun halde ölüme inanmadığın için,  
yaşamak yanı ağır bastığından."*

*Nazım Hikmet Ran,1947*

## DEVELOPMENT AND PHENOTYPE OF NKT<sub>FH</sub> CELLS AND THEIR RELATION TO NKT10 CELLS

Başak Gündüz, Dokuz Eylül University Izmir International Biomedicine and  
Genome Institute, basak.gunduz@msfr.ibg.edu.tr

### ABSTRACT

Invariant natural killer T (*i*NKT) cells are a unique T cell subset that resemble Natural Killer and memory T cells. After TCR-mediated stimulation by the antigen  $\alpha$ GalCer, *i*NKT cells rapidly produce copious amounts of various cytokines. Three to six days later, Bcl6-expressing NKT<sub>FH</sub> cells arise and are detectable for about two weeks *in vivo*. In contrast, IL-10 producing NKT10 cells expand within two and three weeks following the  $\alpha$ GalCer challenge and are detectable for several months *in vivo*. However, little is known to date about the development and phenotype of NKT<sub>FH</sub> cells and their relation to NKT10 cells. To better characterize NKT<sub>FH</sub> cells, we studied the *in vivo* distribution of NKT<sub>FH</sub> cells in different murine organs and how this is influenced by the route of the antigen administration. To this end, we injected  $\alpha$ GalCer either intra-peritoneal or intra-venous and measured the frequency and phenotype of NKT<sub>FH</sub> cells in different organs by flow cytometer. Moreover, we studied the relationship of NKT<sub>FH</sub> and NKT10 cells by analysing the development of NKT10 cells in the absence of NKT<sub>FH</sub> cells in Bcl6<sup>-/-</sup> mice. Our data show, that the route of antigen challenge impacts the frequency and the phenotype of *i*NKT and NKT<sub>FH</sub> cells *in vivo* in different organs. Furthermore, the expansion of NKT10 cells was unimpaired in the absence of Bcl6, indicating that NKT10 cell expansion does not depend on NKT<sub>FH</sub> cells. These findings provide important information to better understand the development of NKT<sub>FH</sub> cells and their relationship with NKT10 cells.

**Keywords: *i*NKT cell subsets, NKT<sub>FH</sub> cells, NKT10 cells, development**

# NKTFH HÜCRELERİNİN GELİŞİMİ, FENOTİPİ VE NKT10 HÜCRELERİ İLE İLİŞKİSİ

Başak Gündüz, Dokuz Eylül Üniversitesi, İzmir Uluslararası Biyotıp ve Genom Enstitüsü, basak.gunduz@msfr.ibg.edu.tr

## ÖZET

Doğala yakın öldürücü T hücreleri (NKT), doğal öldürücü hücrelere (NK) ve hafıza T hücrelerine benzerlik gösteren özgün bir T hücre alt tipidir.  $\alpha$ GalCer ile TCR-aracılı uyarım sonrasında NKT hücreleri, çeşitli sitokinleri yüksek miktarda hızlıca üretir. *In vivo* uyarımdan üç-altı gün sonra, Bcl6 genini ifade eden NKT<sub>FH</sub> hücreleri ortaya çıkar ve yaklaşık iki hafta boyunca tespit edilebilir. IL-10 üretebilen NKT10 hücreleri,  $\alpha$ GalCer uygulaması sonrasında, zıt bir şekilde iki-üç hafta süresince çoğalır ve birkaç ay boyunca tespit edilebilir. Ancak, bugüne kadar NKT<sub>FH</sub> hücrelerinin gelişimi, fenotipi ve NKT10 hücreleriyle ilişkisi hakkında çok az şey bilinmektedir. NKT<sub>FH</sub> hücrelerinin daha iyi karakterize edilmesi için, NKT<sub>FH</sub> hücrelerinin farelerde farklı organlardaki dağılımı ve antijen uygulaması yolundan nasıl etkilendiğini araştırdık. Bu amaç doğrultusunda, intraperitoneal ve intravenöz yollardan  $\alpha$ GalCer enjeksiyonu gerçekleştirildi ve NKT<sub>FH</sub> hücrelerinin frekansı ve fenotipini akış sitometrisi ile ölçüldü. Ayrıca, Bcl6<sup>-/-</sup> farelerde NKT<sub>FH</sub> hücrelerinin yokluğunda NKT10 hücrelerinin gelişimini analiz ederek NKT<sub>FH</sub> hücreleri ile NKT10 hücreleri arasındaki ilişki çalışıldı. Elde ettiğimiz veriler, antijen uygulama yolunun farklı organlarda NKT ve NKT<sub>FH</sub> hücrelerinin fenotipini ve frekansını etkilediğini gösterdi. Buna ek olarak, NKT10 hücrelerinin çoğalmasının Bcl6 yokluğunda zarar görmediğini ve NKT10 hücrelerinin çoğalmasının NKT<sub>FH</sub> hücrelerine bağımlı olmadığını gözlemledik. Bu bulgular NKT<sub>FH</sub> hücrelerinin gelişimi ve NKT10 hücreleri ile ilişkisini daha iyi anlamak açısından önemli bilgiler sağladı.

**Anahtar Sözcükler:** NKT hücre grupları, NKT<sub>FH</sub> hücreleri, NKT10 hücreleri, gelişim

## 1. INTRODUCTION AND OBJECTIVES

Invariant Natural Killer T ( $\mathit{i}$ NKT) cells are a unique subset of T cells. They rapidly produce a wide range of functionally different cytokines and chemokines after stimulation, thus they can influence various different immune reactions.  $\mathit{i}$ NKT cells recognize glycolipids, whereas conventional T cells respond to peptide antigens. Similar to  $\text{CD4}^+$  T helper cells, mouse  $\mathit{i}$ NKT cells can be divided into several distinct subsets. These functional  $\mathit{i}$ NKT cell subsets have been proposed as an explanation for their diverse immune functions. Therefore, it is critical and important to expand our knowledge of  $\mathit{i}$ NKT cell subsets to prevent unpredictable reactions during the treatment of diseases. One  $\mathit{i}$ NKT cell subset, follicular helper NKT ( $\text{NKT}_{\text{FH}}$ ) cells, arise *in vivo* within three - six days after injection with  $\alpha\text{GalCer}$ .  $\text{NKT}_{\text{FH}}$  cells are able to provide cognate help to stimulated B cells, support their proliferation, and thereby enhance antibody responses. Therefore, it is important to improve our knowledge of the development, characterization, and distribution of  $\text{NKT}_{\text{FH}}$  cells *in vivo*, to better understand their role in orchestrating B cells responses.

Two major aims were addressed in this project:

- 1) To improve the characterization of  $\text{NKT}_{\text{FH}}$  cells: Six days after  $\alpha\text{GalCer}$  injection, we analysed their expression of surface markers, transcription factors, and cytokines. We also studied the *in vivo* distribution of  $\text{NKT}_{\text{FH}}$  cells in different murine organs and how this is influenced by the route of the antigen administration, i.e. either intraperitoneal or intra-venous injection. We hypothesized that the *in vivo* distribution of  $\text{NKT}_{\text{FH}}$  cells is impacted by the route of the antigen administration.
- 2) To study the relationship of  $\text{NKT}_{\text{FH}}$  and  $\text{NKT10}$  cells: Following  $\alpha\text{GalCer}$  injection two changes can be observed: i)  $\text{NKT}_{\text{FH}}$  cells arise *in vivo* within three to six days and are undetectable after two to four weeks, and ii) the number of IL-10-producing  $\text{NKT10}$  cells increases within two to four weeks. However, the relationship of  $\text{NKT}_{\text{FH}}$  and  $\text{NKT10}$  cells is unclear to date. Therefore, we compared the phenotype of  $\text{NKT}_{\text{FH}}$  and  $\text{NKT10}$  cells and measured their *in vivo* kinetics over time side-by-side. Furthermore, by utilizing T cell specific Bcl6-deficient mice, we tested whether  $\text{NKT10}$  cells can develop in the absence of



NKT<sub>FH</sub> cells. We hypothesized that NKT<sub>FH</sub> and NKT10 cells are two independent NKT cell subsets.

## 2. LITERATURE SUMMARY

### 2.1. The Immune System

The immune system is an enormous network of many types of immune cells, organs, and proteins that is spread throughout the whole body in order to protect the body against foreign and harmful substances, such as bacteria, viruses, or parasites, and against damage to the tissue. When the body encounters pathogenic substances, the immune system mounts a biological response to protect the body, called an immune response. The immune response is usually accompanied by an inflammation, characterized by five classical signs: redness (*rubor*), swelling (*tumor*), heat (*calor*), pain (*dolor*), and loss of function (*functio laesa*) of the tissues. These processes aim to eliminate harmful substances and to initiate the healing of the tissue.

The immune system is commonly divided into the innate and adaptive immune system. The innate immune system is able to immediately respond following an exposure to a pathogenic substance. In contrast, the adaptive immune system requires an initial maturation phase, leading to a delayed response. These two immune systems together provide a highly coordinated immune responses against e.g. microbes.

### 2.2. The Innate Immune System

The innate immune system is the first line of defence that provides a general antigen-independent defence mechanism, characterized by immediate inflammatory responses following infections (Kimbrell *et al.*, 2001). The innate immune system is always ready to combat a wide variety of different pathogens (Alberts *et al.*, 2002). The effector cells of the innate immune system are monocytes/macrophages, Natural Killer (NK) cells, dendritic cells (DCs), granulocytes (neutrophils, basophils, eosinophils, and mast cells), and innate lymphoid cells (ILCs) (Yatim & Lakkis, 2015). The cells of the innate immune system have limited diversity in their receptors for the recognition of

antigens (Lach, 2005). These receptors recognize common, highly conserved structures of many pathogens (Brubaker *et al.*, 2015). Additionally, most of these cells are not able to generate immunological memory, which means the capability of the cells to respond stronger and faster upon secondary exposure to the particular pathogen (Janeway *et al.*, 2001). Some cells of the innate immune system, such as macrophages and neutrophils, destroy pathogens followed by intracellular killing. However, the prime cytotoxic cells of the innate immune system are NK cells. They play important roles in the early immune defence against tumours (Chan & Housseau, 2008) and against cells infected with viruses and intracellular bacteria (Arnon *et al.*, 2006). NK cells have different mechanisms to trigger the target cell's death: i) granule mediated mechanisms (Sagiv *et al.*, 2013), ii) receptor mediated mechanisms, and iii) antibody-dependent cellular cytotoxicity (Yoon *et al.*, 2015). In the granule mediated mechanism activated NK cells release the content of their cytotoxic vesicles onto the target cells. In particular, the pore-forming molecules perforin and the enzyme granzyme B, which can trigger programmed cell death ones in the cytoplasm, are required for the cytotoxicity (Lord *et al.*, 2003). For the receptor mediated process, NK cells trigger death receptors, such as CD95/Fas or TRAIL, expressed on the target cells that initiate the programmed cell death of the target cells (Wallach *et al.*, 1999). In the antibody-dependent cellular cytotoxicity, NK cells bind via their surface Fc receptors antigen-bound antibodies, which leads to the elimination of the antibody-coated target cells via cytotoxic vesicles (Arnon *et al.*, 2006). These Fc-receptors are an example of activating receptors expressed on NK cells (Arnon *et al.*, 2006). They also express inhibitory receptors that impair the signalling of the activating receptors (Arnon *et al.*, 2006). Therefore, the activation of NK cell-mediated cytotoxicity depends on the balance between the inhibitory and activating receptors (Arnon *et al.*, 2006). Once NK cells are activated, they also secrete cytokines to orchestrate other immune response.

### **2.3. The Adaptive Immune System**

The innate immune system is the first lines of defence against pathogens. It is always ready to attack and ensures a general antigen-independent mechanism. In

contrast, the adaptive immunity system is the second line of defence, as it takes several days from the encounter of the antigen to the peak of the response (Yatim & Lakkis, 2015). The adaptive immune cells are T and B cells. Most of the T and B cells that circulate the body are not functionally active until they recognize their antigen and are, therefore, called naïve cells (Cano & Lopera, 2013). After the activation by a particular antigen, naïve T and B cells undergo further differentiation and become effector lymphocytes (Crotty, 2015). Effector T and B cells are responsible for the cell-mediated and the humoral immune response, respectively. The cell-mediated immunity has an essential role against intracellular bacteria, microbes, and viruses. T cells support the elimination of pathogens either by the killing of infected cells or by orchestrating the immune response via cytokines and surface molecules. The humoral immunity is mediated by antibodies, which are the soluble form of the BCR, secreted by activated B cells. The humoral immune response plays an important role against extracellular microbes and toxins. Antibodies can directly bind to their particular antigen, which might for example be found on a pathogen or toxin. Thereby, antibodies can either neutralize the pathogen/toxin, by inhibiting its functions, or can mark the pathogen for its elimination by other parts of the immune system.

The antigen receptor on T cells is called T cell receptor (TCR). T cells are able to express two different kind of TCR.  $\alpha\beta$  T cells bear TCRs formed from one  $\alpha$  and one  $\beta$  chain, whereas  $\gamma\delta$  T cells bear TCRs that contain one  $\delta$  and  $\gamma$  chain each. The antigen receptor on B cells is called B cell receptor (BCR). Due to the highly diverse receptor repertoire of T and B cells, the adaptive immune system is able to provide defence against a wider range of antigens than the innate immune system (Vivier & Malissen, 2005). The receptors of the innate immune system are encoded by germline genes. In contrast, the receptors of the adaptive immune system are assembled from different gene segments during lymphocyte development. This and other supporting processes allow the generation of billions of distinct TCRs and BCRs, meaning that almost every T and B cell in the body expresses a receptor unique to this cell. Furthermore, and in contrast to the innate immune response, adaptive immune cells are able to form immunological memory, which means that a secondary response against the same antigen is faster and more effective in magnitude and quality (Janeway *et al.*, 2001).

### 2.3.1. B Cells

B lymphocytes are produced in the bone marrow and finalize their differentiation in the spleen (Pieper *et al.*, 2013). Following antigen stimulation, activated B cells proliferate and differentiate into follicular B cells that migrate among secondary lymphoid organs (Natkunam, 2007). This is followed by the generation of specialized, temporary structures in the follicles of the spleen, named germinal centres (GCs) (Allen *et al.*, 2007). In the germinal centres, GC B cells, which are characterized by the surface markers  $GL7^{\text{high}}$ ,  $CD95^{\text{high}}$ , and  $CD38^{\text{low}}$  in mice (Allen *et al.*, 2007), expand numerically and undergo somatic hypermutation (McHeyzer-Williams, 2005). Somatic hypermutation is a mechanism that allows B cells to produce antibodies of higher affinity against their particular antigen (Alberts *et al.*, 2002). Some of the GC B cells eventually differentiate either into short-lived plasma cells that secrete antibodies or into long-lived memory B cells that are the basis of the B cell memory. Plasma B cells and memory B cells leave the GCs as high-affinity cells (Cano *et al.*, 2013).

### 2.3.2. T Cells

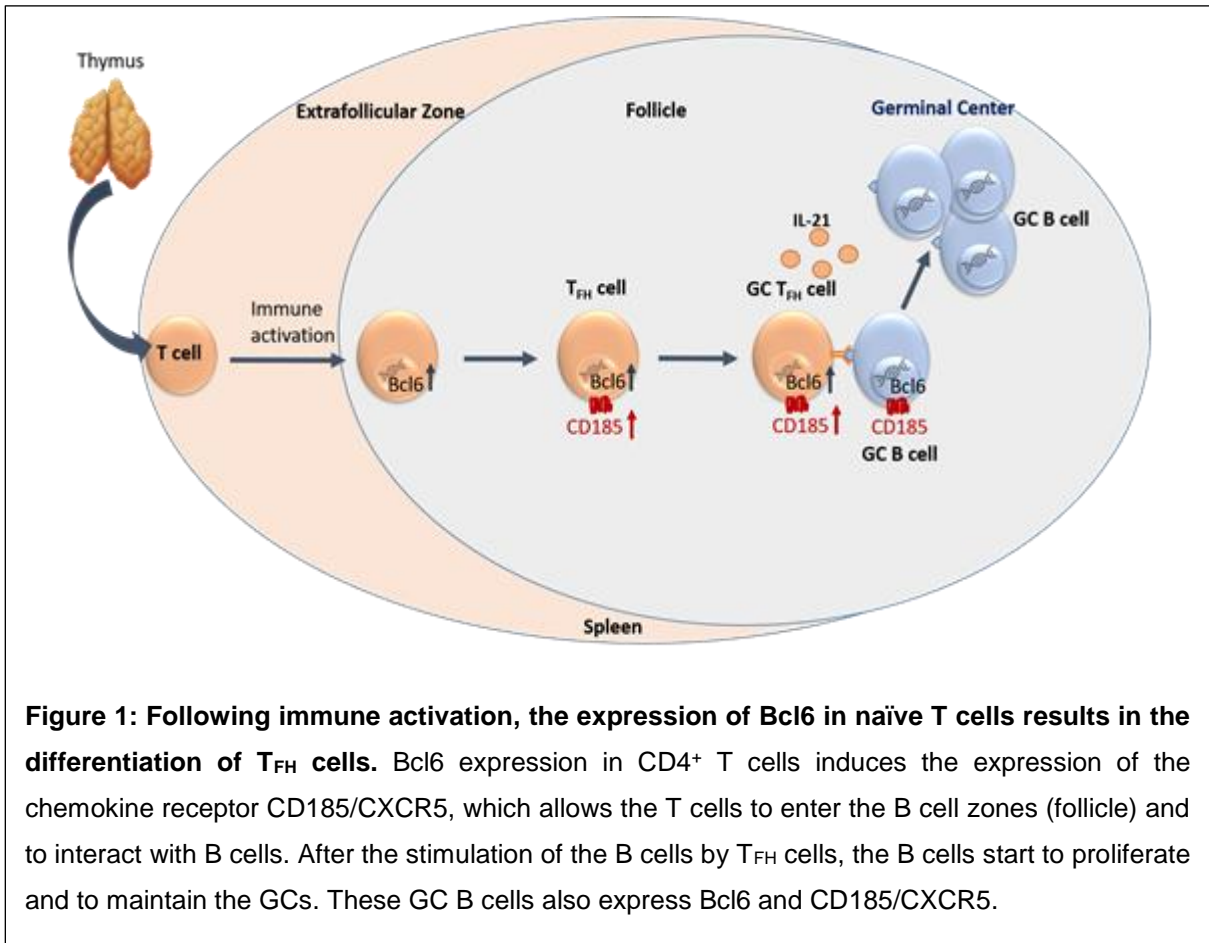
T cell precursors are produced in the bone marrow and migrate to the thymus for their maturation (Cano, 2013). Almost all of  $\alpha\beta$  T cells express either the CD4 or CD8 co-receptors and are, therefore, referred to as  $CD4^+$  or  $CD8^+$  T cells.

$CD8^+$  T cells play important roles in tumour surveillance and in the fight against intracellular pathogens (Zhang & Bevan, 2011). Cells infected with an intracellular pathogen will present some of the pathogen-derived antigens on the surface, which can then be recognized by antigen-specific  $CD8^+$  T cells (Zhang & Bevan, 2011). This antigen recognition by  $CD8^+$  T cells leads to a cytotoxic destruction of the host cells (Vivier & Malissen, 2005).  $CD8^+$  T cells have three major killing mechanisms to kill infected or tumour cells (Chan & Housseau, 2008). The first mechanism is the release of cytokines such as TNF and  $IFN\gamma$ , which have anti-tumour and anti-viral effects (Janeway, 2001). The second mechanism is mediated by perforin and granzymes, stored in cytotoxic granules (Chowdhury & Lieberman, 2008). Perforin is a protein that makes pores in the membrane of the target cells, allowing the entry of granzymes into

the cell (Cullen & Martin, 2007). Granzymes are proteases that initiate a self-destructive process in the cell, called programmed cell death or apoptosis (Cullen & Martin, 2007). In the third killing mechanism the apoptosis of the target cell is not initiated via perforin/granzymes, but via surface receptors (Wallach *et al.*, 1999). Activated CD8<sup>+</sup> T cells express CD178/FasL, which is the ligand for the death receptor CD95/Fas, found particularly on the surface of infected or stressed cells (Wallach *et al.*, 1999). Following CD95/CD178 interaction, signalling molecules down-stream of CD95 can induce apoptosis in the target cell (Wallach *et al.*, 1999). These cytotoxic mechanisms are common between adaptive CD8<sup>+</sup> T cells and innate NK cells (Chan & Housseau, 2008).

The main function of activated CD4<sup>+</sup> T cells is to secrete particular cytokines to help the proliferation and activation of other effector immune cells and to orchestrate the immune response (Luckheeram *et al.*, 2011). Thus, CD4<sup>+</sup> T cells are also called helper T cells. There are several distinct subsets of CD4<sup>+</sup> helper T cells, which are characterized by the particular cytokines they produce and a unique master transcription factor that regulates these functions (Luckheeram *et al.*, 2011).

A distinct subset of CD4<sup>+</sup> helper T cells is called follicular helper T (T<sub>FH</sub>) cells. They are characterized by the expression of the transcription factor Bcl6 (B cell lymphoma 6) (Wali *et al.*, 2016). Among others, Bcl6 also initiate the expression of the chemokine receptor CD185/CXCR5 that can bind the chemokine CXCL13 and is required to allow T<sub>FH</sub> cells to enter the GCs (Haynes *et al.*, 2007). Thus, T<sub>FH</sub> cells are characterized by the expression of Bcl6 and CD185 (Crotty, 2011). Following antigen stimulation, T<sub>FH</sub> cells can stimulate the proliferation and further differentiation of GC B cells as illustrated in **figure 1** (Haynes *et al.*, 2007). Additionally, T<sub>FH</sub> cells can produce the cytokine IL-21 and express the surface markers CD279 (also known as programmed cell death-1, PD-1) and CD278 (also known as inducible T-cell co-stimulatory, ICOS) (Wali *et al.*, 2016).



## 2.4. Antigen Presenting Cells as The Link Between the Innate Immune System and The Adaptive Immune System

A specialized group of immune cells are able to stimulate T cells to mount an adaptive immune response against a particular antigen (Hughes *et al.*, 2016). These cells are named antigen presenting cells (APCs). The main APCs are DCs and macrophages from the innate immune system, and B cells from the adaptive immune system. APCs capture pathogens, microbial products, and antigens (Hughes *et al.*, 2016). They are able to degrade and process the proteins from the captured pathogens or pathogen-infected cells and break them apart into smaller peptides (Hughes *et al.*, 2016). These protein fragments can then be presented on the surface of the APCs for the interaction with T cells by molecules known as major histocompatibility complex (MHC) (Roberts & Girardi, 2008). Indeed, conventional T cells are able to recognize only peptides in the context of MHC molecules (Tjadine *et al.*, 2004). There are two main classes of MHC molecules: MHC class I molecules and MHC class II molecules

(Janeway, 2011). MHC class I molecules are found on all nucleated cells and display peptides derived from proteins found in the cytoplasm to CD8<sup>+</sup> T cells. MHC class II molecules are found mainly on APCs and present peptides derived from proteins that were taken up by the APCs and which are presented to CD4<sup>+</sup> T cells (Janeway, 2011). The CD8 molecules expressed by CD8<sup>+</sup> T cells can bind MHC class I molecules and acts as co-receptor, whereas CD4 on helper CD4<sup>+</sup> T cells acts as co-receptor for the interaction with MHC class II molecules (Cano, 2013). Activated APCs can also secrete cytokines to influence the adaptive and the innate immune responses (Janeway, 2011). By presenting antigens to T cells and by releasing cytokines, innate APCs (DCs, macrophages) can form a bridge between the innate and the adaptive immune system (Janeway, 2011).

## **2.5. Innate-Like T Cells**

Besides the immune cells mentioned above, additional immune cells exist that share features with both of innate and adaptive immune cells (Walker *et al.*, 2013). These cells are also called innate-like lymphocytes (Walker *et al.*, 2013). Like the adaptive immune cells, innate-like lymphocytes express a BCR or TCR (Lanier, 2013). However, their rapid response following activation, e.g. the production of cytokines, is more reminiscent of innate immune cells (Walker *et al.*, 2013). The TCR of these innate-like lymphocytes, also called innate-like T cells, recognize MHC class I like molecules distinct than the one recognized by conventional CD4<sup>+</sup> and CD8<sup>+</sup> T cells (Lanier, 2013). The first and best studied innate-like T cell are invariant Natural Killer T (*i*NKT) cells that received their name due to their similarities with NK and T cells (Brennan *et al.*, 2013; Bendelac *et al.*, 2007).

## **2.6. Invariant Natural Killer T Cells**

Invariant natural killer T (*i*NKT, type I NKT) cells are a distinct subset of innate-like T cells that share features with  $\alpha\beta$  memory T cells and NK cells (Bendelac *et al.*, 2007). *i*NKT cells are characterized by three main features: (i) the expression of an

invariant TCR  $\alpha$ -chain, (ii) the recognition of the CD1d molecule, and (iii) the recognition of glycolipid antigens (Bendelac *et al.*, 2007).

### 2.6.1. The Expression of a Semi-Invariant TCR

Unlike the majority of  $\alpha\beta$  T cells,  $\mathbb{N}$ KT cells express  $\alpha\beta$  TCRs with an invariant  $\alpha$ -chain which pairs with a limited number of TCR  $\beta$ -chains (Park *et al.*, 2001). As strictly speaking only the  $\alpha$ -chain is invariant, their TCR is sometimes also referred to as 'semi-invariant' (Rossjohn *et al.*, 2012). In mice, the  $\alpha$ -chain is composed of V $\alpha$ 14–J $\alpha$ 18 (V $\alpha$ 14i, *Trav11–Traj18*) and pairs mostly with V $\beta$ 8.2 (*Trbv13-2*), V $\beta$ 2 (*Trbv1*), or V $\beta$ 7 (*Trbv29*) (Rossjohn *et al.*, 2012). In humans, the invariant TCR  $\alpha$ -chain consists of V $\alpha$ 24–J $\alpha$ 18 (V $\alpha$ 24i, *Trav10–Traj18*) and pairs mostly with V $\beta$ 11 (*Trbv25-1*) (Porcelli, 1993; Rossjohn *et al.*, 2012). The high sequence similarity of the  $\alpha$ -chains of human and mouse  $\mathbb{N}$ KT cells indicates that  $\mathbb{N}$ KT cells are evolutionarily highly conserved (Godfrey *et al.*, 2005). Besides the structural similarities between human and mouse  $\mathbb{N}$ KT cell TCRs, it has been shown that there is a significant cross-species reactivity (Kjer-Nielsen *et al.*, 2006). This means, that mouse  $\mathbb{N}$ KT cells are able to recognize antigens bound to human CD1d, and that human  $\mathbb{N}$ KT cells can interact with mouse CD1d (Kjer-Nielsen *et al.*, 2006). This remarkable cross-species reactivity of  $\mathbb{N}$ KT cells with CD1d molecule highlights that the immune specificity and function of  $\mathbb{N}$ KT cells are evolutionary conserved between the human and mice (Kjer-Nielsen *et al.*, 2006).

### 2.6.2. The Recognition of CD1d Molecules

In contrast to the classical  $\alpha\beta$  T cells that are restricted by MHC class I or II molecule,  $\mathbb{N}$ KT cells are restricted by the CD1d molecule (Bendelac *et al.*, 2007). The structure of CD1d molecule resembles MHC class I molecules. Like MHC class I molecules, CD1d molecules have a cleft between the ends of the two  $\alpha$ -helices that form a cavity to bind the antigens (Porcelli & Modlin, 1999). However, unlike the peptide binding cavity of MHC class I molecules, the CD1d molecules have a much deeper cavity, which allows them to bind hydrophobic ligands, such as lipids, glycosphingolipid, and glycolipids (Porcelli & Modlin, 1999). The semi-invariant TCR of  $\mathbb{N}$ KT cells



interacts with the CD1d/glycolipid antigen complex like a lock and a key (Porcelli & Modlin, 1999).

### 2.6.3. The Antigens of *i*NKT Cells

Classical  $\alpha\beta$  T cells react against peptide antigen, whereas *i*NKT cells recognize glycolipids (Kawano *et al.*, 1997). The best studied *i*NKT cell antigen is  $\alpha$ -galactosylceramide ( $\alpha$ GalCer) (**Figure 2**), the synthetic version of an antigen originally purified from the marine sponge *Agelas mauritanus* (Kobayashi *et al.*, 1995). However, it is more likely that the antigen was derived from *Sphingomonas* bacteria that were living with the marine sponge (Kinjo *et al.*, 2005).  $\alpha$ GalCer binds strongly to CD1d and activates *i*NKT cells in mice (Benlagha *et al.*, 2000; Matsuda *et al.*, 2000) and humans (Gumperz *et al.*, 2002; Lee *et al.*, 2002). Due to its great anti-tumour effects in mice,  $\alpha$ GalCer caught the attention of scientists from the very beginning (Morita *et al.*, 1995). To detect *i*NKT cells by flow cytometry, mouse CD1d/ $\alpha$ GalCer-tetramers were generated (Matsuda *et al.*, 2000; Benlagha *et al.*, 2000), which are the best experimental tool to identify *i*NKT cells.

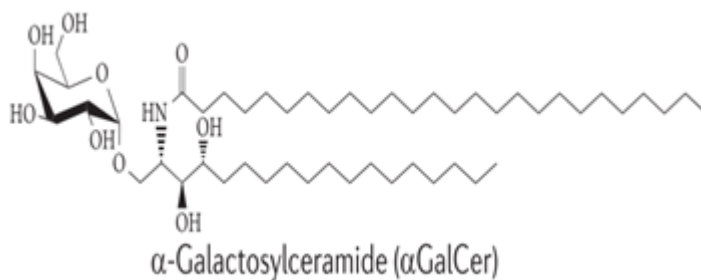


**Figure 2. The chemical structure of  $\alpha$ GalCer.** The figure shows the synthetic lipid structure of  $\alpha$ GalCer (Cohen *et al.*, 2009).

Natural lipid antigens for *i*NKT cells that can be found in a broad range of microorganisms. Activating glycosphingolipids for *i*NKT cells have been found in several bacteria, including *Sphingomonas paucimobilis* (Sriram *et al.*, 2005), *Sphingomonas capsulate*, (Mattner *et al.*, 2005), *Ehrlichia muris* (Mattner *et al.*, 2005), and *Streptococcus pneumonia* (Kinjo *et al.*, 2012), which is the most lethal bacterial

pathogen (O'Brien *et al.*, 2009).  $\mathbb{N}$ KT cells can also recognize diacylglycerol antigens from *Borrelia burgdorferi* (Kinjo *et al.*, 2006), the causative agent of Lyme disease (Orloski *et al.*, 2000), and cholesteryl  $\alpha$ -glucosides from *Helicobacter pylori* (Chang *et al.*, 2011 and Wieland Brown, *et al.*, 2013). Besides bacterial lipids, fungal glycosphingolipids from *Aspergillus fumigatus* have been reported to activate  $\mathbb{N}$ KT cells (Albacker *et al.*, 2013). Interestingly, this structural diversity implies an important role of  $\mathbb{N}$ KT cells in the recognition of a broad range of microbial antigens.

#### 2.6.4. The Effector Functions of $i\mathbb{N}$ KT Cells

$\mathbb{N}$ KT cells share functional similarities with NK and  $\alpha\beta$  T cells. Following TCR stimulation,  $\mathbb{N}$ KT cells rapidly display effector functions without the need of lengthy differentiation (Taniguchi *et al.*, 2003). Following the injection of  $\alpha$ GalCer into mice, activated  $\mathbb{N}$ KT cells undergo clonal expansion, with the peak of the expansion after three days (Crowe *et al.*, 2003).  $\mathbb{N}$ KT cells play an essential role in the immune response against glycolipid antigens (Taniguchi *et al.*, 2003). They display antigen specific cytotoxicity, similar to CTL cells, against target cells via the CD95/CD178 pathway (Wingender *et al.*, 2010). Furthermore,  $\mathbb{N}$ KT cells rapidly produce a wide range of functionally different cytokines and chemokines after activation due to their constitutive expression of mRNA for various cytokines, such as IFN $\gamma$  and IL-4 (Stetson *et al.*, 2003). Via these and other cytokines,  $\mathbb{N}$ KT cells can also connect the innate and the adaptive immune system (Kronenberg, 2005).

#### 2.6.5. The Basic Role of $i\mathbb{N}$ KT Cell in Different Diseases

$\mathbb{N}$ KT cells have been associated with many different diseases, including cancers, autoimmune disease, and allergic reactions (Godfrey & Kronenberg, 2004).  $\mathbb{N}$ KT cells can play advantageous or disadvantages roles under different conditions. They were shown to have antitumor effects in some cancer models (Kuni *et al.*, 2009; Yamasaki *et al.*, 2011), and can prevent allograft rejection, graft-versus-host disease and some autoimmune diseases (Godfrey & Kronenberg, 2004). For example,  $\mathbb{N}$ KT cells are low in numbers and are functionally impaired in mice with type 1 diabetes and

adoptive transfer of wild-type  $\mathbb{N}$ KT cells can ameliorate the disease in these mice (Mak & Saunders, 2006). Consequently,  $\mathbb{N}$ KT cells have great therapeutic potential (Godfrey & Kronenberg, 2004). However, besides these advantageous roles,  $\mathbb{N}$ KT cells can also be detrimental in other contexts. For example,  $\mathbb{N}$ KT cells can respond to lipid antigens in house dust (Wingender *et al.*, 2011) and pollen extracts (Agea *et al.*, 2005), which could lead to allergic reactions and airway hyperactivity in mouse models (Wingender *et al.*, 2011). In a similar way, it has been reported that  $\mathbb{N}$ KT cells can be activated by circulating lipid antigens and can promote cardiovascular disease (Braun *et al.*, 2010). The current theory to explain these divergent roles of  $\mathbb{N}$ KT cells suggests that functional different  $\mathbb{N}$ KT cell subsets exist and that their function determines the outcome.

#### 2.6.6. *The Subsets of $i\mathbb{N}$ KT Cells*

There are four  $\mathbb{N}$ KT cell subsets that develop in the thymus: NKT1, NKT2, NKT10, and NKT17 cells.  $\mathbb{N}$ KT cell subsets are characterized by transcription factors they express and the cytokines they produce (Lee *et al.*, 2013), as shown in **table 1**. These  $\mathbb{N}$ KT cell subsets are named after the CD4<sup>+</sup> T helper subsets they functionally resemble (Lee *et al.*, 2013). NKT1 cells express the transcription factors PLZF and T-bet and produce both IFN $\gamma$  and IL-4 following stimulation (Lee *et al.*, 2013). NKT2 cells express the transcription factor PLZF at high levels and secrete mainly IL-4 (Lee *et al.*, 2013). NKT17 cells express the transcription factors PLZF and ROR $\gamma$ t and secrete mainly IL-17 (Lee *et al.*, 2013). NKT1 cells, but not NKT2 or NKT17 cells, also express several NK cell receptors, like NK1.1 (Kim PJ *et al.*, 2006). The last subset that is found in the steady state is NKT10 cells. NKT10 cells are recently identified regulatory cells that can produce large amounts of the anti-inflammatory cytokine IL-10 (Sag *et al.*, 2014). It was shown that NKT10 cells expand *in vivo* after immunization of mice with  $\alpha$ GalCer and remain elevated for several months (Sag *et al.*, 2014).

**Table 1: The comparison of  $\text{iNKT}$  cell subsets.** The differences on their phenotype and functionality of  $\text{iNKT}$  cell subsets were compared.

Subset name					
	<b>NKT1 cells</b>	<b>NKT2 cells</b>	<b>NKT17 cells</b>	<b>NKT10 cells</b>	<b>NKT<sub>FH</sub> cells</b>
<b>Main transcription factor(s)</b>	Tbet <sup>high</sup> PLZF <sup>low</sup>	GATA3 <sup>high</sup> PLZF <sup>high</sup>	RORγt <sup>high</sup> PLZF <sup>int</sup>	Not known yet	Bcl6 <sup>+</sup>
<b>Surface marker(s)</b>	CD122 <sup>+</sup> NK1.1 <sup>+</sup>	IL17Rb <sup>+</sup>	CD196 <sup>+</sup> IL23R <sup>+</sup>	CD279 <sup>+</sup> (PD-1) CD152 <sup>+</sup> CD127 <sup>+</sup> CD304 <sup>+</sup> FR4 <sup>+</sup>	CD279 <sup>+</sup> (PD-1) CD185 <sup>+</sup> (CXCR5) CD127 <sup>negative</sup>
<b>Main cytokine(s) produced</b>	IFNγ TNF	IL-4 IL-13	IL-17A	IL-10	IL-21

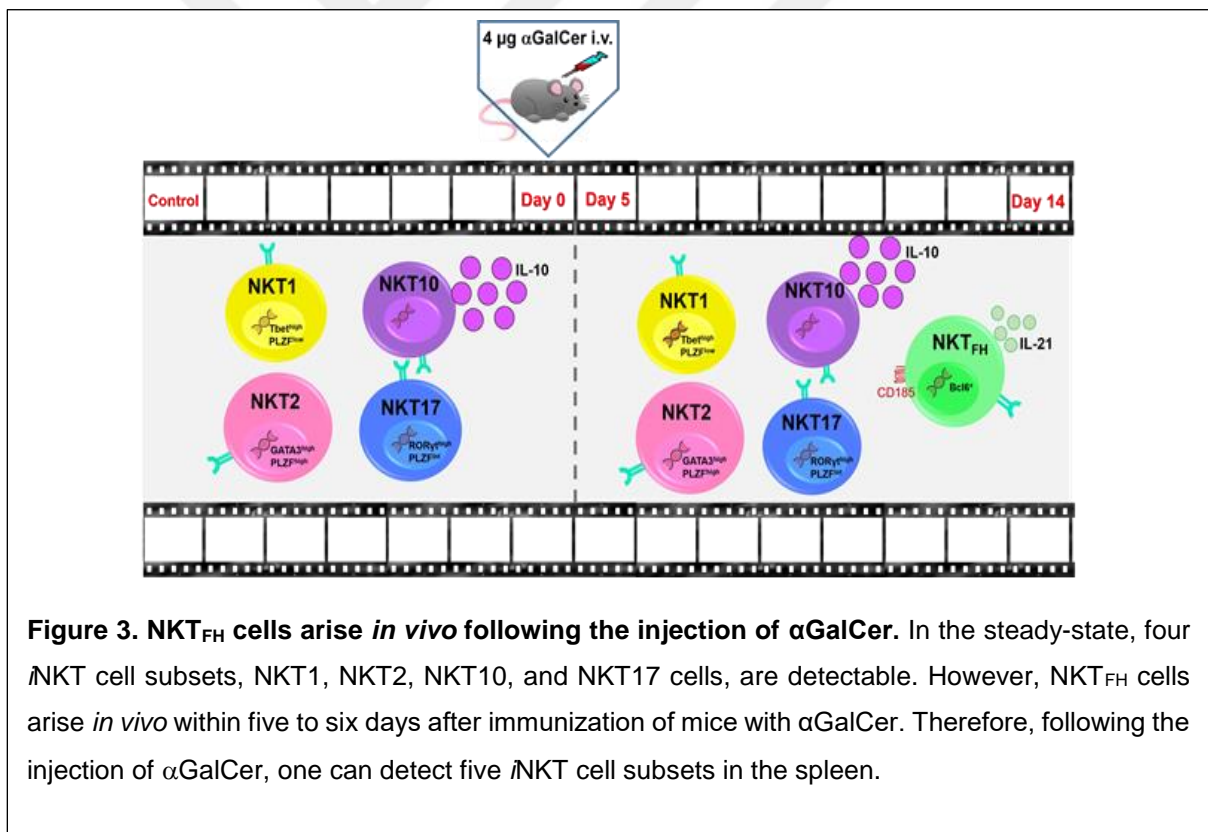
#### 2.6.7. NKT<sub>FH</sub> Cells

In addition to these four subsets of  $\text{iNKT}$  cells found in the thymus, another subset, called follicular helper  $\text{iNKT}$  (NKT<sub>FH</sub>) cells, can arise after stimulation with  $\alpha\text{GalCer}$  (Chang *et al.*, 2012). NKT<sub>FH</sub> cells are found in the germinal centre where they interact with and help GC B cells during the germinal centre reactions (Tonti *et al.*, 2012). NKT<sub>FH</sub> cells express the transcriptional factor Bcl6, which drives the expression of the surface markers CD185/CXCR5, CD278/ICOS, and CD279/PD-1 (Chang *et al.*, 2012). Furthermore, NKT<sub>FH</sub> cells can produce the cytokines IL-4 and IL-21 (Chang *et al.*, 2012). Therefore, NKT<sub>FH</sub> cells resemble phenotypically and functionally conventional T follicular helper (T<sub>FH</sub>) cells (Crotty, 2011). Additionally, NKT<sub>FH</sub> cells were reported to lack expression of the CD127 (Sag *et al.*, 2012).

Although, NKT<sub>FH</sub> cells are able to support antibody responses of B cells in germinal centres, they are not able, unlike T<sub>FH</sub> cells, to support the development of long-lived plasma cells (Vinuesa & Chang, 2013; Tonti *et al.*, 2012). Additionally, once

B cells are activated by NKT<sub>FH</sub> cells they rapidly secrete IgM and IgG antibodies (Barral *et al.*, 2008; Leadbetter *et al.*, 2008). NKT<sub>FH</sub> cells have been detected *in vivo* within three to six days after immunization with  $\alpha$ GalCer (Chang *et al.*, 2012). However, they are undetectable two to three weeks later (Sag *et al.*, 2014). In contrast, the percentage of NKT10 cells remains increased for more than four weeks (Sag *et al.*, 2014). Interestingly, similar to NKT<sub>FH</sub> cells, it has been shown that NKT10 cells can also express CD185 (Sag *et al.*, 2014). However, the relationship of NKT<sub>FH</sub> and NKT10 cells is currently unknown.

Due to the fact that they have advantageous and deleterious functions in the immune system, it is very important to understand the competencies and plasticity of different  $\alpha$ NKT cell subsets to target them safely in immunotherapies.



### **3. MATERIALS AND METHODS**

#### **3.1. Type of The Research:**

Experimental study.

#### **3.2. Location and the time frame of the research:**

All experiments were performed at the Izmir Biomedicine and Genome Center, between 2017 and 2020.

#### **3.3. Research population, sampling and experimental groups:**

Not applicable.

#### **3.4. Research Materials:**

Different organs were obtained from C57BL/6, BALB/c, and Bcl6<sup>-/-</sup> mice, which were housed in IBG's vivarium (May 2018 - February 2020). The CD1d/ $\alpha$ GalCer-tetramers (labelled with BV421 or PE) were kindly provided by the NIH Tetramer Core Facility (Emory University, Atlanta, GA, USA). All other reagents, including chemicals, kits, antibodies, and consumables, were obtained from commercial sources as outlined below.

#### **3.5. Research Variables:**

Variables of our study are cell frequencies and the expression of surface markers, cytokines, and transcription factors.

### **3.6. Data Collection Tools:**

#### **3.6.1. Laboratory Materials**

##### *3.6.1.1. General Laboratory Equipment*

- Autoclave (Systec, VX-150, 166L, SN:8373)
- Biological safety cabinet (ThermoFisher Scientific, class II type A2- SN:41806507)
- Cell analyser, LSR FortessaX20 (BD Biosciences, # 647780S1, SN:H647780S1001, model no:N/A)
- Cell sorter, FACSAria III (BD Biosciences)
- Centrifuge (IKA, model: mini G, SN: 100046858)
- Centrifuge 5702 (Eppendorf, SKU: Z606936EU, SN: 5702DR5336846)
- Centrifuge microCL 17R (ThermoFisher Scientific, # 75002455, SN: 41793777)
- CO<sub>2</sub> incubator (MEMMERT, INCOmed 246 0°C/+50°C, SN: 0215-0125)
- Freezer, -20°C (Bosch, 161x70 cm, SN: GSN51AW30)
- Ice maker (HOSHIZAKI, model number: FM-300AKE-N, SN:E11212)
- Magnet, EasySep – immunomagnetic column-free magnet (StemCell Technologies, #18000)
- Microscope, inverted (Carl Zeiss, model: Axio Vert.A1, SN: 3849001095)
- Pipette pump, electrical (Isolab, 0.1-200 ml, # 010.01.006)
- Pipette stand, carrousel (GILSON, SKU: F161401)
- Pipette, multi-, pipet-lite L8 -200XLS+ (Rainin, # 17013805)
- Pipette, single channel, PIPETMAN classic P2 (GILSON, SKU: F144801)
- Pipette, single channel, PIPETMAN G starter kit, P20G, P200G, P1000G (GILSON, SKU: F167900)

- Refrigerator, +4°C (Bosch, model: KSV36AI31/09)
- Thermal cycler, SimpliAmp (ThermoFisher Scientific, # A24811, SN: 228002716)
- Vortex (ThermoFisher Scientific, LP vortex mixer, SN: EAKT18071, # 88880018)
- Water bath (Nüve laboratory & sterilization technology, model no: NB 9, SN: 02-2531)
- Water purification system (ThermoFisher Scientific, model: Smart2Pure 3 UV/UF, SN:41531232)

#### 3.6.1.2. *Vivarium Laboratory Equipment*

- Anaesthesia machine (E-Z systems, model: classic, # EZ-150C)
- Biological safety cabinet (LABGARD, class II, model no: NU-S677-400E, SN:182313100617)
- Charcoal filter canister (E-Z systems, ReFresh, # EZ-258)
- Forceps (graefe), 10.16 cm long serrated slight curve 0.8 mm tip (ROBOZ, # RS-5135)
- Forceps (semken), 1x2 teeth; 1.6 mm tip width; 15.24 cm length (ROBOZ, # RS-5248)
- Induction chamber (E-Z systems, sure-seal mouse chamber 10.16 cm long x 10.16 cm width x 10.16 cm height, # EZ-177)
- Scissors (delicate operating), 12.065 cm straight sharp/sharp (ROBOZ, # RS-6702)
- Scissors (light operating), 12.7 cm curved sharp/sharp (ROBOZ, # RS-6753)
- Scissors (operating), straight; sharp-blunt; 15.24 cm length (ROBOZ, # RS-6818)



### 3.6.1.3. Consumables

- Parafilm: Wrap, 4" Wide; 125 Ft/Roll (#PM-996)
- Gloves, examination (Small, Medium, Large): MyGlove (Labmarker Dis Ticaret Ltd. Sti., #9604 0203)
- Aluminium foil, 30m, (Migros)
- Tube, 50mL (polypropylene): canonical bottom, (Greiner Bio-One, #227261; Sarstedt, #62.547.254; Orange Scientific, #4440100N)
- Tube, 15mL (polypropylene): canonical bottom (Greiner Bio-One, #188271)
- Tube, 5mL (polypropylene): round bottom (Stem Cell Technologies, #352063)
- Pasteur pipette, glass, 225mm (ISOLAB, #084.01.002)
- Pasteur pipette, polyethylene, 3mL, non-sterilized (ISOLAB, #084.02.001)
- Syringe, single use with needle, 5mL (Genject)
- Filter syringe, 33mm x 0.22µm, (CHROMFILTER, #S33-CA22-S)
- Reservoirs, reagent – disposable, 55mL, non-sterilized (ISOLAB, #006.03.055)
- Microplate, 96-well F- bottom (Greiner Bio-One, #655081)
- Petri dish, 10 cm (ISOLAB, #081.01.100)
- Petri dish, 5 cm (ISOLAB, #081.01.060)
- Multi-well plate, cell culture 96 well (Greiner Bio-One, #655180)
- Cell culture multi-well plate, 48 well (Greiner Bio-One, #677180)
- Cell culture multi-well plate, 24 well (Greiner Bio-One, #662160)
- Cell culture multi-well plate, 6 well (Greiner Bio-One, #657160)
- Flask, cell culture, 250mL (Greiner Bio-One, #658175)
- Flask, cell culture, 50mL (Greiner Bio-One, #690175)
- Reaction tube, 2mL with attached cap (Greiner Bio-One, #623201)

- Reaction tube, 1.5mL with attached cap (Greiner Bio-One, #616201)
- Reaction tube, 0.5mL with attached cap (Greiner Bio-One, #667201)
- Pipet tips, 1mL (Rainin, #17001977)
- Pipet tips, 250mL, LTS for multichannel (Raining, #17000506)
- Pipet tips, 200mL (Corning Inc., #4845)
- Pipet tips, 10mL (Rainin, #17004280)
- Pipettes, serological, 25mL, sterile (Greiner Bio-One, #760180; SPL Lifesciences, #91025)
- Pipettes, serological, 10mL, sterile (Greiner Bio-One, #607180; SPL Lifesciences, #91010)
- Pipettes, serological, 5mL, sterile (Greiner Bio-One; #606180; SPL Lifesciences, #91005)

#### 3.6.1.4. *Chemicals, Reagents, And Commercial Kits*

- 2-Mercaptoethanol (HSCH<sub>2</sub>CH<sub>2</sub>OH, sigma, #M6250-1L, [55 μM], stored at 4°C)
- CytoFix/Perm (BD Biosciences, #554722, stored at 4°C)
- Dynabeads mouse pan B (B220) (ThermoFisher Scientific, #11441D)
- Ethanol Technical Grade (Interlab, #TK.200650.05001)
- Fetal bovine serum (FBS, Biochrome, #s0115, heat inactivated, stored at -20°C)
- GolgiPlug (BD Biosciences, #555029, brefeldin A [1 mg/ml] in DMSO, stored at 4°C)
- GolgiStop (BD Biosciences, #554724, monensin [2 mg/ml] in EtOH, stored at 4°C)
- Ionomycin (C<sub>41</sub>H<sub>72</sub>O<sub>9</sub>, Sigma, #I9657-1MG, [1 mg/mL] in DMSO, stored at -20°C)

- L-Glutamine 100X (ThermoFisher Scientific, #25030081, [200 mM] stored at –20°C)
- Lymphoprep (StemCell Technologies, #07801, stored at 4°C)
- PE positive selection kit II, EasySep™ mouse (StemCell Technologies, #18554)
- Penicillin-streptomycin (10,000 units/mL penicillin and 10,000 µg/mL of streptomycin in 0.85% saline, ThermoFisher Scientific, #15140122, stored at –20°C)
- Percoll plus 1L GE healthcare (Sigma, #17-5445-01, stored at RT)
- Phorbol 12-myristate 13-acetate (PMA, C<sub>36</sub>H<sub>56</sub>O<sub>8</sub>, Sigma, #P8139-1MG, [1 mg/mL] in DMSO, stored at –20°C)
- Phosphate buffered saline (10X PBS, ThermoFisher Scientific, # 70011036, stored at 4°C)
- Phosphate buffered saline (PBS, ThermoFisher Scientific, #10010023, stored at 4°C)
- RPMI 1640 without L-Glutamine (ThermoFisher Scientific, #42401018, stored at 4°C)
- Sodium azide (NaN<sub>3</sub>, Sigma, #S2002-500G, stored at RT)
- Transcription factor buffer set (BD Biosciences, #562574, stored at 4°C)
- α-Galactosylceramide (αGalCer, C<sub>50</sub>H<sub>99</sub>NO<sub>9</sub>, Avanti Polar Lipids, #867000P, [1 mg/mL] in DMSO, stored at -20°C)

### 3.6.1.5. Antibodies for Flow Cytometry

**Table 2: Antibodies used in the study**

Specificity	Clone	Species	Isotype	Conjugate	Ordering number	Company
<b>Bcl-6</b>	K112-91	Mouse	IgG1, κ	APC-Cy7	563581	BD Biosciences
<b>Bcl-6</b>	7D1	Rat	IgG2a, κ	PE-Dazzle 594	358510	BioLegend
<b>CD127</b>	A7R34	Rat	IgG2a, κ	APC-eF780	47-1271-82	eBioscience
<b>CD127</b>	A7R34	Rat	IgG2a, κ	BV510	135033	BioLegend
<b>CD127</b>	A7R34	Rat	IgG2a, κ	BV605	135041	BioLegend
<b>CD127</b>	A7R34	Rat	IgG2a, κ	BV650	135043	BioLegend
<b>CD16/32</b>	2.4G2	Rat	IgG2b	Purified	70-0161-M001	Tonbo Bioscience
<b>CD19</b>	MB19-1	Mouse	IgA, κ	APC	17-0191-82	ThermoFisher Scientific
<b>CD19</b>	1D3	Rat	IgG2a, κ	Biotin	30-0193-U500	Tonbo Biosciences
<b>CD19</b>	6D5	Rat	IgG2a, κ	BV510	115546	BioLegend
<b>CD19</b>	6D5	Rat	IgG2a, κ	BV570	115535	BioLegend
<b>CD19</b>	MB19-1	Mouse	IgA, κ	PE	12-0191-82	ThermoFisher Scientific
<b>CD19</b>	6D5	Rat	IgG2a, κ	PE-Cy5	115510	BioLegend
<b>CD19</b>	6D5	Rat	IgG2a, κ	Pacific Blue	115523	BioLegend
<b>CD19</b>	1D3	Rat	IgG2a, κ	PerCP-Cy5.5	65-0193-U100	Tonbo Biosciences
<b>CD196 / CCR6</b>	29-2L17	Armenian hamster	IgG	BV605	129819	BioLegend
<b>CD1d</b>	1B1	Rat	IgG2b, κ	PE	123510	BioLegend
<b>CD1d</b>	1B1	Rat	IgG2b, κ	Purified	559438	BD Biosciences

<b>CD278 (ICOS)</b>	C398.4A	Armenian hamster	IgG	PerCP-Cy5.5	313518	BioLegend
<b>CD278 (ICOS)</b>	15F9	Armenian hamster	IgG	PE	12-9940-81	ThermoFisher Scientific
<b>CD278 (ICOS)</b>	15F9	Syrian hamster	IgG	PerCP-eF710	46-9940-82	eBioscience
<b>CD3ε</b>	145.2C11	Armenian hamster	IgG1, κ	APC	20-0031-U100	Tonbo Biosciences
<b>CD3ε</b>	145-2C11	Armenian hamster	IgG1, κ	BUV395	563565	BD Biosciences
<b>CD3ε</b>	145-2C11	Armenian hamster	IgG1, κ	PE-Cy5	100310	BioLegend
<b>CD3ε</b>	145-2C11	Armenian hamster	IgG1, κ	PE-eFluor610	61-0031-82	ThermoFisher Scientific
<b>CD3ε</b>	145-2C11	Armenian hamster	IgG1, κ	PerCP-Cy5.5	45-0031-82	ThermoFisher Scientific
<b>CD3ε</b>	17A2	Rat	IgG2b, κ	Purified	70-0032-U500	Tonbo Biosciences
<b>CD4</b>	RM4-5	Rat	IgG2a, κ	AF647	100530	BioLegend
<b>CD4</b>	RM4-5	Rat	IgG2a, κ	AF700	100536	BioLegend
<b>CD4</b>	RM4-5	Rat	IgG2a, κ	APC	17-0042-81	ThermoFisher Scientific
<b>CD4</b>	RM4-5	Rat	IgG2a, κ	eVolve605	83-0042-42	eBioscience
<b>CD4</b>	RM4-5	Rat	IgG2a, κ	PE	100512	BioLegend
<b>CD4</b>	RM4-5	Rat	IgG2a, κ	BV570	100542	BioLegend
<b>CD4</b>	RM4-5	Rat	IgG2a, κ	BV605	563151	BD Biosciences
<b>CD4</b>	GK1.5	Rat	IgG2b, κ	Pacific Blue	100428	BioLegend
<b>CD44</b>	IM7	Rat	IgG2b, κ	APC	17-0441-82	ThermoFisher Scientific
<b>CD44</b>	IM7	Rat	IgG2b, κ	PE	12-0441-83	ThermoFisher Scientific
<b>CD44</b>	IM7	Rat	IgG2b, κ	V500	560780	BD Biosciences

<b>CD45.1</b>	A20	Mouse	IgG2a, κ	AF700	110724	BioLegend
<b>CD45.1</b>	A20	Mouse	IgG2a, κ	BV785	110743	BioLegend
<b>CD8α</b>	53-6.7	Rat	IgG2a, κ	APC-eF780	47-0081-82	ThermoFisher Scientific
<b>CD8α</b>	53-6.7	Rat	IgG2a, κ	BV570	100740	BioLegend
<b>CD8α</b>	53-6.7	Rat	IgG2a, κ	BV650	100741	BioLegend
<b>CD8α</b>	53-6.7	Rat	IgG2a, κ	eFluor 450	48-0081-80	eBioscience
<b>CD8α</b>	53-6.7	Rat	IgG2a, κ	eVolve655	86-0081-42	ThermoFisher Scientific
<b>CD8α</b>	53-6.7	Rat	IgG2a, κ	PE-Cy5	100710	BioLegend
<b>CD8α</b>	53-6.7	Rat	IgG2a, κ	PE-Cy7	25-0081-82	ThermoFisher Scientific
<b>CD8α</b>	53-6.7	Rat	IgG2a, κ	PerCP-Cy5.5	100734	BioLegend
<b>CD8α</b>	53-6.7	Rat	IgG2a, κ	PerCP-eF710	46-0081-82	ThermoFisher Scientific
<b>CD8α</b>	53-6.7	Rat	IgG2a, κ	Biotin	30-0081-U500	Tonbo Biosciences
<b>CD8α</b>	53-6.7	Rat	IgG2a, κ	BV711	100748	BioLegend
<b>CD8β</b>	eBioH35-17.2	Rat	IgG2b, κ	FITC	11-0083-85	ThermoFisher Scientific
<b>CD8β</b>	eBioH35-17.2	Rat	IgG2b, κ	PE	12-0083-81	ThermoFisher Scientific
<b>FoxP3</b>	FJK-16s	Rat	IgG2a, κ	AF700	56-5773-82	ThermoFisher Scientific
<b>FoxP3</b>	FJK-16s	Rat	IgG2a, κ	eF660	50-5773-82	eBioscience
<b>GATA3</b>	L50-823	Mouse	IgG1, κ	BV711	565449	BD Biosciences
<b>GATA3</b>	L50-823	Mouse	IgG1, κ	PE-Cy7	560405	BD Biosciences
<b>GL7</b>	GL7	Rat	IgM, κ	AF488	144612	BioLegend
<b>IFNγ</b>	XMG1.2	Rat	IgG1, κ	BV650	505831	BioLegend

<b>IFN<math>\gamma</math></b>	XMG1.2	Rat	IgG1, $\kappa$	BV785	505838	BioLegend
<b>IFN<math>\gamma</math></b>	XMG1.2	Rat	IgG1, $\kappa$	APC	20-7311-U100	Tonbo Biosciences
<b>IL-10</b>	JES5-16E3	Rat	IgG2b, $\kappa$	APC	505010	BioLegend
<b>IL-10</b>	JES5-16E3	Rat	IgG2b, $\kappa$	PE-Dazzle 594	505034	BioLegend
<b>IL-12/IL-23 p40</b>	C17.8	Rat	IgG2a, $\kappa$	Purified	40-7123-U500	Tonbo Biosciences
<b>Nur77</b>	12.14	Mouse	IgG1, $\kappa$	AF488	4347883	ThermoFisher Scientific
<b>Nur77</b>	12,14	Mouse	IgG1, $\kappa$	PE	12-5965-80	ThermoFisher Scientific
<b>PLZF</b>	9E12	Armenian hamster	IgG	PE	145804	BioLegend
<b>PLZF</b>	9E12	Armenian hamster	IgG	PE-Cy7	145806	BioLegend
<b>Slamf6 / Ly108</b>	330-AJ	Mouse	IgG2a, $\kappa$	APC	134608	BioLegend
<b>Slamf6 / Ly108</b>	330-AJ	Mouse	IgG2a, $\kappa$	Pacific Blue	681304	BioLegend
<b>Tbet</b>	4B10	Mouse	IgG1, $\kappa$	AF647	644804	BioLegend
<b>Tbet</b>	O4-46	Mouse	IgG1, $\kappa$	BV786	564141	BD Biosciences
<b>Tbet</b>	O4-46	Mouse	IgG1, $\kappa$	AF488	561266	BD Biosciences
<b>TCR<math>\beta</math></b>	H57-597	Armenian hamster	IgG	FITC	109206	BioLegend
<b>TCR<math>\beta</math></b>	H57-597	Armenian hamster	IgG	PE	12-5961-83	eBioscience
<b>TCR<math>\beta</math></b>	H57-597	Armenian hamster	IgG	Purified	70-5961-U100	Tonbo Biosciences
<b>TCR<math>\beta</math></b>	H57-597	Armenian hamster	IgG	AF700	109224	BioLegend
<b>TCR<math>\beta</math></b>	H57-597	Armenian hamster	IgG	PerCP-Cy5.5	65-5961-U100	Tonbo Biosciences
<b>TCR <math>\gamma/\delta</math></b>	eBioGL3	Armenian hamster	IgG	FITC	11-5711-82	eBioscience

<b>TCR <math>\gamma/\delta</math></b>	UC7-13D5	Armenian hamster	IgG	FITC	11-5811-85	ThermoFisher Scientific
<b>TNF</b>	MP6-XT22	Rat	IgG1, $\kappa$	FITC	554418	BD Biosciences
<b>TNF</b>	MP6-XT22	Rat	IgG1, $\kappa$	BV711	506349	BioLegend

### 3.6.1.6. Other Reagents for Staining

**Table 3: Other reagents for staining**

<b>Clone</b>	<b>Species</b>	<b>Isotype</b>	<b>Conjugate</b>	<b>Ordering number</b>	<b>Company</b>
Polyclonal	Rat	IgG	Unconjugated	012-000-003	Jackson ImmunoResearch
Polyclonal	Mouse	IgG	Unconjugated	015-000-003	Jackson ImmunoResearch

### 3.6.1.7. Other Fluorescent Reagents for Flow Cytometry

**Table 4: Other fluorescent reagents for flow cytometry**

<b>Specificity</b>	<b>Clone</b>	<b>Species</b>	<b>Isotype</b>	<b>Conjugate</b>	<b>Ordering Number</b>	<b>Company</b>
N/A	N/A	N/A	N/A	Live/Dead-Blue	13-0868-T100	Tonbo Biosciences
CD1d-tetramer	N/A	Mouse	N/A	BV421	N/A	NIH tetramer core facility
CD1d-tetramer	N/A	Mouse	N/A	PE	N/A	NIH tetramer core facility



## 3.6.2. Methods

### 3.6.2.1. Animal Handling and Experimentation

#### 3.6.2.1.1. Mouse Handling

To perform *in vivo* experiments and to collect mouse organs for the subsequent purification of immune cells, the proper handling of mice is essential.

#### **Materials:**

- Polycarbonate cage, with wire lid and drinking bottle

#### **Solutions:**

- 70% ethanol

#### **Method:**

The surface of the mouse cage was sterilized with 70% ethanol, then placed inside of the laminar flow of the procedure room. To open the cage, the lid and the drinking bottle were removed. The mouse was lifted out of its cage by gently holding the tail.

#### 3.6.2.1.2. Mouse Anaesthesia

Mice are anesthetized to limit the pain and stress of the animals during procedures. The lack of resistance from the mice makes the procedures also technically easier for the researchers.

#### **Materials:**

- Anaesthesia machine: induction chamber, precision vaporizer, a waste gas-scavenging unit, isoflurane as liquid anaesthetic

#### **Method:**

The mouse was placed into the induction chamber of the anaesthesia machine and the lid of the chamber was latched to prevent gas leakage. The oxygen flow and then the precision vaporizer of the anaesthesia machine were turned on. The flow of

isoflurane was set to 3 - 4 L/min. After the mouse fell asleep, the lid of the induction chamber was opened and the mouse was taken out. Sufficient depth of the anaesthesia was verified by a lack of reflexes following toe pinch.

### 3.6.2.1.3. *Mouse Injection Methods*

#### *i. Intraperitoneal (i.p.) injection of mice*

Intraperitoneal (i.p.) injection is a common technique for the administration of substance into mice. In contrast to intravenous injection, i.p. injection is faster, does not require anaesthesia, and allows the injection of larger volume.

#### **Materials:**

- 1 ml/cc insulin syringe with 26Gx 12.7 mm needle
- Anaesthesia machine: induction chamber, precision vaporizer, a waste gas-scavenging unit, isoflurane as liquid anaesthetic

#### **Solutions:**

- PBS
- 70% ethanol

#### **Method:**

The cells or reagent to be injected were diluted in 200 µl PBS per mouse and drawn into the syringe. The syringe was held with the needle upwards, air bubbles stuck inside the syringe were collected at the top by gently hitting the syringe with the index finger and removed from the syringe. The mouse was held by the tail with the preferred hand for the injection and placed on the wire grid of the cage. With the thumb and index finger of the free hand, the skin of the mouse's neck was gripped tightly. A sufficient tight grip was indicated by a lack of head movement by the mouse. The tail of the mouse was immobilized between the little finger and the palm of the same hand holding the mouse. The needle was placed into the right lower quadrant of the

abdomen as shown in **figure 4**, kept away from the liver and abdominal midline. The needle was inserted through the skin into the intraperitoneal space, avoiding abdominal organs. Light negative pressure was induced in the needle by pulling the plunger of the syringe for approximately 10 units to verify that no tissue was damaged, which would be indicated e.g. by blood aspiration. When the plunger moved back on its own, due to the lower pressure, then the injection was done with a speed of approx. 200  $\mu$ l/2 seconds. The mouse was placed back into the cage and monitored for about five minutes for any signs of distress.



**Figure 4.** The location for the i.p. injections: The red X at the lower right side of the mouse indicates the location for the intraperitoneal (i.p.) injection.

ii. *Intravenous (i.v.) injection of mice via the retro-orbital route*

Intravenous (i.v.) injection via the retro-orbital route refers to the injection of non-irritating substances directly into the ophthalmic venous sinus of the mouse, located behind the eye. This retro-orbital route requires anaesthesia, but is easier to perform than tail-vein injections and minimizes the distress of the mice.

**Materials:**

- Anaesthesia machine: induction chamber, precision vaporizer, a waste gas-scavenging unit, isoflurane as liquid anaesthetic

- 1 ml/cc insulin syringe with 26Gx 12.7 mm needle

**Solutions:**

- PBS

**Method:**

The cells or reagent to be injected were resuspended in at most 200 µl PBS per mouse and drawn into the syringe. The syringe was held vertically with the needle upwards by the right hand. Air bubbles stuck inside the syringe were collected at the top by gently hitting the syringe with the index finger and pushed out of syringe. The anesthetized mouse was placed onto a solid surface for the procedure. For injections into the right eye, the mouse was laid on its left side with the mouse's head pointing to the right. The palm of left hand was placed on the mouse's body. Using the thumb and index finger of the left hand, the skin around the right eye of the mouse was pulled downwards to bulge the mouse's right eyeball out from the eye socket to expose the eye for the injection. The needle was placed into the medial canthus of the mouse, positioned at an angle of approximately 30°, and inserted behind the eyeball. Overcoming an initial slight resistance indicated entry into the tissue. The solution (max. 200 µl) was then slowly injected into the retro-orbital sinus. The needle was removed and the mouse was placed back into the cage and monitored for approximately five minutes for any signs of distress.

**3.6.2.1.4. Mouse Euthanasia by Cervical Dislocation**

Cervical dislocation is the preferred method for mouse euthanasia, as it is fast, minimizes the pain for the animal, and avoids chemical contamination of the tissue, as it might occur with the use of chemical euthanasia.

**Materials:**

- Scissors (operating), straight; sharp-blunt; 15.24 cm length

**Method:**

The mouse was held by the tail and placed on the wire grid of the cage. Scissors were placed on its neck, behind of the ears, with enough pressure to prevent movement. Then, the tail was pulled while keeping pressure on the neck with the scissors to dislocate the cervical vertebrae. Death was verified by a lack of reflexes following toe pinch.

**3.6.2.1.5. Recovery of Mouse Organs**

To analyse and study immune cells, the organs of interest need to be removed from the animals to allow the purification of cells.

**Materials:**

- Forceps (graefe), 10.16 cm long serrated slight curve 0.8 mm tip
- Forceps (semken), 1x2 teeth; 1.6 mm tip width; 15.24 cm length
- Scissors (delicate operating), 12.07 cm straight sharp/sharp
- Scissors (light operating), 12.7 cm curved sharp/sharp
- Scissors (operating), straight; sharp-blunt; 15.24 cm length
- 15 ml Falcon tubes

**Solutions:**

- PBS
- 70% ethanol
- P2X7 receptor inhibitor A-804598 (Selleckchem) [10  $\mu$ M]

**Method:**

- *Spleen:* The sacrificed mouse was placed on its right side on a clean paper. The fur was sterilized with 70% ethanol in order to prevent contamination. An incision was made perpendicular to the body axis below the rib cage. The skin around of the incision was pulled to opposite directions with both hands to

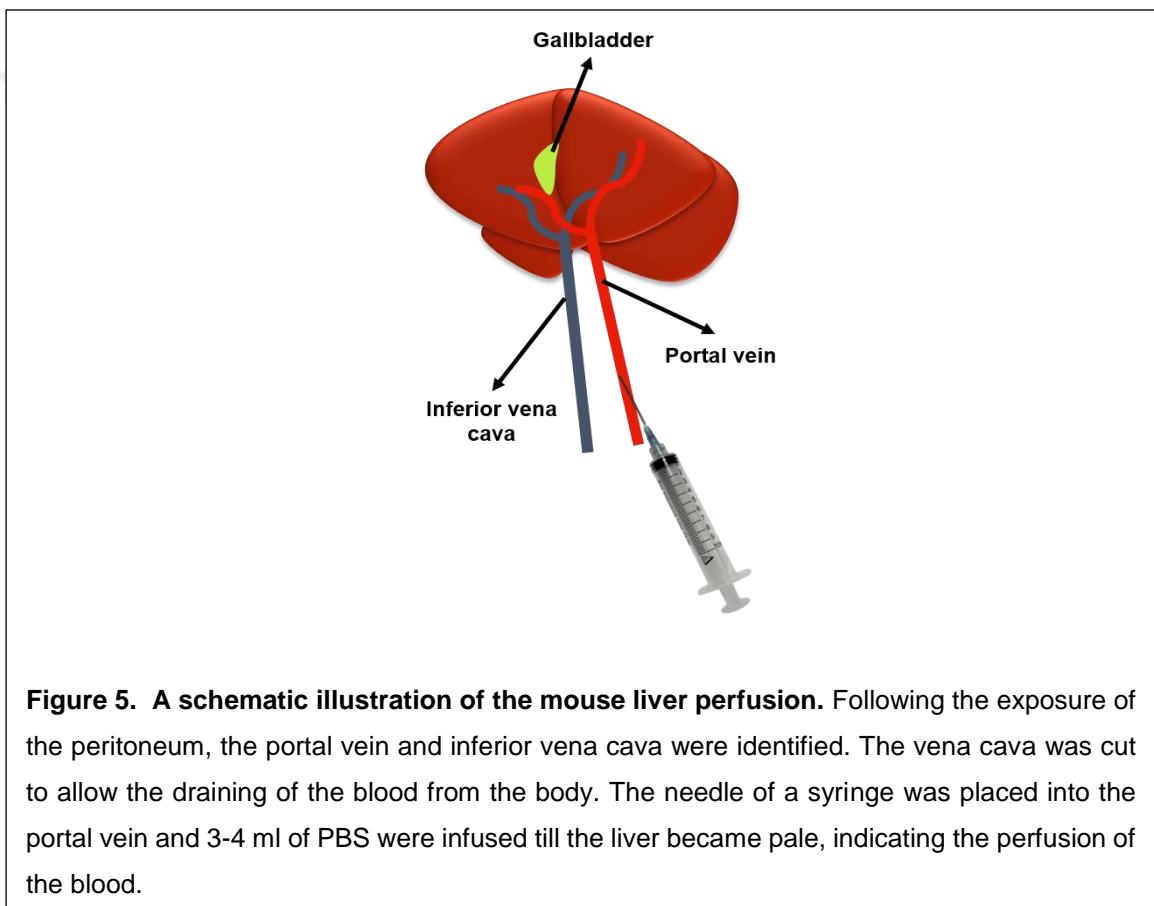
expose the peritoneum. Another incision was made in the peritoneal wall above the spleen. The spleen is a red-elongated organ that is found near the greater curvature stomach under the omentum and is usually visible through the peritoneal wall. The spleen was lifted with curved graefe forceps out of the peritoneum and detached from the body by cutting the connecting tissue with a pair of scissors. The spleen was placed into a 15 ml falcon tube containing approximately 5 ml PBS.

- *Thymus*: The sacrificed mouse was placed on its back on a clean paper. The fur was sterilized with 70% ethanol in order to prevent contamination. An incision was made perpendicular to the body axis below the rib cage. The skin around the incision was pulled to opposite directions with both hands to expose the peritoneum. The lower tip of the sternum was held with forceps and the ribs were cut left and right along the sternum to the top of the rib cage. The ribs were lifted to lateral sides to expose the lungs. The thymus is a white-coloured bi-lobed organ located behind the heart in the anterior superior thorax. With curved graefe forceps, the lobes of the thymus were grasped and removed from the body by cutting the connecting tissue with a pair of scissors. The thymus was placed into a 15 ml falcon tube containing approximately 5 ml PBS.
- *Lymph nodes*: The sacrificed mouse was put on its back on a clean paper. Following the sterilization of the fur with 70% ethanol to prevent contamination, a midline incision was made. The skin was detached from the peritoneal wall using iris scissors. Then, the incision was extended to the neck and the arms with the scissors. The skin was gently pulled to opposite directions with both hands to expose the peritoneum. The inguinal lymph nodes can be found on top of the subcutaneous white adipose tissue, which is attached to the skin, with one lymph nodes on each side of the mouse. The tissue on top of the lymph nodes was ripped apart with two curved forceps. The tissue under the inguinal lymph nodes is then grasped with curved forceps and the lymph nodes is removed by lifting it up with the forceps. The axillary nodes are found in the armpits of the mice, near the triceps area. The tissue under the axillary lymph nodes is then grasped with curved forceps and the lymph nodes is removed by lifting it up with

the forceps. The lymph nodes were placed into a 15 ml falcon tube containing 5 ml of PBS.

- *Lungs*: The sacrificed mouse was placed on a clean paper, and the fur was sterilized with 70% ethanol. An incision was made near midline perpendicular to the body axis below the rib cage. The skin around the incision was pulled to opposite directions with both hands to expose the peritoneum. The lower tip of the sternum was held with forceps and the ribs were cut left and right along the sternum to the top of the rib cage. The ribs were lifted to lateral sides to expose the lungs. The lungs are a large white-pink coloured organ, with five lobes on the right and one lobe on the left side of the mouse. The lobes of the lungs were held with forceps, slightly lifted so that the connective tissue underneath could be cut with scissors. The removed lungs were placed into a 15 ml falcon tube containing 10  $\mu$ M of the P2X7 receptor inhibitor A-804598 in 5 ml of PBS.
- *Bone marrow*: The sacrificed mouse was placed on a clean paper. Following the sterilization of the fur with 70% ethanol, an incision was made to above the hip. The incision was extended until the ankle joint and the skin was pulled back to expose the femur. The fat and muscles around the femur were held with forceps and trimmed off with scissors in order to clean the femur from the extra tissues. Then, the bones were cut off near the joints without cutting the bone marrows.
- *Liver*: The sacrificed mouse was placed on a clean paper. The forelegs were fixed upward side and the hind legs were fixed downward side of the mouse with the needles. Following the sterilization of the fur with 70% ethanol, an incision was made perpendicular to the body axis. The skin around the incision was pulled to opposite directions with both hands to expose the peritoneum. Another incision was made in the peritoneal wall with scissors in order to expose the liver. The liver is a large, red-brownish coloured organ, with three large lobes that places on the right side of the body of the mouse. The inferior vena cava under the liver was identified, which is located next to the portal vein as illustrated in **figure 5**, and cut to allow the draining of the blood. The portal vein, which is thick and dark red coloured vessel found on the bottom of the

liver connecting it with the intestine, was identified. A 25 gauge needle, attached to a 5 ml syringe containing PBS, was inserted into the portal vein and with 3-4 ml of PBS injected into the portal vein the blood from the liver was perfused. Following the injection of PBS, the liver will become pale. The gallbladder, which is green-yellow coloured bladder located within the liver lobes, were held with forceps and removed with scissors. The lobes of the liver were held with forceps, slightly lifted so that the connective tissue underneath could be cut with scissors. The removed livers were placed into a 50 ml falcon tube containing approximately 10 ml of PBS.



- *Adipose tissues:* The sacrificed mouse was put on its back on a clean paper. Following the sterilization of the fur with 70% ethanol to prevent contamination, a midline incision was made. The skin was detached from the peritoneal wall using iris scissors. Then, the incision was extended to the neck and the arms with the scissors. The skin was gently pulled to opposite directions with both hands to expose the peritoneum. The subcutaneous white adipose tissue



(scWAT) is attached to the skin with one lobe on each side of the mouse. The inguinal lymph nodes are on top of the scWAT. Thus, the inguinal lymph nodes were first removed with two curved forceps. Then, the scWAT was slightly lifted with forceps and removed from the underlying skin with a scissor. To reach the visceral white adipose tissue (vWAT) another incision was made in the peritoneal wall with scissors. The vWAT is found on top of the internal organs in the abdominal area as two white lobes. The vWAT lobes were held with forceps and slightly lifted so that the connective tissue underneath could be cut with scissors. The removed adipose tissues were placed into a 15 ml falcon tube containing 10  $\mu$ M of the P2X7 receptor inhibitor A-804598 and 2% BSA in 5 ml of PBS.

### **3.6.2.2. Cell isolation**

Cell isolation is a procedure to isolate single cell suspensions from tissue samples. There are different techniques used, depending on the organ and the composition or purity of the intended cell suspension.

#### *3.6.2.2.1. Single Cell Suspensions from The Bone Marrow*

A 25 gauge needle was attached to a 5 ml syringe filled with PBS. To obtain bone marrow, the femur was held by forceps and its two ends were cut off with scissors. The needle was placed into the end of the femur and the bone marrow was flushed with 1-2 ml of PBS from the bone marrow space into a petri dish containing 1 ml of cRPMI. The cRPMI containing bone marrow was transferred into the 15 ml falcon tube and re-suspended to disrupt large clusters of the bone marrow. Lastly, the tube was centrifuged at 800 g for five minutes at 4°C to pellet the bone marrows, containing the leucocytes.

#### 3.6.2.2.2. *Density gradient separation with Lymphoprep*

Following Lymphoprep density-gradient centrifugation, dead cells are found at the bottom of the tube, due to their shrinking and increased granularity. Therefore, the living cells can easily be harvested at the interphase. The removal of dead cells before the in vitro stimulation improves the detection of cytokines produced by *NKT* cells. (Sag D., *et al.*, 2017) since dead cells can induce *NKT* cells apoptosis. (Lee H, *et al.* 2010)

##### **Materials:**

- 50 ml Falcon tubes
- 70  $\mu$ m mesh
- 5 mL round bottom FACS tubes
- 3 mL syringe plunger
- 15 ml Falcon tubes
- Pasteur pipettes

##### **Solutions:**

- PBS
- Complete medium: Supplement RPMI-1640 medium with 5% (vol/vol) heat-inactivated FBS, 100 U/mL penicillin-streptomycin, 0.05% (vol/vol) 2-Mercaptoethanol, 4  $\mu$ M L-glutamine
- Lymphoprep (stored at RT)

##### **Method:**

The cell pellet was re-suspended in 2 ml of complete medium and transferred into a 5 mL round bottom FACS tube. The cell suspension was underlaid slowly with 1.5 ml Lymphoprep using a 1 ml pipette tip through a glass Pasteur pipette reaching the bottom of the FACS tube. The gradient was centrifuged at 500 *g* for 20-30 min at RT without acceleration or break. Using a 1 ml pipette tip, the interphase containing the live leukocytes was recovered twice and transferred into a new 15 ml falcon tube.

The cells were washed once with 150  $\mu$ l PBS (400 g, 5-10 min, 4 °C).

### 3.6.2.2.3. *Density Gradient Separation with Percoll*

Density gradients allow to separate a heterogeneous cell suspension based on the densities of the cells. Percoll is a commercial solution of colloidal silica that is coated with *polyvinylpyrrolidone* to minimize its toxicity. Due to the low viscosity, it is suitable for the density gradient separation of leukocytes. In this study, this protocol was used to purify lymphocytes from murine livers (Watarai *et al.*, 2008)

#### **Materials:**

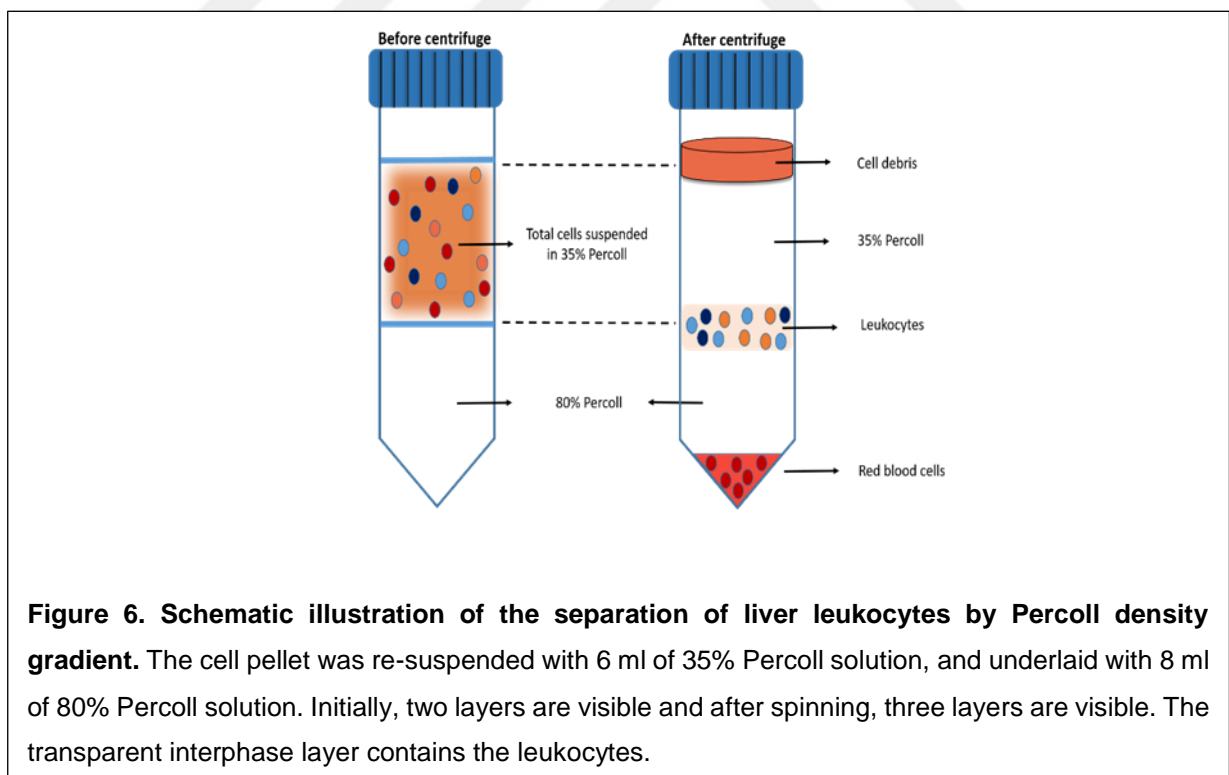
- 50 ml Falcon tubes,
- Glass Pasteur pipettes,
- 5 ml and 25 ml serological pipettes,

#### **Solutions:**

- Percoll Plus (density: 1.131 g/mL),
- PBS,
- 10X PBS,
- 70% Ethanol,
- 100% Percoll solution: 90Volume of Percoll Plus mixed with 10Vol of 10X PBS, stored at RT,
- 80% Percoll solution: 80Volume of 100% Percoll solution mixed with 20Vol of 1X PBS, stored at RT,
- 35% Percoll solution: 35Volume of 100% Percoll solution mixed with 65Vol of 1X PBS, stored at RT,

## Method:

The cell pellet of a cell suspension from a single liver was re-suspended with 6 ml of 35% Percoll solution with a 5 ml serological pipette and the solution was transferred into a 50 ml falcon tube. A glass Pasteur pipette was placed into the tube with the tip reaching the bottom of the tube. Then, 8 ml of 80% Percoll solution was slowly added through the glass Pasteur pipette to the bottom of the 50 ml tube, underneath the cell suspension, resulting in two different layers (**Figure 6**). The glass Pasteur pipette was carefully removed without disturbing the layers. The tube was centrifuged at 800 *g* for 20-30 minutes at room temperature (16-24° C) without acceleration and break. Afterwards, the falcon tube was handled gently, not to disturb the three layers visible now (**Figure 6**). A glass Pasteur pipette was connected to the vacuum and the thick upper layer of cell debris was sucked off. Then, the interphase, the middle transparent layer containing the leukocytes, was slowly removed twice with a 1 ml pipette. The cells from the interphase were washed ones with 25 ml of PBS (400 *g*, 5 min, 4°C). The pellet contained the purified mixture of leukocytes.



### 3.6.2.3. *In Vitro* Stimulation of Single Cell Suspensions

$\alpha$ NKT cells produce large amounts of different cytokines after stimulation. Since cytokines typically are secreted proteins, they must first be trapped inside the cell with a protein transport inhibitor. The two most commonly used protein transport inhibitors are monensin and brefeldin A. Both interrupt the intracellular transport processes leading to an accumulation of the cytokine in the Golgi complex, allowing the detection of cytokines inside the producing cells. (Schuerwegh, *et.al.*, 2001)

#### **Materials:**

- Flat-bottom 24-well plates
- V-bottom 96-well plates

#### **Solutions:**

- GolgiPlug (Brefeldin A [1 mg/ml] in DMSO, stored at 4 °C)
- GolgiStop (Monensin [2 mg/ml] in EtOH, stored at 4 °C)
- PMA ([1 mg/mL] in DMSO)
- Ionomycin ([1 mg/mL] in DMSO)
- Complete medium: Supplement RPMI-1640 medium with 5% (vol/vol) heat-inactivated FBS, 100 U/mL penicillin-streptomycin, 0.05% (vol/vol) 2-mercaptoethanol, 4  $\mu$ M L-glutamine (stored at 4 °C)

#### **Method:**

Cells were resuspended in complete medium and stimulated in flat-bottom 24 well-plates at  $2 \times 10^6$  cells in 500  $\mu$ l. The cells were stimulated either with

(i) PMA [50 ng/mL] and ionomycin [500 ng/mL]; (ii)  $\alpha$ GalCer [100 ng/mL]; or with plate-coated  $\alpha$ -CD3 $\epsilon$  Ab. The cells were stimulated in the presence of GolgiPlug (final concentration 0.5  $\mu$ l/mL), GolgiStop (final concentration 0.33  $\mu$ l/mL) for 4 hours (PMA/ionomycin;  $\alpha$ -CD3 $\epsilon$  Ab) or for 5 hours ( $\alpha$ -GalCer) at 37°C in a CO<sub>2</sub> incubator.

### 3.6.2.4. Cell Staining for Flow Cytometry

#### 3.6.2.4.1. Cell Surface Staining for Flow Cytometry

Cell surface markers are expressed on the cell surface and can be used to define cell types. To this end, the surface markers are labelled with fluorochrome-conjugated antibodies and analysed by flow cytometry.

#### **Materials:**

- V-bottom 96-well plates

#### **Solutions:**

- PBS
- FACS buffer: PBS, 1% FBS, 0.1% NaN<sub>3</sub> (stored at 4°C)
- CytoFix/Perm (stored at 4°C)

#### **Method:**

Cells were stained in V-bottom 96-well plates with up to  $3 \times 10^6$  cells per well. 50 µL FACS buffer per well of master mix was prepared containing pre-titrated amounts of the antibodies, plus 5 µl/mL of α-CD16/32-Ab (clone 2.4G2), unconjugated IgGs (1:1, 10 µg/mL mix of mouse IgG and rat IgG). The master mix was added to the cells, resuspended, and incubated for 15-30 minutes on ice in the dark. After incubation, the cells were centrifuged and the pellet was washed twice with 150 µl PBS (400 g, 5 min, 4°C). Then, 150 µl of CytoFix/Perm buffer per well was added to the cell pellet and immediately re-suspended. They were fixed for 10 min on ice or at 37 °C in the dark and then washed twice with 150 µl PBS (400 g, 5 min, 4°C).

#### 3.6.2.4.2. Intracellular Staining for Flow Cytometry

To stain intracellular molecules, like cytokines or transcription factors, the cells need to be fixed in suspension and then permeabilized before the detection antibody is added. This fixation/permeabilization treatment allows the antibody to pass through

the plasma membrane into the cell interior, while maintaining the morphological characteristics.

### *i. Transcription Factors*

#### **Materials:**

- 70  $\mu\text{m}$  mesh
- V-bottom 96-well plates
- 5 ml round bottom FACS tubes

#### **Solutions:**

- PBS
- FACS buffer: PBS, 1% FBS, 0.1% NaN<sub>3</sub> (stored at 4°C)
- 1X TF Fix/Perm buffer (stored at 4°C)
- 1X TF Perm/Wash buffer (stored at 4°C)

#### **Method:**

Surface-stained cells were pelleted (400 g, 5 min, 4°C), resuspended in 150  $\mu\text{l}$  of TF Fix/Perm buffer and incubated for 75 min at 4°C in the dark. Then, the cells were washed twice with TF Perm/Wash buffer (400 g, 5 min, 4°C). The intracellular staining cocktail was prepared using 50  $\mu\text{l}$  per sample of Perm/Wash buffer containing pre-titrated amounts of the antibodies for the transcription factors and unconjugated IgGs (1:1, 10  $\mu\text{g}/\text{mL}$  mix of mouse IgG and rat IgG). The intracellular staining cocktail was added to the cell pellet, the cells were re-suspended and incubated overnight at 4°C in the dark. Afterwards, the cells were washed once with TF Perm/Wash buffer, re-suspended with 150  $\mu\text{l}$  TF Perm/Wash buffer and incubated five minutes on ice to permit unbound antibodies to diffuse out of the cells. The cells were washed once more with 150  $\mu\text{l}$  TF Perm/Wash buffer and once with FACS buffer (400 g, 5 min, 4°C), then re-suspended in 150  $\mu\text{l}$  of FACS buffer and filtered through a 70  $\mu\text{m}$  mesh into a 5 mL round bottom FACS tube.

## ii. Cytokines

### **Materials:**

- 70 µm mesh
- V-bottom 96-well plates
- 5 ml round bottom FACS tubes

### **Solutions:**

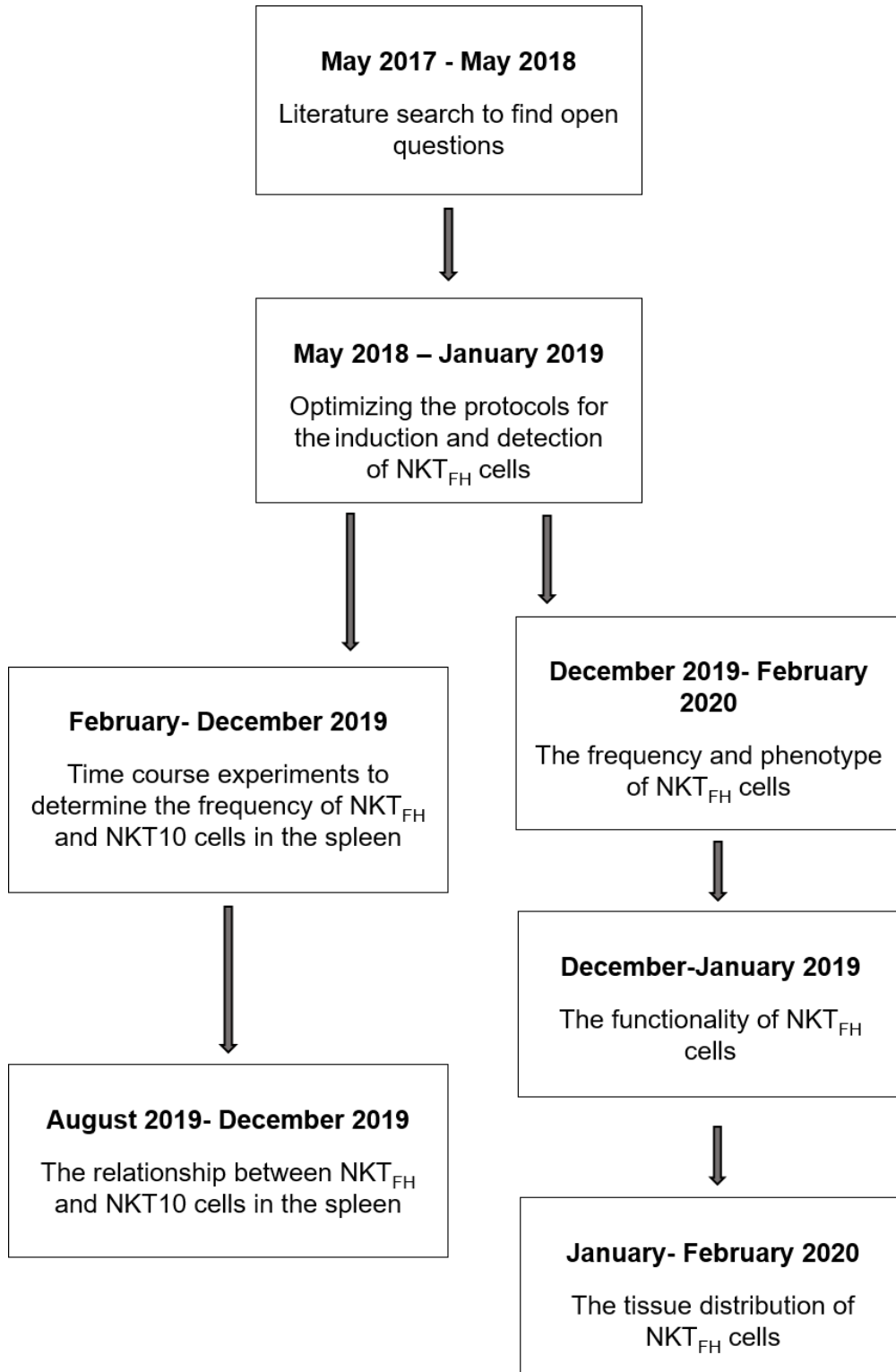
- PBS
- FACS buffer: PBS, 1% FBS, 0.1% NaN<sub>3</sub> (stored at 4°C)
- CytoFix/Perm buffer (stored at 4°C)
- 1X Perm/Wash (stored at 4°C)

### **Method:**

Surface-stained cells were pelleted (400 g, 5 min, 4°C), resuspended in 150 µl of CytoFix/Perm buffer and fixed for 10 minutes at 37 °C. Then, the cells were washed twice with Perm/Wash buffer to permeabilize the cells (500 g, 5 min, 4°C). The intracellular cytokine staining (ICCS) cocktail was prepared with 50 µl per test of Perm/Wash buffer containing pre-titrated amounts of the antibodies for the cytokines and unconjugated IgGs (1:1, 10 µg/mL mix of mouse IgG and rat IgG). The ICCS cocktail was added to the cell pellet, the cells were re-suspended and incubated for 30 min or overnight at 4°C in the dark. Then, the cells were washed once with Perm/Wash buffer (500 g, 5 min, 4°C), re-suspended with 150 µl Perm/Wash buffer, and incubated five minutes on ice to permit unbound antibodies to diffuse out of the cells. The cells were washed once more with Perm/Wash buffer and once with FACS buffer (500 g, 5 min, 4°C). Then, the cells were re-suspended with 70 µl FACS buffer and filtered through a 70 µm mesh into a 5 mL round bottom FACS tube.



### 3.7. Research Plan



### **3.8. Evaluation of Data**

Statistical analysis: Results are expressed as the mean  $\pm$  SEM. Statistical comparisons were drawn using a 2-tailed Student's *t* test (Excel; Graphpad Software). *P* values less than 0.05 were considered statistically significant and are indicated as \**P* < 0.05, \*\* *P* <0.01, and \*\*\**P* <0.001 in the figures. Graphs were generated with GraphPad Prism.

### **3.9. Limitation of the Research**

There were no limitations in our study.



## 4. RESULTS

### 4.1. Optimizing the Bcl6 Staining for The Detection of NKT<sub>FH</sub> Cells

#### 4.1.1. The gating strategy for the identification of iNKT cells

Single cell suspensions of spleens from C57BL/6, BALB/c, and Bcl6<sup>-/-</sup> mice were prepared for flow cytometric analysis to identify iNKT cells. Lymphocytes were gated by physical parameters (FSC-Area versus SSC-Area) (**Figure 7A**) and cell doublets and aggregates were eliminated based on their high FSC-Width (**Figure 7B**) and SSC-Width (**Figure 7C**) values. Live cells were gated by excluding cells labelled with a live/dead marker (**Figure 7D**). B cells are characterized by their expression of CD19 (Wang *et al.*, 2012), thus αCD19-Abs were used to exclude B cells (**Figure 7E**). Because murine iNKT cells do not express CD8α (Bendelac *et al.*, 1997), αCD8α-Abs were used to exclude CD8<sup>+</sup> T cells (**Figure 7E**). Like other memory cells, iNKT cells express the activation marker CD44 (Bendelac *et al.*, 2007), which was used to improve the gating for iNKT cells (**Figure 7F**). Finally, iNKT cells were identified as CD3ε<sup>+</sup> CD1d/αGalCer-tetramer<sup>+</sup> cells (Godfrey *et al.*, 2005) (**Figure 7G**).

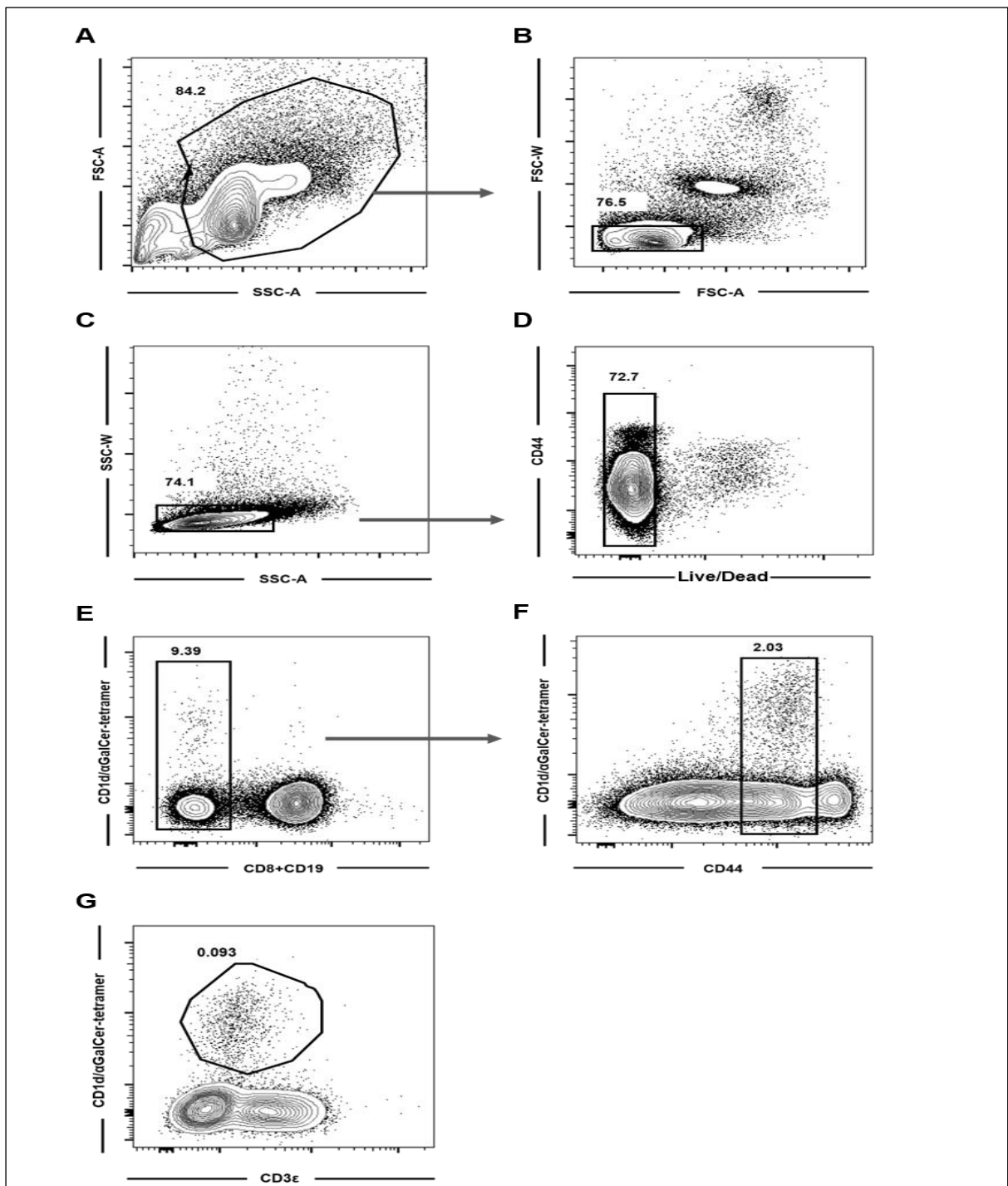


**Figure 7. The gating strategy used to identify *NKT* cells.** After gating for lymphocytes (SSC-A vs. FSC-A) and single cells (excluding FSC-W vs. FSC-A and SSC-W vs. SSC-W high cells), live splenocytes were gated as cells negative for the live/dead marker. *NKT* cells were gated as CD8 $\alpha$ - and CD19- negative, CD44<sup>high</sup>, CD3 $\epsilon$ <sup>int</sup>, and CD1d/ $\alpha$ GalCer-tetramer<sup>+</sup> cells. A representative gating tree for splenic *NKT* cells from C57BL/6 control mice is shown. The numbers in the graphs represent the percentage of cells within the gate.

#### 4.1.2. Germinal centre B cells are used as positive control for the Bcl6-expression

GC B cells express the transcription factor Bcl6 (Fearon *et al.*, 2002), and thus were used as positive control for the staining with  $\alpha$ Bcl6-Abs (clone 7D1). Single cell suspensions of spleens from C57BL/6 mice were stained for the surface markers, followed by the transcription factor staining to detect the transcription factor Bcl6. Lymphocytes were gated by SSC-Area versus FSC-Area (**Figure 8A**), singlet cells were gated by excluding of SSC-A versus SSC-W (**Figure 8B**) and FSC-A versus FSC-W high cells (**Figure 8C**). Then, live cells were gated as cells negative for the live/dead marker (**Figure 8D**). Finally, GC B cells were identified as CD19<sup>+</sup> CD185<sup>+</sup> GL7<sup>high</sup> CD95<sup>+</sup> and Bcl6<sup>+</sup> cells (Allen *et al.*, 2007) (**Figure 8E, 8F, and 8G**). As shown in **figure 8G**, Bcl6<sup>+</sup> GC B cells are detectable as a separate population from the Bcl6<sup>neg</sup> B cells. Therefore, it was concluded that we can identify GC B cells with the  $\alpha$ Bcl6-Ab (clone 7D1).

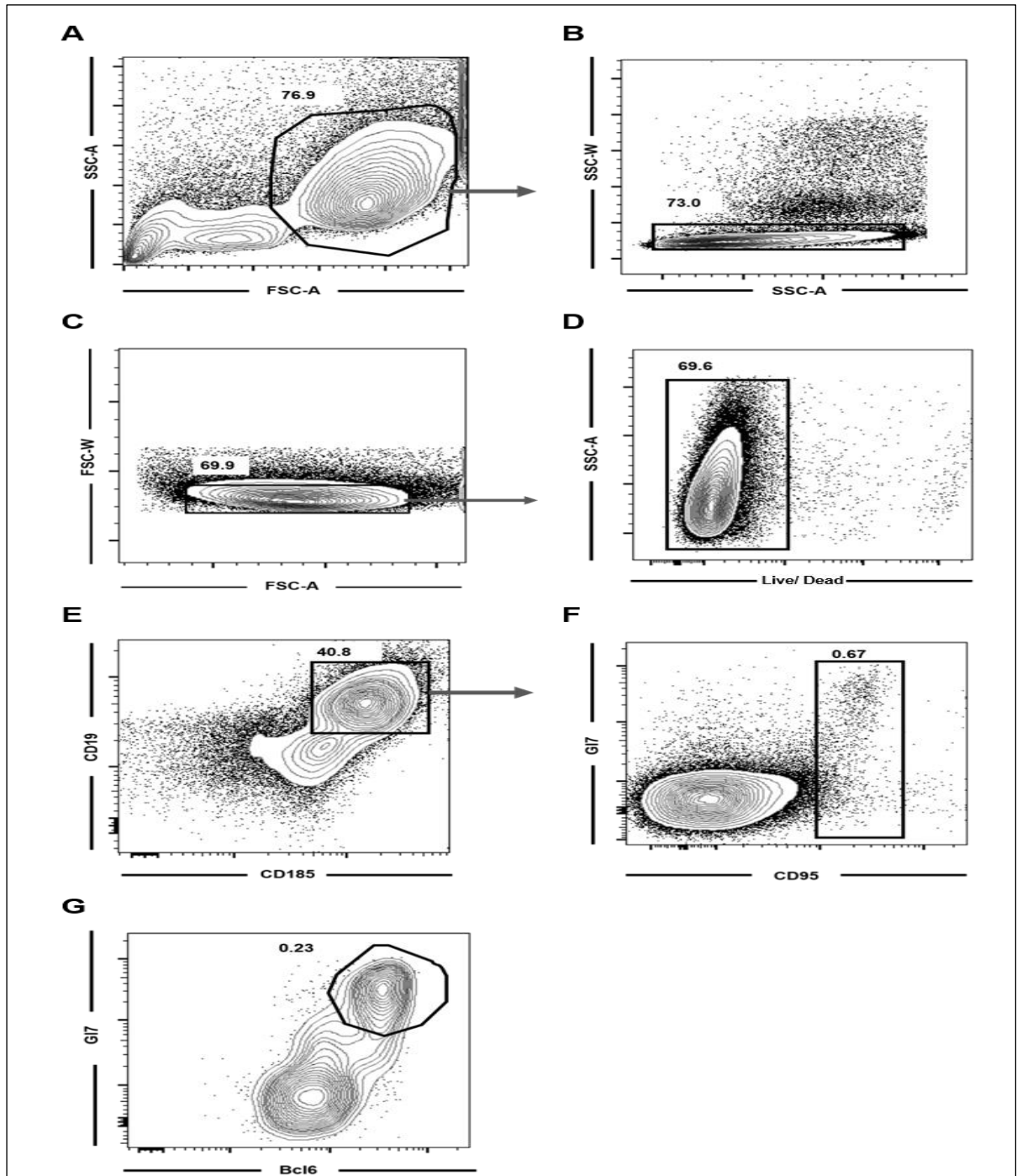
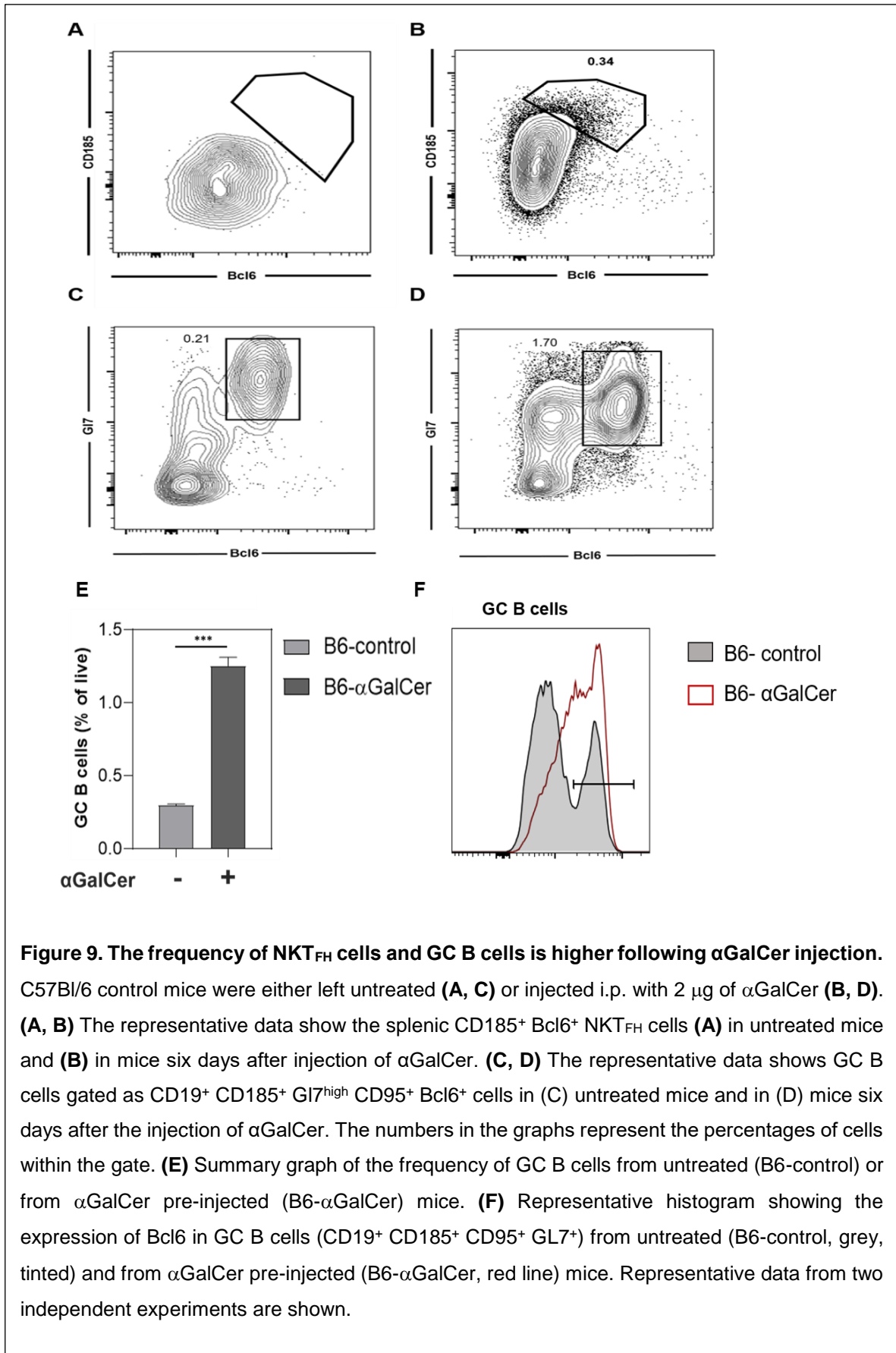


**Figure 8. The gating strategy used to detect GC B cells.** Splenic lymphocytes (A; SSC-A vs. FSC-A) and single cells (B and C; excluding SSC-W and FSC-W high cells), were gated, and dead cells were excluded (D). GC B cells were identified as CD19<sup>+</sup> CD185<sup>+</sup> GL7<sup>high</sup> CD95<sup>+</sup> and Bcl6<sup>+</sup> cells (E-G). A representative gating tree for splenic GC B cells from C57BL/6 control mice is shown. The numbers in the graphs represent the percentage of cells within the gate.

#### 4.1.3. $NKT_{FH}$ cells are detectable in C57BL/6 mice six days after injection of $\alpha GalCer$

$NKT_{FH}$  cells arise within five to six days following antigen challenge (Chang *et al.*, 2011). Thus, 2  $\mu g$   $\alpha GalCer$  were injected into C57BL/6 mice and splenocytes were analysed six days later for  $NKT_{FH}$  cells. Similar to  $T_{FH}$  cells,  $NKT_{FH}$  cells are characterized by the expression of the transcription factor Bcl6 (Chang *et al.*, 2011). Once  $\bar{N}KT$  cells were gated as described above (**Figure 7**),  $NKT_{FH}$  cells were identified as  $CD185^+ Bcl6^+$  cells. As shown in **figure 9A**, the untreated mice did not contain  $CD185^+ Bcl6^+$  double positive  $\bar{N}KT$  cells. In contrast, in the  $\alpha GalCer$  pre-injected mice,  $CD185^+ Bcl6^+$  double positive  $\bar{N}KT$  cells were detected and defined as  $NKT_{FH}$  cells (**Figure 9B**). It has been reported that  $NKT_{FH}$  cells can provide cognate help to B cells and can support the proliferation of GC B cells (Chang *et al.*, 2011). Therefore, the frequency of GC B cells was also examined in these experiments. As expected, splenic GC B cells were more frequent in the  $\alpha GalCer$  pre-injected mice (1.25%  $\pm$  0.06%) compared to the untreated mice (0.01%  $\pm$  0.01%) (**Figure 9A**). This higher frequency of GC B cells in the  $\alpha GalCer$  pre-injected mice is another indication for the development of  $NKT_{FH}$  cells.





#### 4.1.4. A pre-fix step using Cytofix/Cytoperm at 37°C improves the Bcl6 staining

As NKT<sub>FH</sub> cells are less frequent than GC B cells in the spleen, we first tested the Bcl6 staining protocol by analysing GC B cells. In these optimization experiments, four different protocols were tested for the detection of Bcl6, which differed only in the initial fixation (pre-fix step). To this end, splenocytes from untreated C57BL/6 mice were divided into four groups to test the different pre-fix approaches in parallel. After the surface staining, the samples were differently treated for the pre-fix step. For the first sample, the pre-fix step was skipped (**Figure 10A**). For the second sample, the pre-fix step was performed using 2% formaldehyde for 60 min at 4°C (**Figure 10B**). In the third sample, the pre-fix step was performed using Cytofix/Cytoperm for 10 min on ice (**Figure 10C**). Lastly, for the fourth sample the pre-fix step was performed using Cytofix/Cytoperm for 10 min at 37°C (**Figure 10D**). The rest of the transcription factor staining protocol was the same for all the groups.

In **figure 10**, the contour plots (left panel) show the gating of GC and other B cells and the Bcl6 expression levels are shown in representative histograms (right panel). These data indicated that the protocol with the pre-fix step using 2% formaldehyde was not able to identify Bcl6<sup>+</sup> cells (**Figure 10B**). Following the pre-fix with Cytofix/Cytoperm the difference between Bcl6<sup>+</sup> and Bcl6<sup>-</sup> cells was weaker when performed on ice (**Figure 10C**) than at 37°C (**Figure 10D**). The percentage of Bcl6<sup>+</sup> GC B cells in the protocol without prefix step (**Figure 10A**) was 0.12% ± 1.48% within total cells. Even though the percentage of Bcl6<sup>+</sup> GC B cells in the protocol with the pre-fix step using Cytofix/Cytoperm at 37°C was lower (0.065% ± 1.78%), the separation between Bcl6<sup>+</sup> and Bcl6<sup>-</sup> cells was clearer (**Figure 10D**). Therefore, it was decided to use the pre-fix with Cytofix/Cytoperm for 10 min at 37°C for our Bcl6 staining.

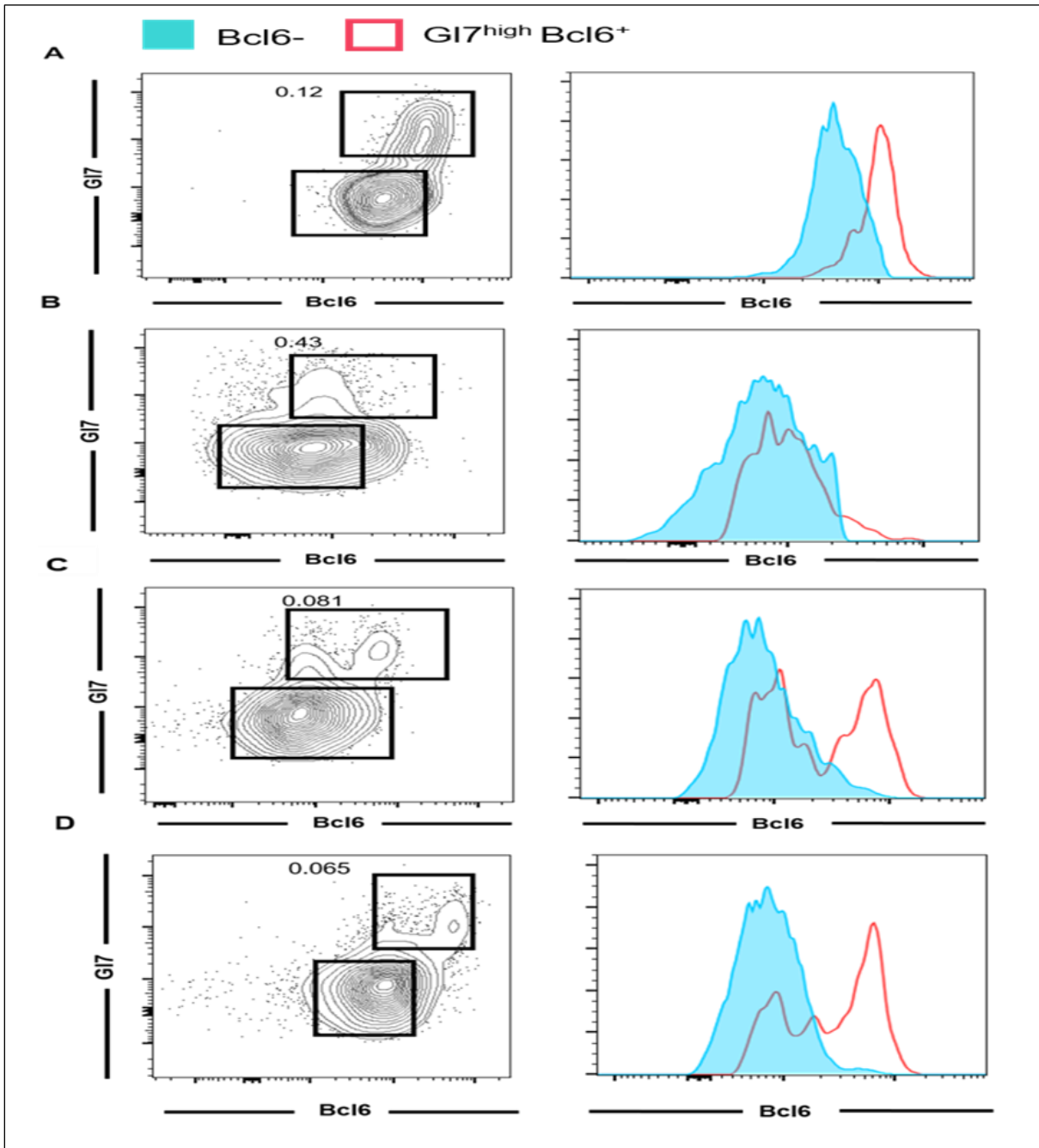
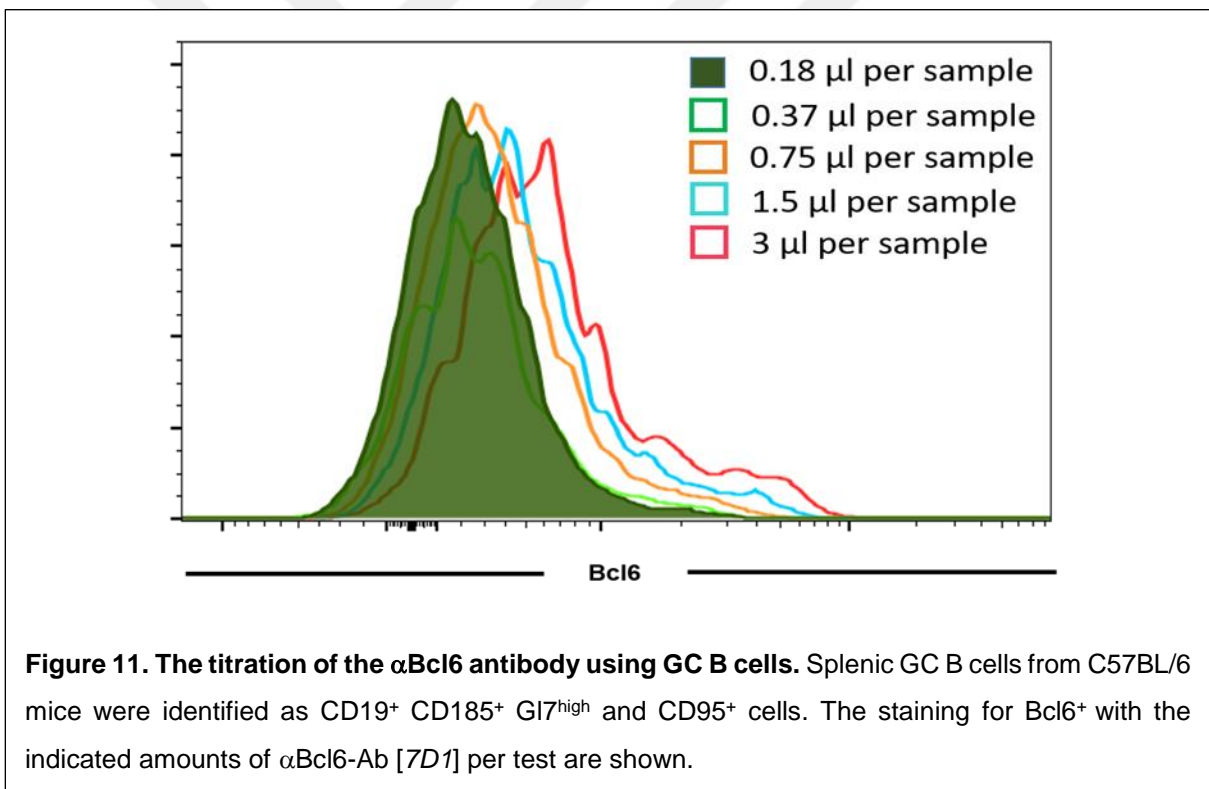


**Figure 10. The different pre-fix protocols tested for the optimization of the Bcl6 staining in GC B cells.** The expression of Bcl6 was compared in GL7<sup>+</sup> (red line) and GL7<sup>neg</sup> (blue, tinted) B cells (CD19<sup>+</sup> CD185<sup>+</sup> CD95<sup>+</sup>). Four different protocols were tested for the Bcl6 transcription factor staining. The representative data show the result of the protocol **(A)** without the prefix step, **(B)** with the prefix step using 2% formaldehyde for 60 min at 4°C, **(C)** with the prefix step using Cytofix/Cytoperm for 10 min on ice, and **(D)** with the prefix step using Cytofix/Cytoperm for 10 min at 37°C. Representative data for splenic GC B cells from C57BL/6 control mice are shown. The numbers in the graphs represent the percentage of cells within the GL7<sup>+</sup> gate.

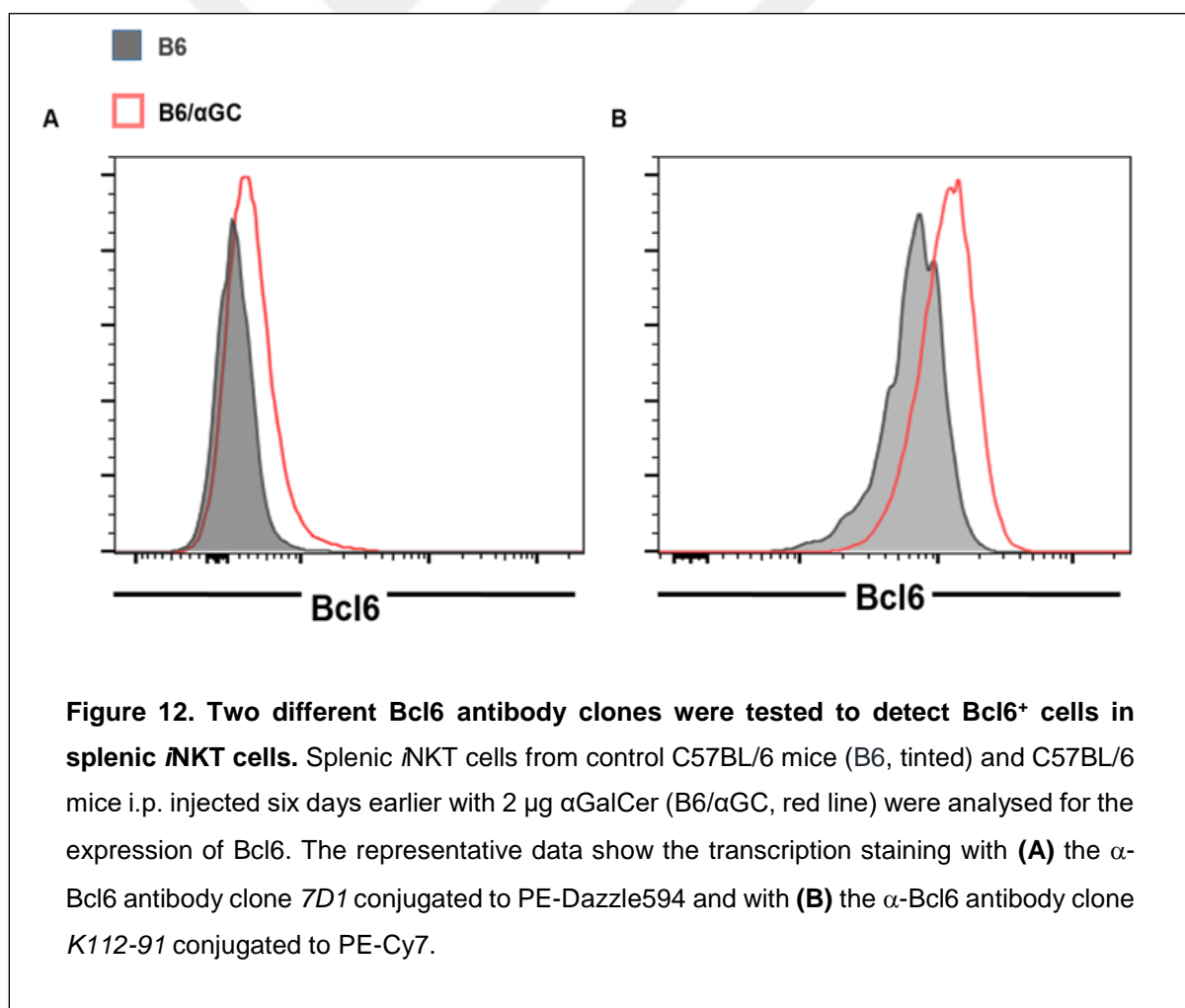
#### 4.1.5. The working concentration of $\alpha$ Bcl6-Ab [7D1] was established

To prevent unspecific binding due to an excess amount of antibody, we performed titration experiments with the  $\alpha$ Bcl6-Ab [7D1] to determine the best working concentration. Splenocytes from untreated C57BL/6 mice were divided into five aliquots. The flow cytometric panel identified GC B cells and the antibody concentrations were the same for all antibodies except the  $\alpha$ Bcl6-Ab [7D1]. For the  $\alpha$ Bcl6-Ab [7D1], five two-fold dilutions were performed, starting with 3  $\mu$ l per sample. After gating for GC B cells, the histogram graph in **figure 11** was prepared to decide the best working concentration of  $\alpha$ Bcl6-Ab [7D1]. 3  $\mu$ l of the  $\alpha$ Bcl6-Ab [7D1] per sample gave the clearest separation of Bcl6<sup>+</sup> and Bcl6<sup>-</sup> cells and, therefore, it was decided to use this concentration for further experiments.



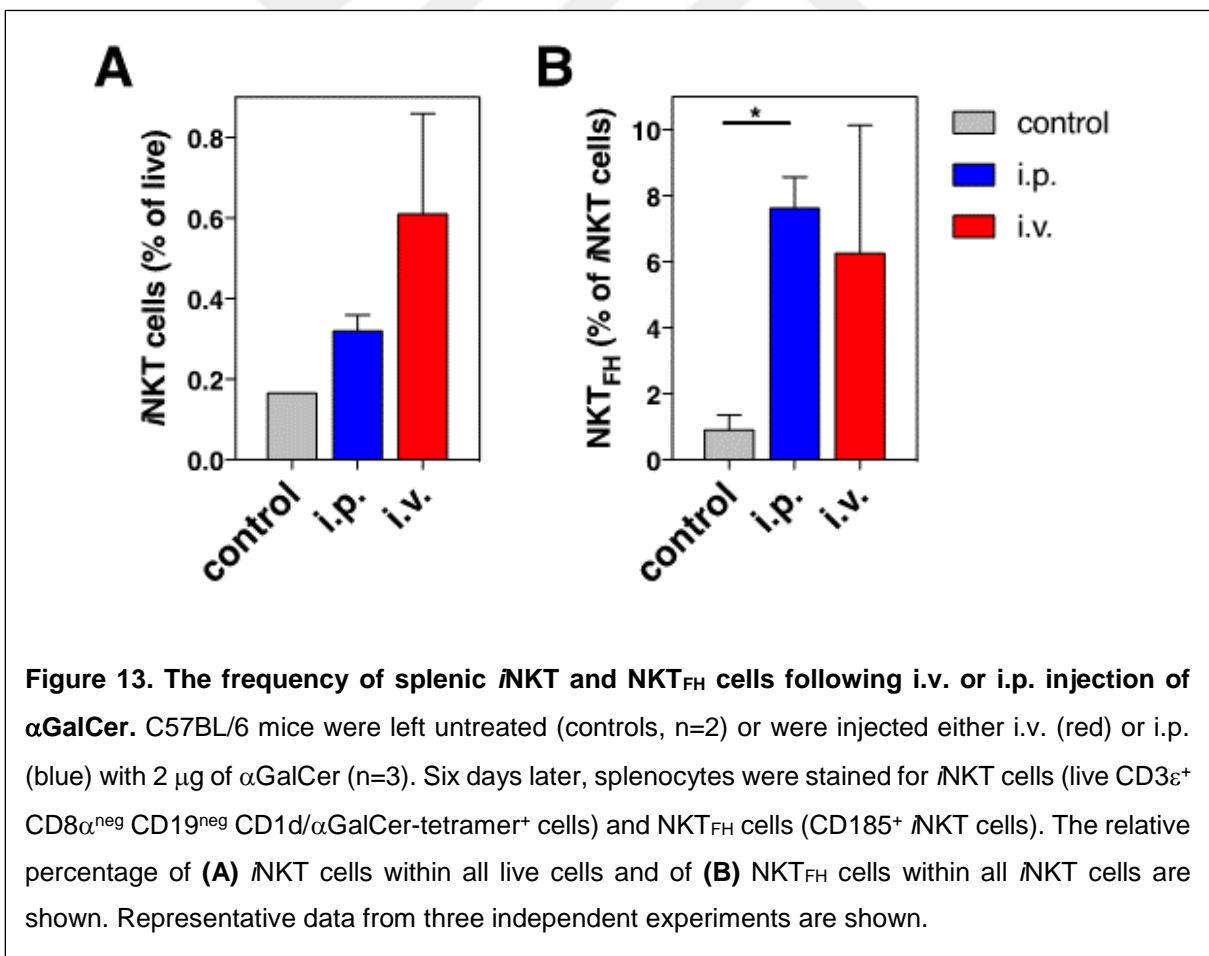
#### 4.1.6. Differences in The Bcl6 Detection Between the $\alpha$ Bcl6-Ab Clones K112-91 and Clone 7D1

The experiments under 4.1.5 were performed with  $\alpha$ Bcl6-Abs of the clone 7D1. To test whether the antibody clone may affect the detection of Bcl6, two different clones were tested in parallel. Purified splenocytes from  $\alpha$ GalCer pre-injected mice were divided in two aliquots. The flow cytometric panel identified  $\mathbb{N}$ KT cells and differed only in the  $\alpha$ Bcl6-Ab clone used. After surface staining, the transcription factor staining with pre-titrated antibody concentrations was performed: one sample was stained with the  $\alpha$ Bcl6-Ab clone K112-91 conjugated to PE-Cy7 (**Figure 12B**) and the other sample with the  $\alpha$ Bcl6-Ab clone 7D1 conjugated to PE-Dazzle594 (**Figure 12A**). Due to the clearer separation of expression Bcl6<sup>+</sup> and Bcl6<sup>-</sup> cells (**Figure 12A**), the  $\alpha$ Bcl6-Ab clone K112-91 was used for future experiments.



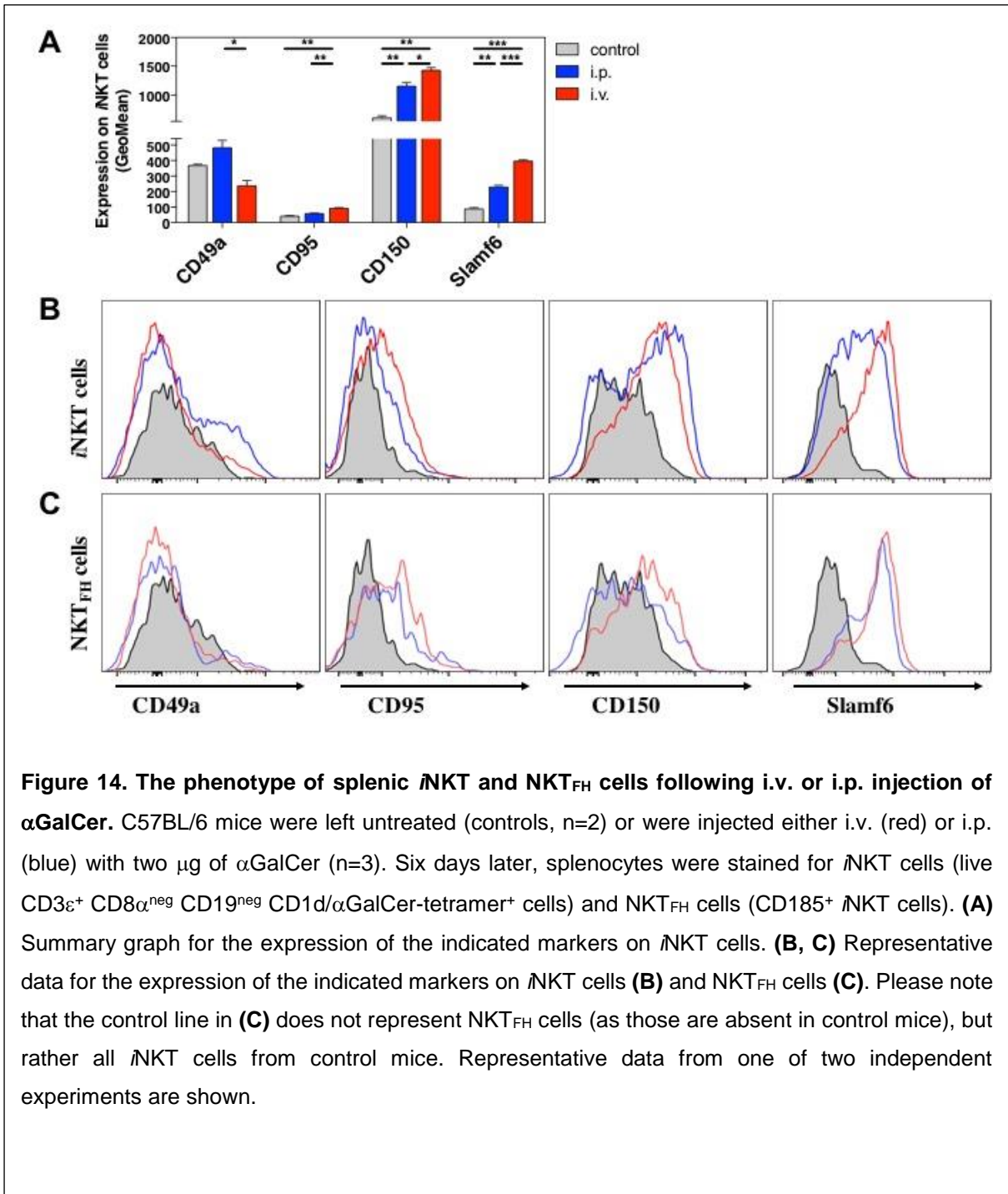
## 4.2. The Frequency and Phenotype of Splenic NKT<sub>FH</sub> Cells

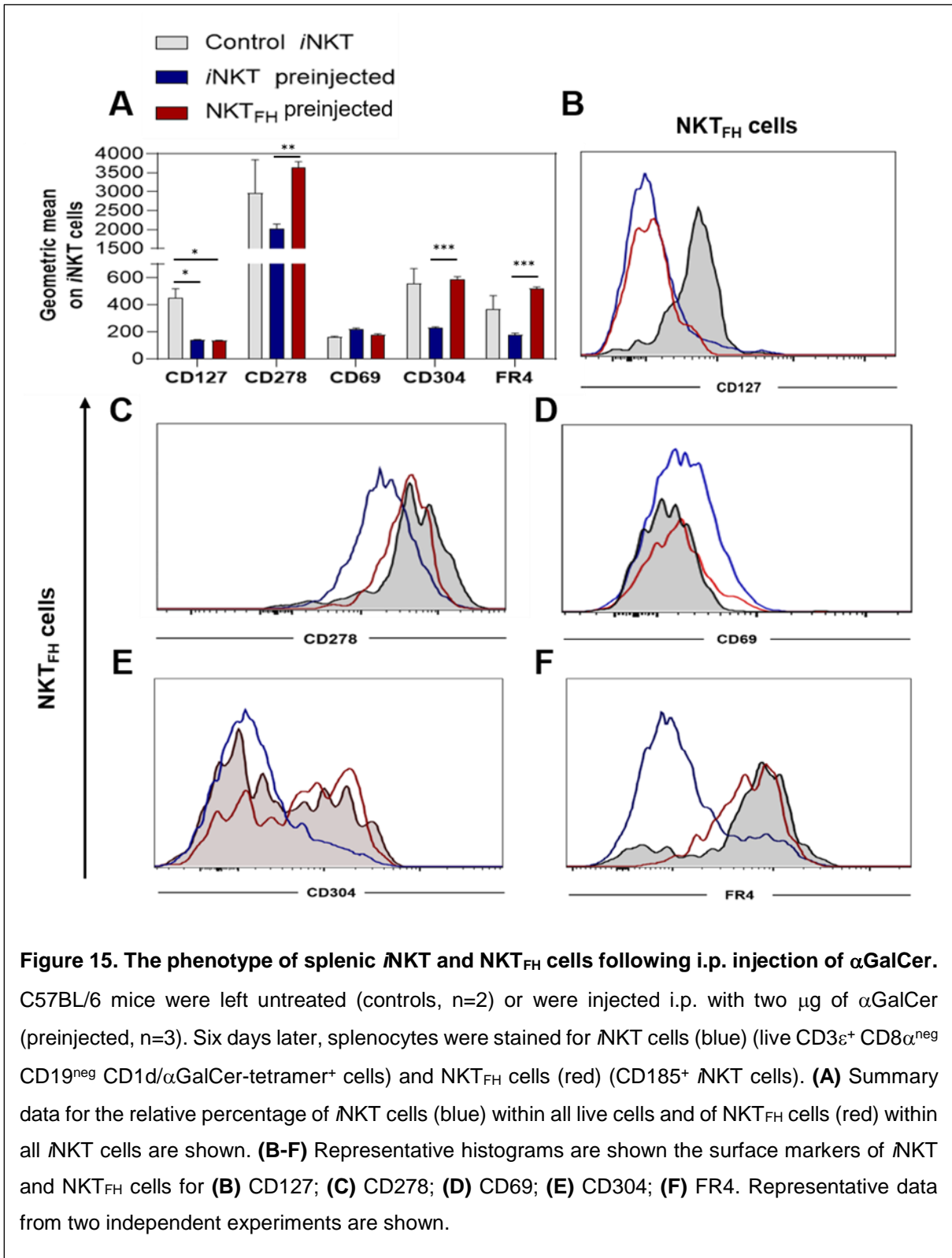
Having established the flow cytometric protocol to identify NKT<sub>FH</sub> cells, we next measured the *in vivo* expansion of NKT<sub>FH</sub> cells. However, previous publications on NKT<sub>FH</sub> cells used different routes of  $\alpha$ GalCer injection, either sub-cutaneous (Tonti *et al.* 2012), intra-venous (i.v.) (Chang *et al.* 2012, Sag *et al.* 2014), or intra-peritoneal (i.p.) (Chang *et al.* 2012, King *et al.* 2012). Therefore, we initially compared the impact of i.v. versus i.p. injection of  $\alpha$ GalCer on splenic  $\text{iNKT}$  cells and NKT<sub>FH</sub> cells six days later. The frequency of  $\text{iNKT}$  cells increased following the injection of  $\alpha$ GalCer and this tended to be more pronounced following i.v. than i.p. injection (**Figure 13A**), however, this did not reach statistical significance in most experiments (data not shown). When analysing NKT<sub>FH</sub> cells, we observed a clear induction of NKT<sub>FH</sub> cells in the spleen six days after  $\alpha$ GalCer injection, which was comparable for the injection via the i.v. or i.p. route (**Figure 13B**).



So far, the expression of only a few surface markers have been reported for NKT<sub>FH</sub> cells. In particular, NKT<sub>FH</sub> cells were shown to be positive for CD185/CXCR5, CD272/BTLA, CD278/ICOS, and CD279/PD1, but negative for CD127/IL7R $\alpha$  (Chang *et al.* 2012, King *et al.* 2012, Sag *et al.* 2014, Tonti *et al.* 2012). To improve the characterization of NKT<sub>FH</sub> cells, we determined the expression of several additional surface markers on  $\bar{N}KT$  and NKT<sub>FH</sub> cells six days after the injection of  $\alpha GalCer$  (**Figure 14**). For some of these experiments the i.v. and i.p. challenge of  $\alpha GalCer$  was performed in parallel. **Figure 14** shows the results for those surface markers where a change following  $\alpha GalCer$  was noticed on splenic  $\bar{N}KT$  cells. For most of these markers, the route of  $\alpha GalCer$  challenge also influenced the extent of the observed changes (**Figure 14**). In contrast, no  $\alpha GalCer$ -induced differences were observed on  $\bar{N}KT$  cells for the markers CD11b (integrin  $\alpha M$ ), CD49b (integrin  $\alpha 2$ ), CD49d (integrin  $\alpha 4$ ), CD103 (integrin  $\alpha E$ ), and CD335/NKp46 (data not shown).

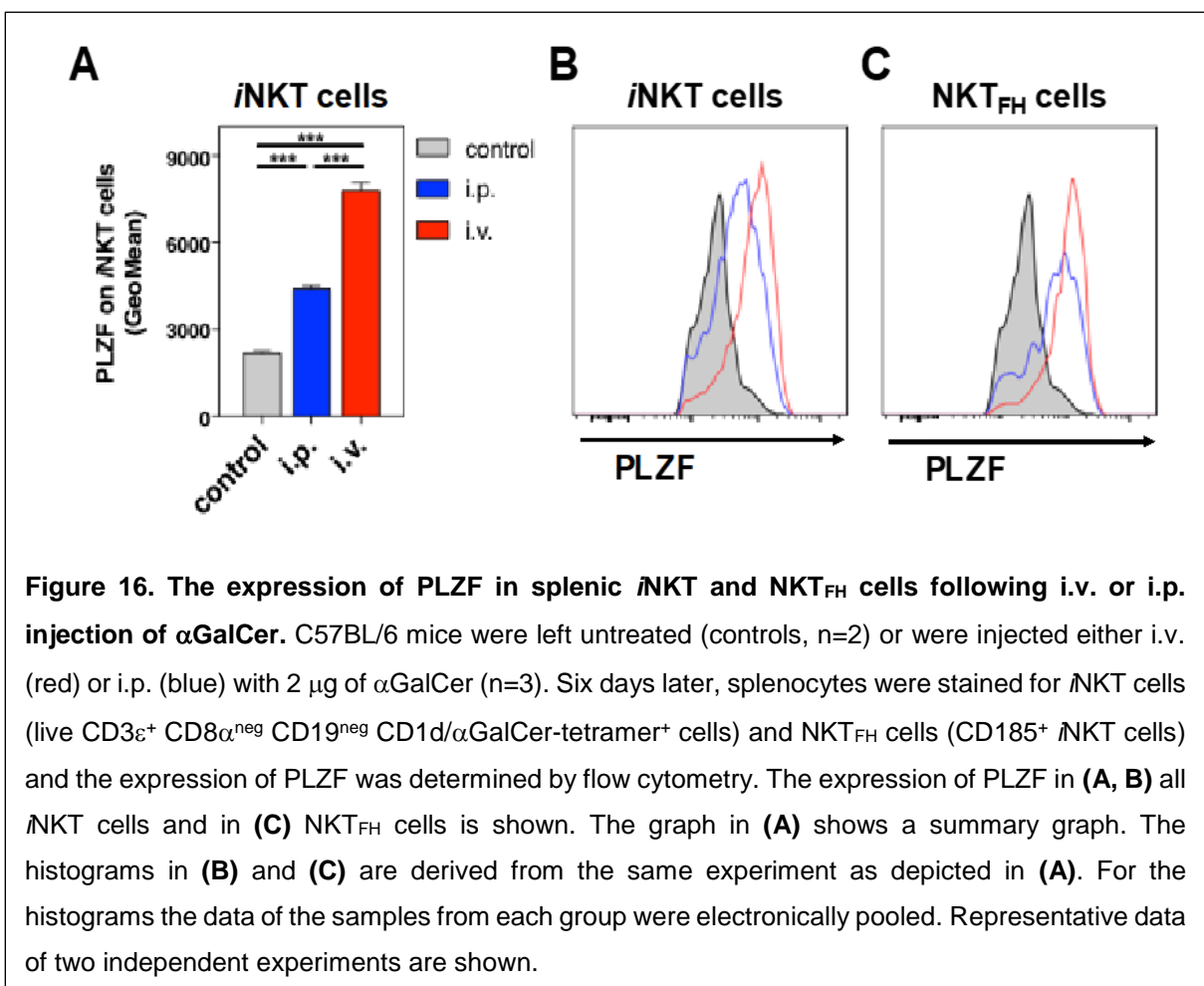
We next analysed the expression of above surface markers specifically on NKT<sub>FH</sub> cells. Interestingly, the expression differences we noticed following the injection of  $\alpha GalCer$  either i.v. or i.p. were only seen on the  $\bar{N}KT$  cell level, but not when focusing exclusively on NKT<sub>FH</sub> cells (**Figure 14**).



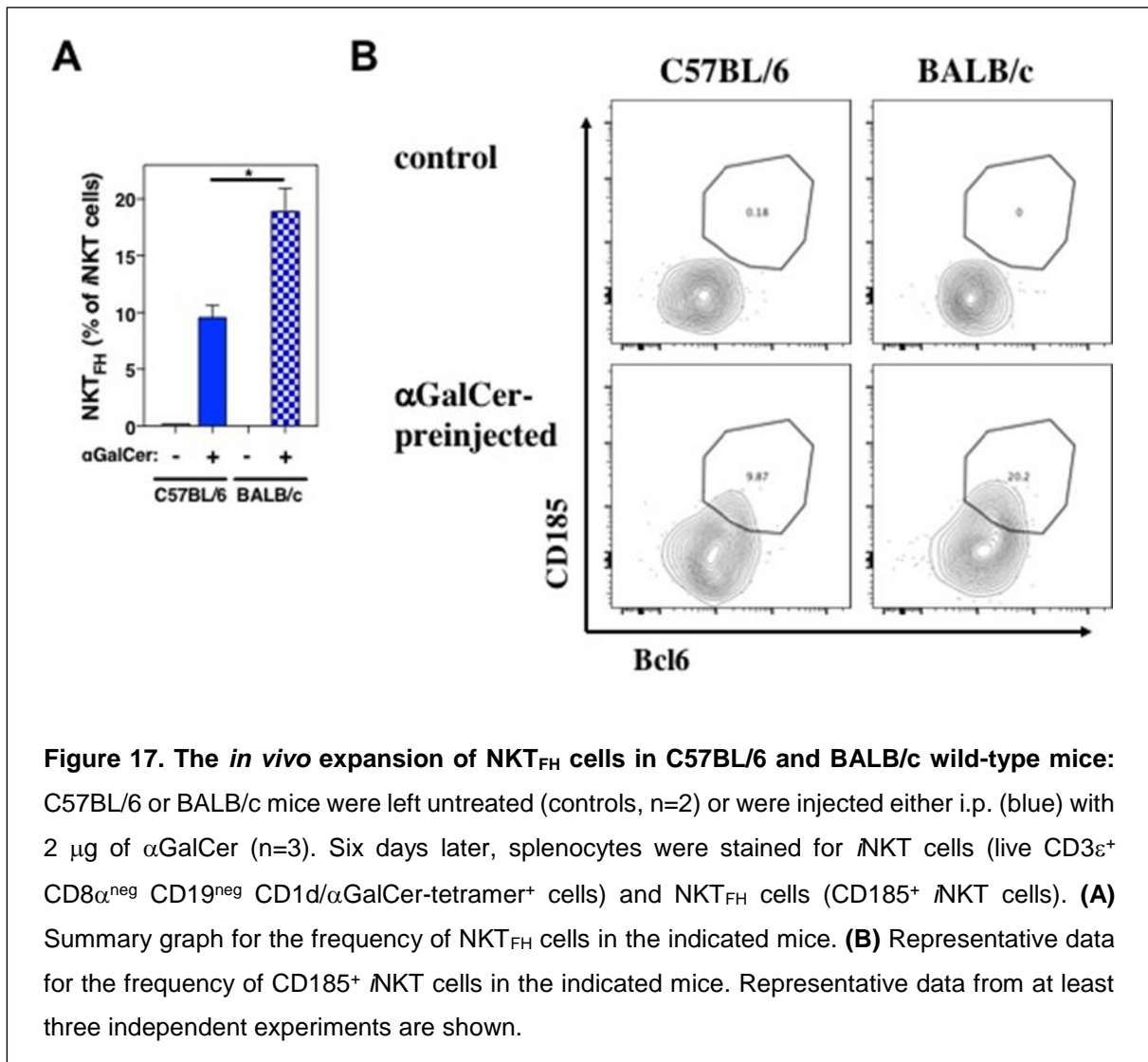




Additional to the surface markers, we also analysed the expression of several transcription factors besides Bcl6, namely PLZF, ROR $\gamma$ t, and Tbet. No changes were observed for ROR $\gamma$ t and Tbet six days after the injection of  $\alpha$ GalCer for all  $i$ NKT cells or specifically for NKT<sub>FH</sub> cells (data not shown). However, a clear increase in the expression of PLZF was visible when all  $i$ NKT cells were analysed, which was more pronounced after i.v. injection of  $\alpha$ GalCer (**Figure 16A and 16B**). Similar to the expression of the surface markers (**Figure 15**), the difference between the i.v. versus i.p. injected cells were not seen when NKT<sub>FH</sub> cells were analysed (**Figure 16C**).



The frequency of  $\text{NKT}$  cell subsets under resting conditions differs between C57BL/6 and BALB/c mice (Lee *et al.* 2013, Lee *et al.* 2015, Sag *et al.* 2014). Therefore, we wondered if the induction of  $\text{NKT}_{\text{FH}}$  cells following  $\alpha\text{GalCer}$  challenge would also differ between these two mouse strains. As shown in **figure 17**, the expansion of  $\text{NKT}_{\text{FH}}$  cells, on day six following  $\alpha\text{GalCer}$  injection, was clearly stronger in the BALB/c than in the C57BL/6 mice.

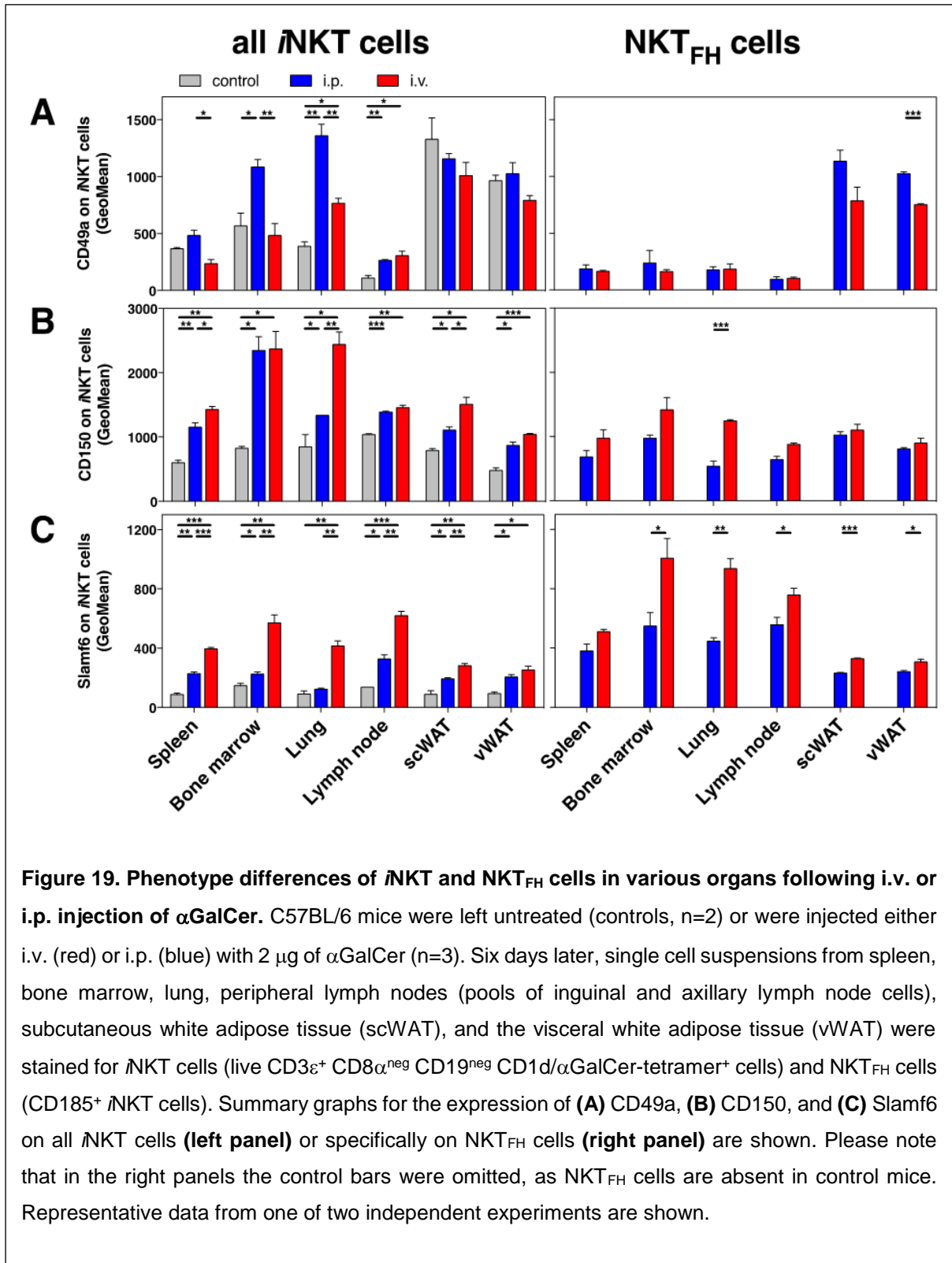


### 4.3. The Tissue Distribution of NKT<sub>FH</sub> Cells

So far, NKT<sub>FH</sub> cells have been reported following the injection of  $\alpha$ GalCer only in the spleen and the peripheral lymph nodes (Chang *et al.* 2012, King *et al.* 2012, Tonti *et al.* 2012). Therefore, we determined whether NKT<sub>FH</sub> cells could be also detected in other organs. As we noticed slight differences in the phenotype of  $\mathcal{N}$ KT cell in the spleen following i.p. versus i.v. injection (**Figure 14**), we decided to compare these two routes of  $\alpha$ GalCer injection side-by-side. To this end,  $\alpha$ GalCer was injected either i.v. or i.p. and six days later the frequency of NKT<sub>FH</sub> cells was determined in several organs.

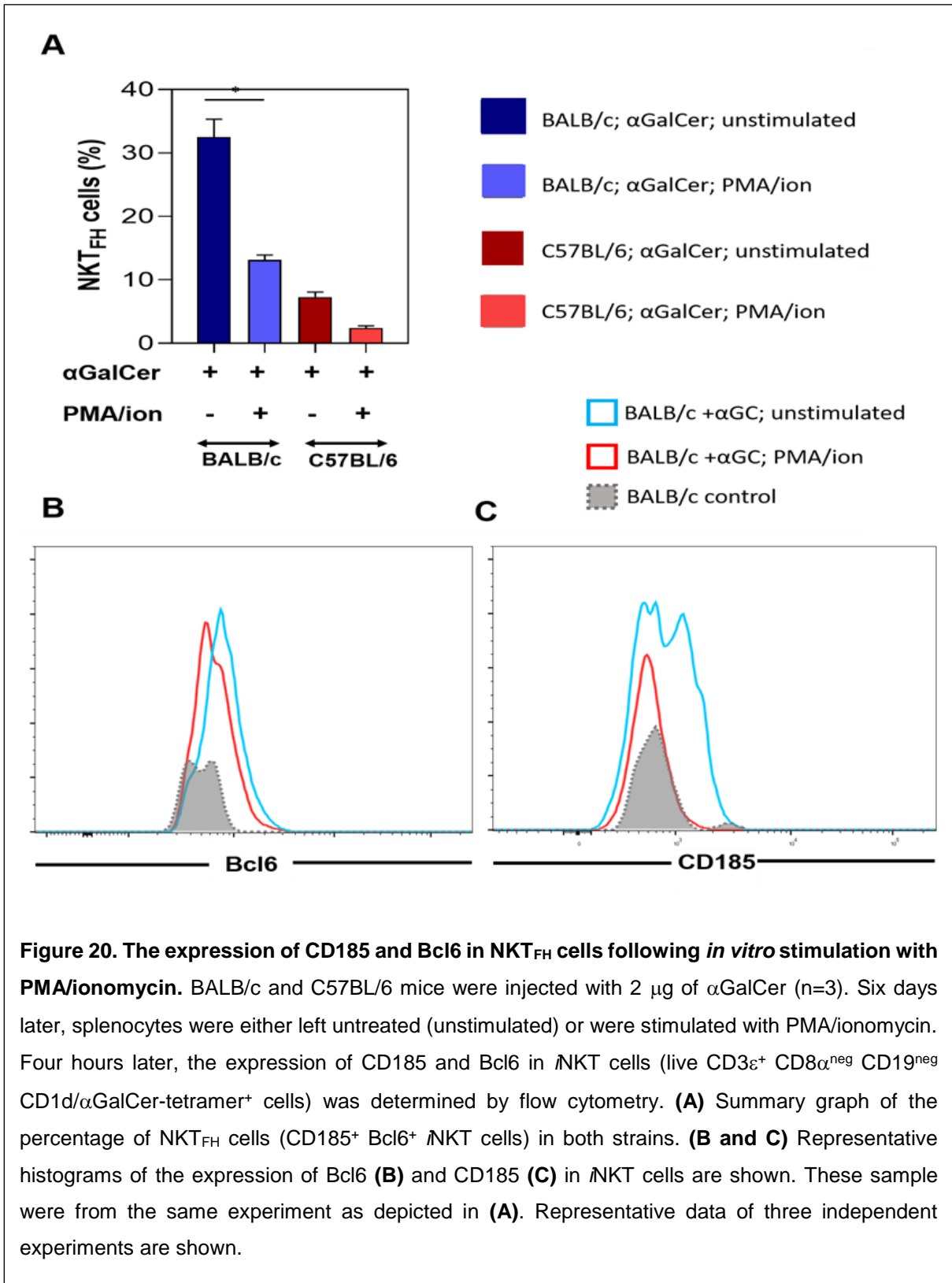
Six days after the injection of  $\alpha$ GalCer, the frequency of  $\mathcal{N}$ KT cells increased in some (bone marrow, lung, adipose tissue), but not all (spleen, lymph nodes, liver) organs (**Figure 18A**). No statistically significant differences were observed for the frequency of  $\mathcal{N}$ KT cells for the application of  $\alpha$ GalCer via the i.v. or the i.p. route (**Figure 18A**). We next analysed the frequency of NKT<sub>FH</sub> cells six days after the injection of  $\alpha$ GalCer. A clear population of NKT<sub>FH</sub> cells was visible above background (control) in spleen, bone marrow, lung, and the lymph nodes (**Figure 18B**). In contrast, preliminary results suggest that NKT<sub>FH</sub> cells were not or only weakly induced in the adipose tissue and the liver (**Figure 18B**). The induction of NKT<sub>FH</sub> cells was also influenced by the route of the antigen injection in most (bone marrow, lung, lymph nodes), but not all (spleen) organs, as we observed more NKT<sub>FH</sub> cells following the i.v. injection (**Figure 18B**).

As we noticed differences in the frequency of NKT<sub>FH</sub> cells in different organs following i.v. versus i.p. injection (**Figure 18**), we decided to analyse in detail the phenotype of NKT<sub>FH</sub> cells following these two routes of  $\alpha$ GalCer injection side-by-side. To this end,  $\alpha$ GalCer was injected either i.v. or i.p. and six days later the phenotype of NKT<sub>FH</sub> cells was analysed in several organs via flow cytometry. However, the expression of most of the tested surface markers (CD44, CD49a, CD95, CD150, and Slamf6) on NKT<sub>FH</sub> cells of most of the analysed organs was not impacted by the route of antigen challenge (**Figure 19**). To illustrate this point, **figure 19** shows a side-by-side comparison of the expression levels of CD49a (**Figure 19A**), CD150 (**Figure 19B**), and Slamf6 (**Figure 19C**) on all  $\mathcal{N}$ KT cells and specifically on NKT<sub>FH</sub> cells.



#### 4.4. The Cytokine Production of NKT<sub>FH</sub> Cells

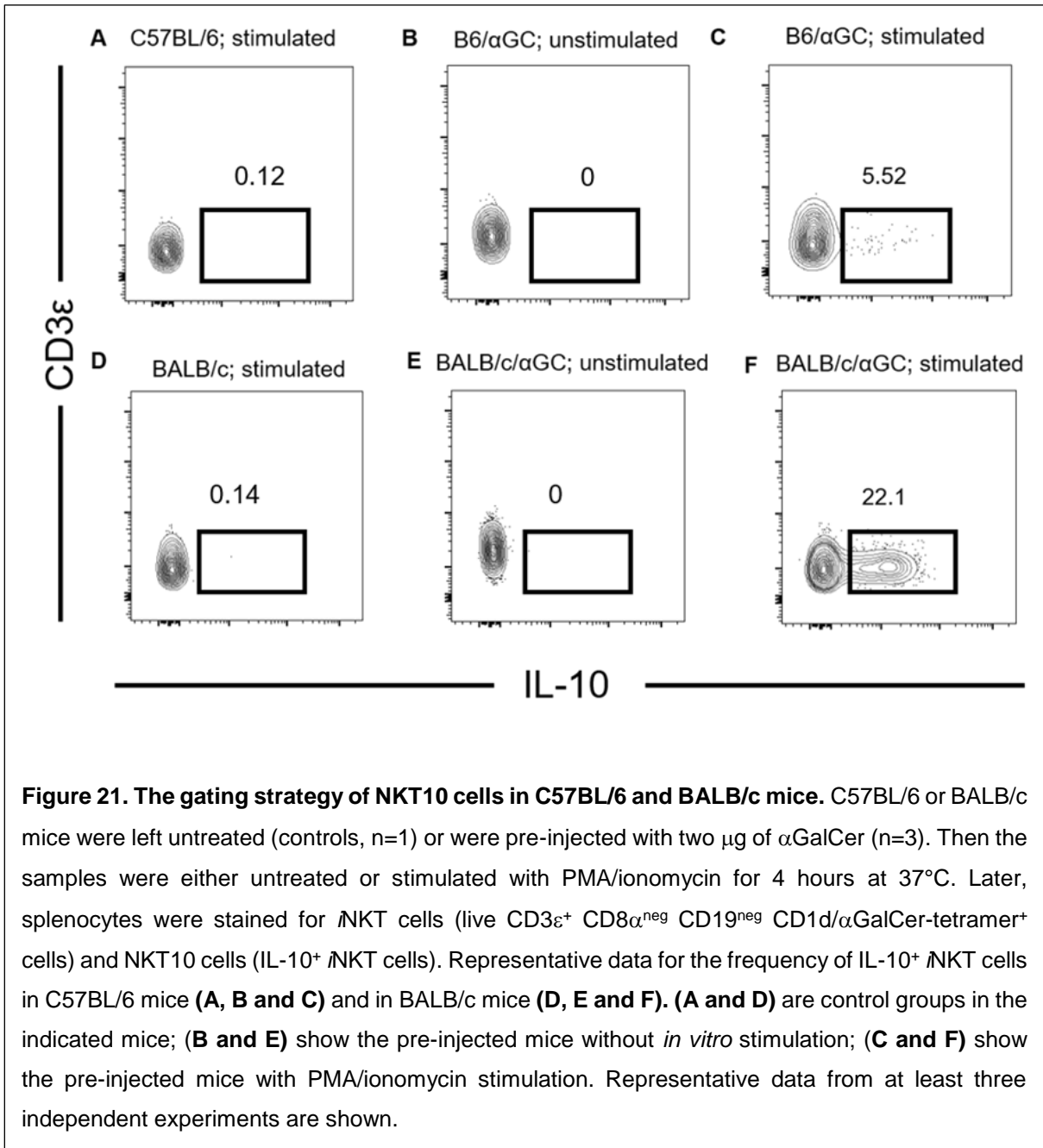
So far, it has only been reported that NKT<sub>FH</sub> cells can produce the cytokine IL-21 (Chang *et al.*, 2011). In order to improve our knowledge on their function, we wanted to analyse whether NKT<sub>FH</sub> cells can produce several additional cytokines. Splenocytes from  $\alpha$ GalCer pre-injected and untreated mice were stimulated with PMA and ionomycin *in vitro* for four hours in the presence of protein transport inhibitors. This was followed by the intracellular cytokine and transcription factor staining. However, the percentage of NKT<sub>FH</sub> cells, measured as Bcl6 and CD185 double-positive cells, after the stimulation was significantly lower than in the unstimulated samples (**Figure 20A**). This was seen in both mouse strains tested, C57BL/6 and BALB/c mice. In  $\alpha$ GalCer pre-injected BALB/c mice, the percentage of NKT<sub>FH</sub> cells in unstimulated samples was with  $32.5\% \pm 2.80\%$  significantly higher than in stimulated samples ( $13.1\% \pm 0.8\%$ ) (**Figure 20A**). This was similar for pre-injected C57BL/6 mice, where the percentage of NKT<sub>FH</sub> cells in unstimulated samples was  $7.28\% \pm 0.8\%$ , but in stimulated samples  $2.37\% \pm 0.37\%$ . This reduced frequency of NKT<sub>FH</sub> cells was caused by a clear decrease in the expression of both Bcl6 and CD185 after the stimulation (**Figure 20B** and **20C**). Due to the greatly reduced cell numbers of NKT<sub>FH</sub> cells that we could measure after the stimulation, we were not able to obtain conclusive results on the cytokine production of NKT<sub>FH</sub> cells.



## 4.5. The Relationship of NKT<sub>FH</sub> And NKT10 Cells

### 4.5.1. The frequency of NKT<sub>FH</sub> and NKT10 cells changes over time following antigenic stimulation

Four  $\text{iNKT}$  cell subsets, namely NKT1, NKT2, NKT10 and NKT17 cells, can be detected in mice in the steady state. Following  $\alpha\text{GalCer}$  injection, several changes have been reported. Firstly, Sag and others have reported that  $\alpha\text{GalCer}$  injection can expand the frequency of IL-10 producing NKT10 cells (Sag *et al.*, 2014; **Figure 21**). Secondly, Chang and others have shown that NKT<sub>FH</sub> cells arise within five to six days following  $\alpha\text{GalCer}$  injection (Chang *et al.*, 2011). As  $\alpha\text{GalCer}$  injection causes changes in the frequency of NKT10 and NKT<sub>FH</sub> cells, we decided to analyse how the percentage of IL-10 producing NKT10 cells and Bcl6<sup>+</sup> expressing NKT<sub>FH</sub> cells changes over time. For this, C57BL/6 mice were injected i.p. with 4  $\mu\text{g}$   $\alpha\text{GalCer}$  and analysed six to eighty-five days later. To detect NKT<sub>FH</sub> cells, the transcription factor Bcl6 was measured and were gated as described in **figure 9**. As IL-10 production is currently the only way to identify NKT10 cells, lymphocytes were purified from splenocytes via lymphoprep and stimulated with PMA/ionomycin for five hours at 37°C to detect cytokine production. Once  $\text{iNKT}$  cells were gated as described above (**Figure 7**), NKT10 cells were identified as IL-10<sup>+</sup> cells. As shown in **figure 21**, stimulated  $\text{iNKT}$  cells from  $\alpha\text{GalCer}$  pre-injected mice produced significantly more (18.03%  $\pm$  1.19%, 0,006) IL-10 than control  $\text{iNKT}$  cells (0.14%  $\pm$  0.007%, 0.105).





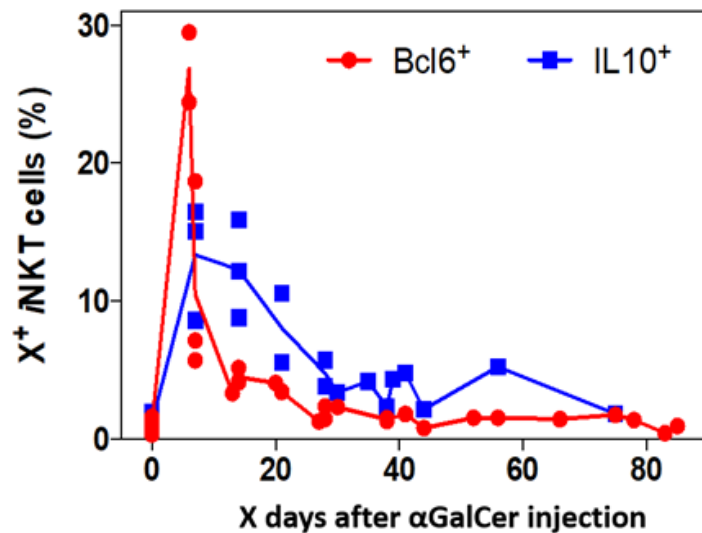


**Figure 22. Time course of the expression of Bcl6 and IL-10 in  $\mathbb{N}$ KT cells following  $\alpha$ GalCer injection.** C57BL/6 mice were left untreated (day 0) or were injected i.v. with 4  $\mu$ g of  $\alpha$ GalCer. Six to 85 days later, splenocytes were stained for  $\mathbb{N}$ KT cells (live CD3 $\epsilon$ <sup>+</sup> CD8 $\alpha$ <sup>neg</sup> CD19<sup>neg</sup> CD1d/ $\alpha$ GalCer-tetramer<sup>+</sup> cells) and the frequency of either Bcl6<sup>+</sup>  $\mathbb{N}$ KT cells (*ex vivo*) or of IL-10<sup>+</sup>  $\mathbb{N}$ KT cells (intracellular cytokine staining after stimulation with PMA/ionomycin for 4h) was determined by flow cytometry. In the summary graph, each data point displays the average values from one independent experiment with at least two mice per group.

As shown in **figure 22**, the percentage of Bcl6<sup>+</sup>  $\mathbb{N}$ KT cells reached its peak on day six after  $\alpha$ GalCer injection, rapidly declines thereafter and returned to background levels within about three weeks. In contrast, the percentage of IL-10<sup>+</sup>  $\mathbb{N}$ KT cells peaked after one to two weeks and clearly remained elevated over the background levels throughout the experiment. These data demonstrate that, following the injection of  $\alpha$ GalCer, the NKT<sub>FH</sub> cell expansion preceded the NKT10 cell expansion (**Figure 22**). Due to this kinetic we wondered if these two recently identified  $\mathbb{N}$ KT cell subsets might be functionally linked, i.e. whether NKT<sub>FH</sub> cells could be required precursors for NKT10 cells *in vivo*.

#### 4.5.2. The Importance of $\text{NKT}_{\text{FH}}$ Cells for The Development of $\text{NKT10}$ Cells

To test the hypothesis that  $\text{NKT}_{\text{FH}}$  cells are required precursors for  $\text{NKT10}$  cells, we tested the response of  $\text{iNKT}$  cells towards  $\alpha\text{GalCer}$  injection in mice lacking  $\text{Bcl6}$ . Chang and others reported that in mice with a T cell specific deficiency of  $\text{Bcl6}$  ( $\text{Bcl6}^{\text{flx/flx}} \times \text{CD4-Cre}$  mice; Kaji *et al.*, 2012) lacked both  $\text{T}_{\text{FH}}$  cells and  $\text{NKT}_{\text{FH}}$  cells, demonstrating that the transcription factor  $\text{Bcl6}$  is required for their development (Chang *et al.*, 2011). To directly address the requirement of  $\text{Bcl6}$  in the development of  $\text{NKT10}$  cells we analysed the presence of  $\text{NKT10}$  cells in these  $\text{Bcl6}^{-/-}$  mice.  $\text{Bcl6}^{-/-}$  mice were injected i.v. with  $\alpha\text{GalCer}$  and the production of IL-10 by  $\text{iNKT}$  cells was measured after *in vitro* stimulation of splenocytes with PMA/ionomycin for five hours at  $37^{\circ}\text{C}$ .

The percentage of IL-10 producing  $\text{iNKT}$  cells in the  $\text{Bcl6}^{-/-}$  mice was not lower, but even higher than in the C57BL/6 wild-type mice (**Figure 23**). These results demonstrate that  $\text{NKT10}$  cells can develop in the absence of  $\text{Bcl6}$  and, therefore, suggest that  $\text{NKT10}$  cell development does not depend on  $\text{NKT}_{\text{FH}}$  cells.

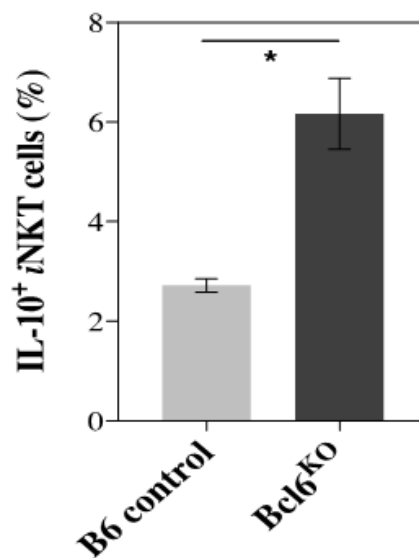


**Figure 23.  $\text{NKT10}$  cell expansion after  $\alpha\text{GalCer}$  does not depend on  $\text{Bcl6}$ .** C57BL/6 (B6 control) and  $\text{Bcl6}$ -deficient ( $\text{Bcl6}^{\text{KO}}$ ) mice were injected i.v. with four  $\mu\text{g}$  of  $\alpha\text{GalCer}$  and eight weeks later, splenocytes were stimulation with PMA/ionomycin for 4h, and the frequency of IL-10 in  $\text{iNKT}$  cells (live  $\text{CD3}\epsilon^+ \text{CD8}\alpha^{\text{neg}} \text{CD19}^{\text{neg}} \text{CD1d}/\alpha\text{GalCer-tetramer}^+$  cells) was determined by flow cytometry. Representative data of two independent experiments with at least two mice per group is shown.

## 5. DISCUSSION

In this study, we provide a detailed characterization of NKT<sub>FH</sub> cells. Although NKT<sub>FH</sub> cells could have important functions in supporting B cell responses during infections, little information on NKT<sub>FH</sub> cells has been reported. Here, for the first time, we defined the impact of antigen administration on the frequency of NKT<sub>FH</sub> cells in different organs and how this is influenced by the route of the antigen administration. Importantly, our data demonstrates that the development of NKT10 cells does not depend on NKT<sub>FH</sub> cells. Our data suggest that NKT10 and NKT<sub>FH</sub> cells are two independent NKT cell subsets.

So far it has been reported that NKT<sub>FH</sub> cells are positive for CD185/CXCR5, CD272/BTLA, CD278/ICOS, and CD279/PD-1, but negative for CD127 (Chang *et al.*, 2012; King *et al.*, 2012; Tonti *et al.*, 2012; Sag *et al.*, 2014). To improve the characterization of NKT<sub>FH</sub> cells, we measured the expression of several additional surface markers (**Figure 15**). We next addressed the functionality of NKT<sub>FH</sub> cells. So far, IL-21 was the only reported cytokine that NKT<sub>FH</sub> cells can produce (Chang *et al.*, 2011). We stimulated splenocytes of  $\alpha$ GalCer-preinjected mice *in vitro* with PMA/ionomycin in order to induce cytokine production. However, we noticed that the frequency of NKT<sub>FH</sub> cells was significantly lower after stimulation compared to the unstimulated samples. This was due to the downregulation of CD185 and Bcl6, which are required to identify NKT<sub>FH</sub> cells. Similar results were seen with splenocytes from BALB/c and C57BL/6 mice. Therefore, we were not able to measure the cytokine production of NKT<sub>FH</sub> cells. The downregulation of CD185 and Bcl6 might also be happen *in vivo* during inflammations and that might be a problem for the detection of NKT<sub>FH</sub> cells *ex vivo* during such conditions. To avoid this issue, it would be helpful to find additional markers, besides CD185 and Bcl6, for the identification of NKT<sub>FH</sub> cells. As an alternative approach for this problem, we could use Bcl6 reporter mice (Kaji *et al.*, 2012) to improve the detection of NKT<sub>FH</sub> cells in order to analyse their cytokine production. By sorting of NKT<sub>FH</sub> cells via the surface marker CD185 we could purify NKT<sub>FH</sub> cells first in order to analyse then their cytokine production.

Previous publications on NKT<sub>FH</sub> cells used different antigen-administration routes, such as subcutaneous (Tonti *et al.*, 2012), intravenous (Chang *et al.*, 2012, Sag *et al.*, 2014), or intraperitoneal (Chang *et al.*, 2012, King *et al.*, 2012). Therefore, we compared whether the route of the antigen administration influences the induction of NKT<sub>FH</sub> cells. We described here for the first time that the route of  $\alpha$ GalCer challenge (i.v. vs. i.p.) impacts the expansion and *in vivo* distribution of NKT<sub>FH</sub> cells six days later. Our analysis revealed that the frequency of NKT<sub>FH</sub> cells is higher following the injection of  $\alpha$ GalCer via the i.p. route than the i.v. route. As  $\alpha$ NKT cells are activated by APCs, this may be explained by APCs. It was published that i.p. injection of an antigen could drain directly to the mesenteric lymph nodes in the peritoneal cavity (Fritz and Waag, 1999). Therefore, the antigen administration from the peritoneal cavity could stimulate different kinds of APCs or increase the frequency of activated APCs. These activated APCs may circulate faster from one lymph node to another and could therefore strengthen the stimulation of  $\alpha$ NKT cells. Another important implication is the potential response of NKT<sub>FH</sub> cells during infections *in vivo*, as how the pathogen enters the body should also impact the NKT<sub>FH</sub> cell induction. In this context, the impact of an injection of the antigen via the subcutaneous route on the NKT<sub>FH</sub> cell expansion would be worthwhile to include. Furthermore, it would be of interest to compare the NKT<sub>FH</sub> cell development following the challenge with different kinds of  $\alpha$ NKT cell antigens. As NKT<sub>FH</sub> cells can support B cell responses *in vivo*, such knowledge would be important to decide the route of administration for therapeutic applications.

Lee and others reported that the frequency of NKT1, NKT2, and NKT17 cells differs between C57BL/6 and BALB/c mice at the steady state (Lee *et al.* 2015). Therefore, we measured the NKT<sub>FH</sub> cell expansion in these two mouse strains side-by-side. Our data show that the *in vivo* frequency of NKT<sub>FH</sub> cells is significantly higher in BALB/c than in C57BL/6 mice. This data may be explained by the genetic tendency of BALB/c mice towards Th2 immune response, like during helminth infections (Mills *et al.*, 2000). It was reported that T<sub>FH</sub> cells could differentiate from Th2 cells during helminths infection (Gladman *et al.*, 2009). It is also known that BALB/c mice have a higher frequency of NKT2 cells than C57BL/6 mice (Lee *et al.*, 2013). As  $\alpha$ NKT cell subsets mimic CD4<sup>+</sup> T cell subsets, it might be possible that NKT2 cells could differentiate into NKT<sub>FH</sub> cells. Furthermore, this tendency towards Th2 immune

response also affects the balance of the cytokine production. This could result in a different environment, which could also affect the activation of  $\mathbb{N}$ KT cells. To clarify these points, one would need to determine the cellular origin of  $\mathbb{N}$ KT<sub>FH</sub> cells.

$\mathbb{N}$ KT cell subsets are characterized by the transcription factors they express and the cytokines they produce (Lee *et al.*, 2013). NKT1, NKT2, NKT10, and NKT17 cells develop in the thymus at the steady-state (Lee *et al.*, 2013; Birkholz *et al.*, 2015; Sag *et al.*, 2014; Coquet *et al.*, 2008). However,  $\mathbb{N}$ KT<sub>FH</sub> cells arise after immunization. It was reported that the frequency of NKT10 cells is increased 20 days following  $\alpha$ GalCer injection (Sag *et al.*, 2014). Our data indicates that the expansion of NKT10 cells starts even earlier. Although,  $\mathbb{N}$ KT<sub>FH</sub> cells were more frequent than NKT10 cells first six days after the injection of  $\alpha$ GalCer, a clear increase of NKT10 cells was already visible (**Figure 22**). This raised the question of the relationship of  $\mathbb{N}$ KT<sub>FH</sub> and NKT10 cells. It is known that there is *plasticity* among CD4<sup>+</sup> T cell subsets, meaning that some CD4<sup>+</sup> T cell subsets are able to differentiate into each other under certain conditions (Caza *et al.*, 2015; Geginat *et al.*, 2014).

As  $\mathbb{N}$ KT cell subsets mimic CD4<sup>+</sup> T cell subsets in many aspects of phenotype and function, it could be argued that  $\mathbb{N}$ KT<sub>FH</sub> cells differentiate into NKT10 cells. To test this hypothesis, we measured the expansion of NKT10 cells in mice in which all T cells lack Bcl6, the essential transcription factor for the development of  $\mathbb{N}$ KT<sub>FH</sub> and T<sub>FH</sub> cells (Chang *et al.*, 2012). Surprisingly, our data show that the frequency of IL-10<sup>+</sup> producing  $\mathbb{N}$ KT cells, i.e. NKT10 cells, was increased in  $\alpha$ GalCer pre-injected Bcl6<sup>-/-</sup> mice four weeks after the injection. This demonstrates that NKT10 cells are independent from  $\mathbb{N}$ KT<sub>FH</sub> cells and that  $\mathbb{N}$ KT<sub>FH</sub> cells are not essential precursors for NKT10 cells. Given the increased frequency of NKT10 cells in the Bcl6<sup>-/-</sup> mice could suggest that  $\mathbb{N}$ KT<sub>FH</sub> cells impair the development of NKT10 cells. However, the T cell-specific Bcl6<sup>-/-</sup> mice also lack T<sub>FH</sub> cells and potential other Bcl6-dependent developmental aspects, which might influence NKT10 cell expansion. To clarify this point, we will test whether *in vivo* treatment of wild-type mice with Bcl6 inhibitors would also augment NKT10 cell differentiation. Such a therapeutic increase of anti-inflammatory NKT10 cells could provide a new approach for the treatment of e.g. autoimmune diseases.

## 6. CONCLUSION

$\mathbb{N}$ KT cells are a unique subset of T lymphocytes that phenotypically and functionally resemble NK cells as well as memory T cells.  $\mathbb{N}$ KT cells recognize glycolipids and can be activated by  $\alpha$ GalCer. After activation with  $\alpha$ GalCer,  $\mathbb{N}$ KT cells rapidly produce cytokines, like IFN- $\gamma$  and IL-4. Similar to CD4<sup>+</sup> T helper cells, mouse  $\mathbb{N}$ KT cells can be divided into several distinct subsets. One  $\mathbb{N}$ KT cell subset, NKT<sub>FH</sub> cells provide help for the proliferation of B cells during infection. This study provides new knowledge on the development and phenotype of NKT<sub>FH</sub> cells. In particular, we show that the route of antigen challenge impacts the frequency of NKT<sub>FH</sub> cells and their *in vivo* distribution. This information is important for the development of new vaccination strategies that target NKT<sub>FH</sub> cells. Furthermore, we show that NKT10 cells do not depend on NKT<sub>FH</sub> cells *in vivo*. This demonstrates that these two  $\mathbb{N}$ KT cell subsets are developmentally independent and can, therefore, be targeted independently, e.g. for therapeutic interventions.

## 7. REFERENCES

Agea, E., Russano, A., Bistoni, O., *et al.*, Human CD1-restricted T cell recognition of lipids from pollens. *The Journal of experimental medicine* 2005; 202(2), 295–308. doi:10.1084/jem.20050773,

Albacker LA, Chaudhary V, Chang YJ, *et al.*, A fungal glycosphingolipid directly activates Natural Killer T cells and rapidly induces airways disease. *HHS Public Access*. 2014;19(10):1297-1304. doi:10.1038/nm.3321.

Alberts B, Johnson A, Lewis J, *et al.* Innate Immunity. *Molecular Biology of the Cell*, 4th edition, New York: Garland Science; 2002.

Allen, C.D., Okada, T., and Cyster, J.G. Germinal-center organization and cellular dynamics. *Immunity* 2007; 27, 190–202

Arnon TI, Markel G, Mandelboim O. Tumor and viral recognition by natural killer cells receptors. 2006;16:348-358. doi:10.1016/j.semcancer.2006.07.005-1-36

Barral P, Eckl-Dorna J, Harwood NE *et al.*, B cell receptor-mediated uptake of CD1d-restricted antigen augments antibody responses by recruiting invariant NKT cell help *in vivo*. *Proc Natl Acad Sci USA* 2008;105:8345–50.

Bendelac A, Savage PB. *The Biology of NKT Cells*. 2007. doi:10.1146/annurev.immunol.25.022106.141711

Benlagha BK, Weiss A, Beavis A, Teyton L, Bendelac A. *In vivo* identification of glycolipid antigen – specific T cells using fluorescent CD1d tetramers. 2000; 191(11).

Braun NA, Major AS. Natural Killer T Cells and atherosclerosis : form and function meet pathogenesis. 2010;316-324. doi:10.1159/000296915

Brennan PJ, Brigl M, Brenner MB. Invariant natural killer T cells: An innate activation scheme linked to diverse effector functions. *Nat Rev Immunol*. 2013;13(2):101-117. doi:10.1038/nri3369

Brien KLO, Wolfson LJ, Watt JP, *et al.*, Burden of disease caused by *Streptococcus pneumoniae* in children younger than 5 years : global estimates. *Lancet*. 2005;374(9693):893-902. doi:10.1016/S0140-6736(09)61204-6

Brubaker, S. W., Bonham, K. S., Zanoni, I., *et al.*, Innate immune pattern recognition: a cell biological perspective. *Annual review of immunology*, 33. 2015; 257–290. doi:10.1146/annurev-immunol-032414-112240

Cano RLE, Lopera HDE. Introduction to T and B lymphocytes. El Rosario University Press; 2013 Jul 18; Chapter 5.

Caza T, Landas S. Functional and Phenotypic Plasticity of CD4(+) T Cell Subsets. *Biomed Res Int*. 2015;2015:521957. doi:10.1155/2015/521957

Chan CW, Housseau F. The ' kiss of death ' by dendritic cells to cancer cells. 2008:58-69. doi:10.1038/sj.cdd.4402235

Chang PP, Barral P, Fitch J, *et al.* Identification of Bcl-6-dependent follicular helper NKT cells that provide cognate help for B cell responses. *Nat Immunol*. 2012;13(1):35-43. doi:10.1038/ni.2166

Chang Y, Kim HY, Albacker LA, *et al.*, Influenza infection in suckling mice expands an NKT cell subset that protects against airway hyperreactivity. 2011;121(1):57-69. doi:10.1172/JCI44845DS1

Chen J, Yang J, Qiao Y, Li X. Understanding the regulatory roles of Natural Killer T cells in rheumatoid arthritis : T helper cell differentiation dependent or independent ? 2016:197-203. doi:10.1111/sji.12460

Chowdhury D, Lieberman J. Death by a thousand cuts : granzyme pathways of programmed cell death. 2008. doi:10.1146/annurev.immunol.26.021607.090404

Crotty S. A brief history of T cell help to B cells. *Nature reviews. Immunology*, 2015; 15(3), 185–189. doi:10.1038/nri3803

Crotty, S. Follicular helper CD4 T cells (TFH). *Annu. Rev. Immunol*. 2011; 29, 621–663

Crowe, N. Y. *et al.* Glycolipid antigen drives rapid expansion and sustained cytokine production by NKT cells. *J. Immunol*. 2003; 171, 4020–4027.

Cullen SP, Martin SJ. Mechanisms of granule-dependent killing. 2008: 251-262. doi:10.1038/sj.cdd.4402244

Geginat J, Paroni M, Maglie S, *et al.* Plasticity of human CD4 T cell subsets. *Front Immunol*. 2014;5:630. Published 2014 Dec 16. doi:10.3389/fimmu.2014.00630



Glatman Zaretsky A, Taylor JJ, King IL, Marshall FA, Mohrs M, Pearce EJ. T follicular helper cells differentiate from Th2 cells in response to helminth antigens. *J Exp Med*. 2009;206(5):991–999. doi:10.1084/jem.20090303

Godfrey DI, Kronenberg M, Godfrey DI, *et al.*, Going both ways : Immune regulation via CD1d- dependent NKT cells 2004; 114(10):1379-1388. doi:10.1172/JCI200423594.

Godfrey DI, Macdonald HR, Kronenberg M. NKT cells : what's in a name ? 2004; 4(March):1-7.

Godfrey DI, Mcconville MJ, Pellicci DG. Chewing the fat on natural killer T cell development. *JEM* 2006; 203(10):2229-2232. doi:10.1084/jem.20061787

Gumperz JE, Miyake S, Yamamura T, *et al.*, Functionally distinct subsets of CD1d-restricted Natural Killer T cells revealed by CD1d tetramer staining. 2002; 195(5):625-636.

Haynes, NM., Allen, C.D., Lesley, R., *et al.*, Role of CXCR5 and CCR7 in follicular Th cell positioning and appearance of a programmed cell death gene-1high germinal center-associated subpopulation. *J Immunol*. 2007; 179:5099-5108

Huughes C, Benson RA, Bedaj M, Maffia P. Antigen-Presenting cells and antigen presentation in tertiary lymphoid organs. 2016; 7(November). doi:10.3389/fimmu.2016.00481

Janeway CA Jr, Travers P, Walport M, *et al.* Generation of lymphocytes in bone marrow and thymus; *Immunobiology: The immune system in health and disease*; 5th edition; New York: Garland Science; 2001

Kaji T, Ishige A, Hikida M, *et al.* Distinct cellular pathways select germline-encoded and somatically mutated antibodies into immunological memory. *J Exp Med*. 2012;209(11):2079–2097. doi:10.1084/jem.20120127

Kawano, T., J. Cui, Y. Koezuka, *et al.*, CD1d-restricted and TCR- mediated activation of Va14 NKT cells by glycosylceramides. *Science* 1997; 278: 1626–1629.

Kim PJ, *et al.*, GATA-3 regulates the development and function of invariant NKT cells. *J Immunol*. 2006; 177:6650–6659

Kimbrell DA, Beutler B. The evolution and genetics of innate immunity. 2001; 2(April):256-267.

Kinjo Y, Tupin E, Wu D, *et al.* Natural killer T cells recognize diacylglycerol antigens from pathogenic bacteria. 2006; 7(9):978-986. doi:10.1038/ni1380

Kinjo Y, Wu D, Kim G, *et al.*, Recognition of bacterial glycosphingolipids by Natural Killer T cells. 2005; 434(March). doi:10.1038/nature03398.

Kjer-nielsen L, Borg NA, Pellicci DG, *et al.*, A structural basis for selection and cross- species reactivity of the semi-invariant NKT cell receptor in CD1d/glycolipid recognition. 2006; 203(3):661-673. doi:10.1084/jem.20051777

Kobayashi E, Motoki K, Uchida T, *et al.*, A novel immunomodulator, and its antitumor activities. *Oncol. Res.*; 1995; KRN7000,7:529–34

Kronenberg M. Toward an understanding of NKT cell biology : progress and paradoxes. 2005; 877-900. doi:10.1146/annurev.immunol.23.021704.115742

Kunii, N. *et al.* Combination therapy of *in vitro*-expanded natural killer T cells and  $\alpha$ -galactosylceramide-pulsed antigen-presenting cells in patients with recurrent head and neck carcinoma. *Cancer Sci.* 2009; 100, 1092–1098

łach-Olszewska Z. Innate immunity: cells, receptors, and signaling pathways. *Archivum Immunologiae et Therapiae Experimentalis.* 2005 May-Jun;53(3):245-253.

Lanier LL. Innate and adaptive immunity. *Nat Rev Immunol.*, 2013; 13(2):73-74. doi:10.1038/nri3389

Lee H, Hong C, Shin J, *et al.*, The presence of CD8+ invariant NKT cells in mice. 2009; 41(12):866-872. doi:10.3858/emm.2009.41.12.092

Lee YJ, Holzapfel KL, Zhu J, *et al.*, Steady-state production of IL-4 modulates immunity in mouse strains and is determined by lineage diversity of iNKT cells *Nat Immunol.* 2013; 14(11):1146–1154. doi:10.1038/ni.2731

Lord SJ, Rajotte R V, Korbitt GS, *et al.*, Granzyme B : a natural born killer. 2003; 193:31-38.

Matsuda, J. L. *et al.*, Tracking the response of natural killer T cells to a glycolipid antigen using CD1d tetramers. *J. Exp. Med.* 2000; 192, 741–754

Mattner J, Debord KL, Ismail N, *et al.*, Exogenous and endogenous glycolipid antigens activate NKT cells during microbial infections. 2005; 523(2003):525-530.

Mattner J, Debord KL, Ismail N, *et al.*, Exogenous and endogenous glycolipid antigens activate NKT cells during microbial infections. 2005; 523(2003):525-530.

McHeyzer-Williams LJ, McHeyzer-Williams MG. Antigen-specific memory B cell development. *Annu Rev Immunol* 2005; 23:487–513.

Morita M., K. Motoki, K. Akimoto, *et al.*,. Structure-activity relationship of  $\alpha$ -galactosylceramides against B16-bearing mice. *J. Med. Chem.* 1995; 38: 2176–2187

Natkunam Y. Follicular Lymphoma *The Biology of the Germinal Center.*

Park BS, Weiss A, Benlagha K, *et al.*, The mouse CD1d-restricted repertoire is dominated by a few autoreactive T cell receptor families. 2001; 193(8).

Pieper K, Grimbacher B, Eibel H. B-cell biology and development. *J Allergy Clin Immunol.* 2013;131(4):959-971. doi:10.1016/j.jaci.2013.01.046

Porcelli SA, Modlin RL. The CD1 system : Antigen-presenting molecules for T Cell recognition of lipids and glycolipids. 1999:297-329.

Roberts, S., & Girardi, M. Conventional and Unconventional T Cells. In: Gaspari A.A., Tying S.K. (eds) *Clinical and Basic Immunodermatology*, 2008

Rossjohn J, Pellicci DG, Patel O, *et al.*, Recognition of CD1d-restricted antigens by natural killer T cells. *Nat Rev Immunol.* 2012; 12(12):845-857. doi:10.1038/nri3328

Schuerwegh AJ, *et al.*, Evaluation of monensin and brefeldin A for flow cytometric determination of interleukin-1 beta, interleukin-6, and tumor necrosis factor alpha in monocytes. *Cytometry.* 2001;46:172-176)

Sriram V, Du W, Gervay-hague J, *et al.*, Cell wall glycosphingolipids of *Sphingomonas paucimobilis* are CD1d-specific ligands for NKT cells. 2005:1692-1701. doi:10.1002/eji.200526157

Stetson, D. B. *et al.*, Constitutive cytokine mRNAs mark natural killer (NK) and NKT cells poised for rapid effector function. *J. Exp. Med.* 2003; 198, 1069–1076

Tak W.Mak Mary E.Saunders, Bridging innate and adaptive immunity, *Cells N. K. T.* 2003; 517–552.

Taniguchi M, Harada M, Kojo S, *et al.*, The regulatory role of V $\alpha$ 14 NKT cells in innate and acquired immune response. *Annu. Rev. Immunol.* 2003; 21:483–513

Tjadine M, Holling, Erik Schooten, Peter J van Den Elsen, Function and regulation of MHC class II molecules in T-lymphocytes: of mice and men, *Human Immunology*, 2004; Volume 65, Issue 4, 2004, Pages 282-290.

Tonti E, Fedeli M, Napolitano A, Iannacone M, Von UH. Europe PMC Funders Group Follicular helper NKT cells induce limited B cell responses and germinal center formation in the absence of CD4+ T cell help. 2013; 188(7):3217-3222. doi:10.4049/jimmunol.1103501.Follicular

Vinuesa CG, Chang PP. Innate B cell helpers reveal novel types of antibody responses. *Nat Immunol* 2013; 14:119–26.

Vivier E, Malissen B. Innate and adaptive immunity : specificities and signaling hierarchies revisited. 2005; 6(1):17-22. doi:10.1038/ni1153

Wali, S., Sahoo, A., Puri, S., *et al.*, Insights into the development and regulation of T follicular helper cells. *Cytokine*,2016; 87, 9–19. doi:10.1016/j.cyto.2016.06.010

Walker JA, Barlow JL, Mckenzie ANJ. Innate lymphoid cells — how did we miss them? *Nat Rev Immunol.* 2013;(January). doi:10.1038/nri3349

Wallach D, Varfolomeev EE, Malinin NL, *et al.*, Tumor necrosis factor receptor and Fas signaling mechanisms. 1999.

Wang K, Wei G, Liu D. CD19 : a biomarker for B cell development, lymphoma diagnosis and therapy. 2012;1(1):1. doi:10.1186/2162-3619-1-36

Wieland Brown LC, Penaranda C, Kashyap PC, *et al.* Production of  $\alpha$ -galactosylceramide by a prominent member of the human gut microbiota. *PLoS Biol.* 2013;11(7):e1001610. doi:10.1371/journal.pbio.1001610

Wingender G, Krebs P, Beutler B, Kronenberg M. Antigen-specific cytotoxicity by Invariant NKT cells in vivo is CD95/CD178-dependent and is correlated with antigenic potency. *J Immunol.* 2010; 185(5):2721-2729. doi:10.4049/jimmunol.1001018

Wingender G. From the deep sea to everywhere: environmental antigens for iNKT cells. *Arch Immunol Ther Exp (Warsz).* 2016; 64(4):291-298. doi:10.1007/s00005-015-0381-7

Yamasaki, K. *et al.* Induction of NKT cell-specific immune responses in cancer tissues after NKT cell-targeted adoptive immunotherapy. *Clin. Immunol.* 2011; 138, 255–265

Yatim KM, Lakkis FG. A brief journey through the immune system. 2015:1-8. doi:10.2215/CJN.10031014

Zhang N, Bevan MJ, CD8+ T cells: foot soldiers of the immune system, 2012; 35(2):161-168. doi:10.1016/j.immuni.2011.07.010.CD8



## 8. ADDENDA

### 8.1. Research Ethics Committee Approval



Date of the Meeting	21/12/2016	Day of the Meeting	Wednesday
Number	15 <sup>th</sup>	Meeting Hour	09:00

To Assist. Prof. Dr. Gerhard Wingender,

It is hereby resolved by unanimous vote that the applications of your research on "Functional characteristics and transcription factor usage of mouse NKT10 cells" are ethically appropriate.

Respectfully submitted for your attention.

**Prof.Dr.Sedef AKGÜNGÖR**  
Chair

**Prof.Dr. H. Alper BAĞRIYANIK**  
Vice-chair

**Prof. Dr. Ensari GÜNELİ**  
Member

**Assoc. Prof.Dr. H. Güneş ÖZHAN**  
Member

**Assoc. Prof. Dr. Ralph Meuwissen**  
Member

**Assoc. Prof. Dr. Devrim PESEN OKVUR**  
Member

**Spec. Umur KELEŞ**  
Member

**Spec. Kerem ESMEN**  
Member

**Phrm. Ferdane KAHRAMAN**

Member

IBG-izmir  
Dokuz Eylül Üniversitesi  
İzmir Uluslararası Biyotıp ve Genom Enstitüsü  
Sağlık Kampüsü  
Balçova 35340 - İzmir / TURKEY  
Phone : +90 (232) 412 6501  
Fax : +90 (232) 412 6509

<https://www.ibg.deu.edu.tr>  
<https://www.facebook.com/ibgizmir>  
<https://twitter.com/ibgizmir>





T.C.  
DOKUZ EYLÜL ÜNİVERSİTESİ  
İZMİR ULUSLARARASI BİYOTİP VE GENOM ENSTİTÜSÜ  
HAYVAN DENEYLERİ YEREL ETİK KURULU (İBG-HADYEK)  
KARARI



TOPLANTI TARİHİ	21/12/2016	TOPLANTI GÜNÜ	Çarşamba
TOPLANTI SAYISI	15	TOPLANTI SAATI	09:00

Sayın Yrd.Doç. Dr. Gerhard Wingender,

19/2016 Protokol No'lu; yürütücüsü olduğunuz "Functional characteristics and transcription factor usage of mouse NKT10 cells" isimli projenin uygulanmasında etik açıdan sakınca olmadığına oy birliği ile karar verilmiştir.

Bilgilerinizi ve gereğini rica ederiz.

Prof.Dr.Sedef AKGÜNGÖR  
Başkan

Prof.Dr. H. Alper BAĞRIYANIK  
Başkan Yardımcısı

Prof. Dr. Ensari GÜNELİ  
Üye

Doç.Dr. H. Güneş ÖZHAN  
Üye

Doç.Dr. Ralph Meuwissen  
Üye

(Katılmamıştır)

Doç.Dr. Devrim PESEN OKVUR  
Üye

Uzm. Umur KELEŞ  
Üye

Uzm. Kerem ESMEN  
Üye

Ecz. Ferdane KAHRAMAN

Üye  
(Katılmamıştır)

## 8.2. Curriculum Vitae

### PERSONAL INFORMATION

### BAŞAK GÜNDÜZ

**Address:** Izmir Biomedicine and Genome Center (IBG),  
Dokuz Eylul University Health Campus,  
Mithatpasa St. No: 58/5, Balçova 35340, Izmir/TURKEY

**E-mail address:** basak.gunduz@msfr.ibg.edu.tr, basakgndz@gmail.com,

**Mobile Phone:** +905373855496

**Date of Birth:** 10/04/1991

### EDUCATION:

**2017- present: MSc in Molecular Biology and Genetics**

Dokuz Eylul University,  
Izmir International Biomedicine and Genome Institute (IBG)  
Molecular Biology and Genetics Department

**2012-2017: BSc in Molecular Biology and Genetics**

Izmir Institute of Technology (IZTECH)  
Molecular Biology and Genetics Department

**2011-2012: English Preparation School**

Izmir Institute of Technology (IZTECH), School of Foreign Languages

### Research Experience:

**05/2017 – present: M.Sc at iBG**

Wingender Laboratory  
Izmir Biomedicine and Genome Center (IBG), Asst. Prof. Gerhard Wingender

**06/2016 – 09/2016:** Internship at Max Planck Institute for Evolutionary Biology

**06/2015 – 07/2015:** Internship at Max Planck Institute for Evolutionary Biology

### Personal Skills

**Language:** Turkish (native), English

### Computer Skills:

Bioinformatics tools, MS Office Applications, C programming, KNIME, Microsoft Access, FLOWJO



**Congress Participated:**

**05/2019:** International Molecular Immunology & Immunogenetics Congress IV (poster presentation)

**Poster:** Basak Gunduz, Yusuf Cem Eskiocak, Gerhard Wingender *NKT10 and NKTFH cells represent two independent iNKT cell subsets that can counter-regulate each*, 2019.

**10/11/2017:** New Frontiers in Life Sciences Symposium, Dokuz Eylul University, Izmir Biomedicine and Genome Center (IBG)

**30/01/2017 – 04/02/2017:** Evolutionary Genomics Winter School

**Research Experience:** Master Thesis

**2017-Present:** The development and phenotype of NKT<sub>FH</sub> cells and their relation to NKT10 cells  
Izmir Biomedicine and Genome Center (IBG), Dokuz Eylul University

Supported by: TUBITAK

**Practised Laboratory Method During M.Sc Education:** Cell Culture Techniques, Cell sorting, FACS- Flow Cytometry, Mouse handling and dissection

**Certifications:** Certificate of Experimental Animal Usage for Researchers, Dokuz Eylul University, 2017

**Academic Reference**

- 1) Asst. Prof. Gerhard Wingender,  
Izmir Biomedicine and Genome Center (IBG) Dokuz Eylul University Health Campus,  
Mithatpasa St. No: 58/5, Balçova 35340 Izmir / TURKEY.  
Email: gerhard.wingender@ibg.edu.tr
- 2) Assoc. Prof. Duygu Sag  
Izmir Biomedicine and Genome Center (IBG) Dokuz Eylul University Health Campus,  
Mithatpasa St. No: 58/5, Balçova 35340 Izmir / TURKEY.  
Email: duygu.sag@ibg.edu.tr
- 3) Dr. Derek Caetano- Anolles,  
Max Planck Institute for Evolutionary Biology  
Plön, GERMANY,  
Email : caetano@evolbio.mpg.de

